

IL NUOVO CIMENTO

ORGANO DELLA SOCIETÀ ITALIANA DI FISICA

SOTTO GLI AUSPICI DEL CONSIGLIO NAZIONALE DELLE RICERCHE

VOL. VII, N. 4

Serie decima

16 Febbraio 1958

Remarks on the Weak Lepton Processes (*).

K. SENBA

Department of Physics, Hiroshima University - Hiroshima

(ricevuto il 29 Aprile 1957)

Summary. — A tentative model, a modification of Konopinski-Mahmoud's model concerning the leptons is developed for the classification of the processes where leptons take part. By means of this model, we obtain a good selection rule, and also the redundant neutral particle has not been introduced which always appears in the model based on the charge independence hypothesis extended to leptons. We have referred to the relation between the N-G model and our scheme and shortly discussed the interaction structure with this scheme. And though we obtain a good selection rule for lepton processes, we conclude that for a classification of leptons, their interaction structure is always to be taken into account.

1. - Introduction.

To interpret the contradiction between the copious production of the new particles and their metastabilities, several ways ⁽¹⁾ have been proposed. Their common idea consists in the introduction of new quantum numbers by which the appropriate selection rules have been expressed. In this way, GELL-MANN and NISHIJIMA ⁽¹⁾ have presented a scheme for classifying the fundamental particles which belong to the baryon- and meson-families under the charge independence hypothesis and characterized these particles by means

(*) Preliminary reports of the present paper have been published in *Prog. Theor. Phys.*, **17** (1957).

⁽¹⁾ A. PAIS: *Physica*, **19**, 869 (1953); *Proc. Nat. Acad. Sci. U.S.*, **40**, 484 (1954); M. GELL-MANN: *Phys. Rev.*, **92**, 833 (1953); T. NAKANO and K. NISHIJIMA: *Prog. Theor. Phys.*, **10**, 581 (1953); K. NISHIJIMA: *Prog. Theor. Phys.*, **13**, 285 (1955); B. D'ESPAGNAT and J. PRENTKI: *Nuovo Cimento*, **3**, 1045 (1956).

of the isotopic spin and strangeness. Thus as far as these particles are concerned they could explain successfully the phenomena concerning strongly interacting particles and discriminate whether the interactions are strong or weak.

On the other hand, from the phenomenological point of view, three kinds of interaction have been found among the baryons, mesons and leptons; namely, strong, electromagnetic and weak interactions. Among these three kinds of interactions, as to weak interactions, there seems to exist the regularity relating to all the families; baryon-, meson- and lepton-families, as pointed out by OGAWA ⁽²⁾. This suggests that the weak interactions have a more fundamental character than the strong interactions. Therefore it is desirable to formulate a theory of weak interactions governing both the baryons and leptons. For this purpose it is desired to introduce some new quantities by which the appropriate selection rules can be expressed retaining the GELL-Mann-Nishijima scheme.

There seems to exist two ways of approach for such programs. The first is to consider the isotopic spin as having some intrinsic significance for all the fundamental particles including leptons ⁽³⁾. This may be justified from the fact that in the electromagnetic interaction the charge operator $Q = I_3 + \alpha$ associates always with the 3rd component of the isotopic spin. The second is to seek some other new quantum numbers not based on the charge independence hypothesis. This standpoint, which takes the extension of the charge independence hypothesis to the lepton family as to be wrong, will be supported from the following facts: 1) no strong interactions have been found in the transition processes where the leptons take part; 2) the ratios of mutual mass difference between the leptons are large and 3) the weak interactions involving leptons are weaker than the electromagnetic interactions which violate the charge independence. It might be required in this approach to treat the lepton processes as dynamical problems rather than kinematical ones, leaving a delicate problem whether those processes should be forbidden by some selection rules or by the detailed structure of the interactions concerned.

In this note we would like to discuss on a tentative scheme for the classification of the fundamental particles including leptons taking into account their interaction structures. The first approach is abandoned because it requires the introduction of the redundant neutral particles, though it is the simplest way for the classification and produces good selection rules. We take the second approach and assign the η_1 -charge to the leptons in an analogous manner as in the N-G model in addition to the conservation of the lepton number proposed by KONOPINSKI-MAHMOUD ⁽⁴⁾. In our approach useful selection

⁽²⁾ S. OGAWA: *Prog. Theor. Phys.*, **15**, 487 (1956).

⁽³⁾ T. OUCHI and K. SENBA: *Prog. Theor. Phys.*, **16**, 528 (1956); S. GOTÔ: *Prog. Theor. Phys.*, **17**, 107 (1957); Y. KATAYAMA: *Prog. Theor. Phys.*, **17** (1957).

⁽⁴⁾ E. J. KONOPINSKI and H. M. MAHMOUD: *Phys. Rev.*, **92**, 1045 (1953).

rules can be obtained by means of η_i -charge and the difficulty concerning the redundant neutral particles can be overcome.

The conservation of the lepton number has not so clear physical meaning as that of the baryon number which relates to the stabilities of matter satisfying the experimental requirement since we take the lepton as Dirac particles. However, if it happens that the neutrino is proved to be a Majorana particle, our model will be ruled out. Fortunately the analysis carried out by F. REINS *et al.* ⁽⁵⁾, seems to support our assumption that the neutrino is a Dirac particle. Hereafter, for the sake of simplicity, only one kind of neutrino is assumed.

In the following sections, the selection rules by means of η_i -charge will be presented so that

- 1) $|\Delta\eta_i| = 2$ for the processes:

$$[\text{baryon}] + [\text{meson}] \rightarrow [\text{baryon}] + [\text{meson}] + [\text{lepton}];$$

- 2) $\Delta\eta_i = 0$ for the processes:

$$[\text{lepton}] \rightarrow [\text{lepton}].$$

We discuss in detail about the lepton processes and also shortly refer to the interaction structure which causes the mutual transition between the various families.

2. - Assignments of a new quantum number for the lepton family.

About the lepton processes several attempts ⁽⁶⁻⁸⁾ have been presented assuming the existence of Fermi interactions among four fermions. But they cannot forbid the unwanted processes completely though these processes are consistent with the various conservation laws. To avoid this defect YANG and TIOMNO ⁽⁶⁾ tried to introduce the intrinsic «generalized parity» in such a way that the generalized parity conservation is violated in the unwanted processes. CAIANIELLO ⁽⁷⁾ reported that all the unwanted processes can be successfully eliminated if the coupling constants are permitted to change in a certain way corresponding to the changes of co-ordinates. And TIOMNO ⁽⁸⁾ proposed to choose the suitable combination of coupling types by imposing the «mass reversal» invariance on the Fermi interactions.

⁽⁵⁾ F. REINS and C. L. COWAN JUN: *Nature*, **178**, 446 (1956).

⁽⁶⁾ C. N. YANG and J. TIOMNO: *Phys. Rev.*, **79**, 495 (1950).

⁽⁷⁾ E. R. CAIANIELLO: *Nuovo Cimento*, **8**, 534 and 749 (1951); **9**, 336 (1952).

⁽⁸⁾ J. TIOMNO: *Nuovo Cimento*, **1**, 226 (1955).

In comparison with these attempts Konopinski-Mahmoud's model ⁽⁴⁾ is quite interesting. They showed that the unwanted processes can be forbidden by the conservation of lepton numbers if the positively charged μ -meson, the negatively charged electron and the neutrino are assumed to be normal particles. With the accumulation of the experimental facts for new unstable particles, the K-M model has been found insufficient to exclude the unwanted processes concerning strange particles.

To complete the K-M model, let us assign the η_l -charge to leptons under the hypothesis of the conservation of the lepton number in an analogous manner as in the Nishijima model, assuming the relationship between electric charge Q and η_l -charge as follows:

$$(1) \quad Q = \frac{1}{2}(n + \eta_l).$$

The η_l -charge was assigned to each particles in the following table.

TABLE I. - *Types of fields.*

| Name | Lorentz space | Q | n | η_l |
|-------|---------------|-----|-----|----------|
| μ | spinor | 1 | 1 | 1 |
| e | » | -1 | 1 | -3 |
| ν | » | 0 | 1 | -1 |

In order to avoid the introduction of the redundant neutral particles appearing in the charge-independent model of leptons, the leptons are assumed here to be scalar quantities in the isotopic spin space. An anti-particle, i.e., the charge conjugate particle, has an opposite η_l -charge to that of the normal particle as is the case for the electric charge, and we have

$$(2) \quad QC = -CQ, \quad \eta_l C = -C\eta_l,$$

where C is the charge conjugation operator.

Under these assumptions we shall go on into the detailed investigation of lepton processes in the following sections.

3. - Interaction structure and the classification of fundamental particles.

As one of the phenomenological approaches to the investigation of the structure of interactions, it seems to be most attractive to classify the elementary particles into several families 1) baryon-family, 2) lepton-family, 3) meson-family and 4) photons.

Among these families the electromagnetic field (photon) interacts with all the charged particles with a universal coupling constant « e », satisfying the requirement of gauge invariance. Therefore we take this constant « e » to

characterize the electro-magnetic field « A_μ ». Moreover, for the electromagnetic field there exists an invariance principle under gauge transformation, but no invariance principle like this has yet been found for other families. However there seems to be some peculiar regularity concerning the weak interaction among these families as has been recently stressed by OGAWA ⁽²⁾. The coupling constants of these interactions take a unique value of the order of magnitude (10^{-14}) in the natural unit regardless of coupling type or the kinds of particles concerned. Because this weak interaction occurs not only among the baryon- and meson-families, but also among the lepton family, we may ask why the particles belonging to all these families have a coupling constant of an unique order of magnitude, and what is the source of weak interaction. This question will offer a key to the study of the interaction structure among these particles. Further, the fact that the weak interaction associates with all the families suggests that the weak interaction has more fundamental and elementary character than the strong interaction which appears only between baryon- and meson-families.

It may be a clue to the above question to remind the fact that the lepton processes involve at least one neutrino. But with the accumulation of the experimental data about new unstable particles, there exists the other weak interaction that does not involve neutrino. So, we cannot take the neutrino as the unique origin of the weak interaction. On the other hand, on the belief that all the weak interactions come from a single base, OGAWA has proposed an attractive model in which new unobserved charged Bose fields (simply called « B -field») have been introduced and are assumed to interact with all Fermi particles with a unique coupling constant. His fundamental idea consists rather in the introduction of the B -field which plays a similar role as the electromagnetic field does in the electromagnetic interaction.

From the phenomenological investigation we know as universal weak interaction the following three kinds; 1) weak fermion-boson interaction, 2) universal weak Fermi interaction extended to baryons and 3) weak boson-boson interaction. We assume in this paper for the sake of simplicity that the interactions occur through the universal weak

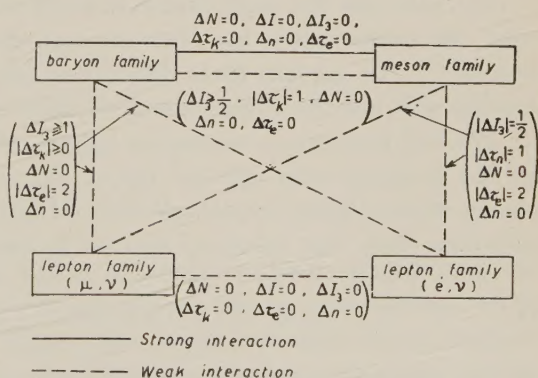


Fig. 1.

Fermi interaction. Then the transition scheme among these families is as follows (Fig. 1):

Analogously to the N-G scheme for the strong interactions, we assume another hypothesis than the charge independence for the fundamental weak interactions. Though it may be more reasonable to treat both the weak interaction between the baryon- and meson-families and the weak lepton processes on the same footing, we are forced to treat them differently because of the peculiar character of lepton processes. But η_l -charges of leptons are shown to produce a good selection rule.

Now we shall go further to investigate the transition processes from the view-point of family mentioned above as follows:

1) The strong interactions; [baryon] and/or [meson] \rightarrow [baryon] and/or [meson].

Since these processes are strong and not concerned with the leptons, we do not enter into a detailed discussion here. The isotopic spin I , its 3rd component I_3 and η_l -charge are conserved in this case.

2) The weak interactions: [baryon] or [meson] \rightarrow [baryon] and/or [meson]. This processes are governed by the rule

$$(3) \quad |\Delta I| \geq \frac{1}{2}, \quad \Delta N = 0 \quad \text{and} \quad |\Delta \eta_h| \geq 1.$$

For these processes it will be an interesting problem to examine whether these are due to direct interactions or to indirect ones. Here the indirect processes are meant to be the processes that occur through the intermediary of the universal weak Fermi interaction extended to baryons.

3) The weak interactions: [baryon] and/or [meson] \rightarrow [baryon] and/or [meson] + [lepton].

For this case the main task is to exclude the processes which are consistent with the conservation law, but are not observed experimentally: several attempts ^(6,7) to explain these difficulties have been published so far. Our attention will also be concentrated on such processes.

We will here give a scheme to rule out the unwanted processes for leptons by the η_l -charge rule and the lepton-number conservation law instead of the charge independence hypothesis without introduction of the redundant neutral particles. Thus the following scheme is assumed

$$(4) \quad |\Delta I_3| = 1, \quad \Delta N = 0, \quad |\Delta \eta_h| \geq 0 \quad \Delta n = 0 \quad \text{and} \quad |\Delta \eta_l| = 2$$

for the process: [baryon] \rightarrow [baryon] + [lepton],

$$(5) \quad |\Delta I_3| = \frac{1}{2}, \quad \Delta N = 0, \quad |\Delta \eta_h| = 1 \quad \Delta n = 0 \quad \text{and} \quad |\Delta \eta_l| = 2$$

for the processes: [meson] \rightarrow [meson] + [lepton].

4) The weak interactions: $[\text{lepton}] \rightarrow [\text{lepton}]$.

Only one process belonging to this case is known so far ($\mu \rightarrow e + \nu + \nu$). For this process, the following assumption will be adequate

$$(6) \quad \Delta n = 0 \quad \text{and} \quad \Delta \eta_i = 0.$$

It is interesting to investigate the interaction structure of this process in connection with the problem of the elementarity of the interactions. Compared with the case 3) this assumption seems somewhat unreasonable. Perhaps it may be due to the difference of the interaction structure of leptons from that of baryons.

4. - Allowed lepton processes.

In this section we would like to discuss the processes which are allowed by our model and consistent with the conventional conservation laws. As is referred in Sect. 3 the following characteristic features are recognized experimentally for the phenomena involving leptons: 1) The lepton processes involve at least one neutrino, 2) they take place always in pairs (μ, ν) or (e, ν) and 3) in two body decay μ and e appear only in an asymmetrical manner.

The established lepton processes so far are as follows ⁽⁹⁾:

$$(7) \quad N \rightarrow p + e^- + \tilde{\nu},$$

$$(8) \quad P + \mu^- \rightarrow N + \tilde{\nu},$$

$$(9) \quad \mu^+ \rightarrow e^+ + \nu + \nu,$$

$$(10) \quad \pi \rightarrow \mu + \nu,$$

$$(11) \quad K_{\mu 2}^+ \rightarrow \mu^+ + \tilde{\nu},$$

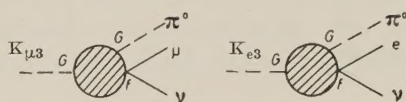
$$(12) \quad K_{\mu 3}^+ \rightarrow \pi^0 + \mu^+ + \tilde{\nu},$$

$$(13) \quad K_{e 3}^+ \rightarrow \pi^0 + e^+ + \nu.$$

The processes except the decay of heavy mesons have been analyzed on the hypothesis that the elementary interactions are strong interactions (π -N) and that weak universal Fermi interaction occurs not only among nucleon and lepton, but also among leptons themselves, and that reasonable results have been obtained. As for the process (12), the accumulated experimental facts indicate that one of the two neutral decay-products is π^0 . This process

⁽⁹⁾ See, for example, A. M. SHAPIRO: *Rev. Mod. Phys.*, **28**, 164 (1956).

might be taken as an alternative mode of decay of the same K particle decaying according to the reaction $K_{\pi 2}^{\pm} \rightarrow \pi^{\pm} + \pi^0$, that is the K-meson decays virtually into $\pi^+ + \pi^0$ and then the charged pion decays into a $\mu + \nu$ pair. Even if this turned out to be acceptable for the $K_{\mu 3}$, a similar explanation can not be applied to the $K_{e 3}$ because the decay of a pion into an electron is highly forbidden so that the $K_{e 3}$ -decay should be much less probable than $K_{\mu 3}$, while experimentally $K_{e 3}$ are found as often as $K_{\mu 3}$. Therefore we will assume that bosons interact through virtual fermion pairs and that universal weak Fermi interactions exist not only between nucleons and leptons, but also between hyperons and leptons. Accordingly $K_{\mu 3}$ - and $K_{e 3}$ -decays occur through the baryon family loop shown as follows ⁽¹⁰⁾:



where G is the strong coupling constant ($1 \sim 10^{-1}$) and f is the weak coupling constant ($\sim 10^{-14}$). We get in this way for the transition probabilities ⁽¹¹⁾,

$$(14) \quad \left\{ \begin{array}{l} \omega_{K_{\mu 3}} = \frac{0.044}{128\pi^5} \cdot \frac{1}{\hbar} \left(\frac{G}{4\pi\hbar c} \right)^2 \frac{f M^4 c^2}{\hbar^6} \cdot \frac{(\mu_{\pi} c^2)^4}{M^2 c^4 \mu_{\pi} c^2} \int_0^{\eta_{\max}} \left[\frac{1}{4} \eta^4 - \left(\frac{Q}{p_{\pi} c^2} + \frac{1}{3} \right) \eta^2 + \frac{Q^2}{\mu_{\pi}^2 c^4} \right] d\eta, \\ \eta = \frac{p_{\pi}}{\mu_{\pi} c}, \end{array} \right.$$

where Q is the Q -value of the K reaction and M is the mass of the baryon and their ratios to the decay probability of the $K_{\pi 2}$ are given by

$$(15) \quad \left\{ \begin{array}{l} \frac{\omega_{K_{\pi 2}}}{\omega_{K_{\mu 3}}} = \frac{1}{\pi} \cdot \frac{G^2}{4\pi\hbar c} \cdot \frac{p_{\pi}^2 c^2}{\omega_{\pi}^2} \cdot \frac{c}{v_1 + v_2} \cdot \left(\frac{M}{\mu_{\pi}} \right)^4 \left\{ \int_0^{\eta_{\max}} \left[\frac{1}{4} \eta^4 - \left(\frac{Q}{\mu_{\pi} c^2} + \frac{1}{3} \right) \eta^2 + \frac{Q^2}{\mu_{\pi}^2 c^4} \right] d\eta \right\}^{-1}, \\ \frac{\omega_{K_{\pi 2}}}{\omega_{K_{\mu 3}}} = 2.7, \quad \frac{\omega_{K_{\pi 2}}}{\omega_{K_{e 3}}} = 1.05, \end{array} \right.$$

where v_1 and v_2 are the velocities of the two final pions of $K_{\pi 2}$ respectively. These results are in good agreement with the experimental data. A similar consideration can be also applied to $K_{\mu 2}$ -decay. Although the perturbation calculation may not be adequate for the strong interaction, these consideration

⁽¹⁰⁾ S. FURUICHI, T. KODAMA, S. OGAWA, Y. SUGAHARA, A. WAKASA and M. YONEZAWA: *Prog. Theor. Phys.*, **17**, 89 (1957).

⁽¹¹⁾ G. COSTA and N. DALLAPORTA: *Nuovo Cimento*, **2**, 519 (1955).

might be sufficient to give an indirect test concerning the elementarity of the weak Fermi interaction.

If we assume the generalized weak Fermi interaction as the elementary one, the η_1 -charge selection rule of our model allows the following lepton processes besides the transition processes (7)–(13). Here the processes are restricted to two or three body decays ⁽¹²⁾.

1) The transition processes due to the generalized weak Fermi interaction:

$$(16) \quad \left\{ \begin{array}{l} \Lambda^0 \rightarrow p + e^- + \tilde{\nu}, \\ \Lambda^0 \rightarrow p + \mu^- + \nu, \\ \dots \end{array} \right.$$

and the charge conjugate of these processes. The analysis of these processes has been done basing on the generalized weak Fermi interaction by IWATA *et al.* ⁽¹³⁾, and they obtained the life times for the above processes

$$(17) \quad \tau(\Lambda^0 \rightarrow p + e^- + \tilde{\nu}) \sim (10^{-8} \div 10^{-10}) \text{ s},$$

showing the detection of them as possible in future. And their detection will give a clue for the investigation of the interaction structure.

2) The transition processes occurring through the combination of the strong and the generalized weak Fermi interaction:

$$(18) \quad \left\{ \begin{array}{l} K^0 \rightarrow \pi^- + e^+ + \nu, \\ K^0 \rightarrow \pi^- + \mu^+ + \tilde{\nu}, \\ \dots \end{array} \right.$$

Though these are not yet firmly established, they are expected to be observed with frequency comparable to the $K_{e3} \rightarrow \pi^0 + e + \nu$ and $K_{\mu 3} \rightarrow \pi^0 + \mu + \nu$ because they can be considered as the neutral counter particle of the K.

3) The transition processes through a combination of the strong and the

⁽¹²⁾ This restriction would be reasonable because the matrix elements of the other transition processes, containing the weak elementary interactions twice or more and having small phase volume, should be much smaller than the usual observed weak processes.

⁽¹³⁾ K. IWATA, S. OGAWA, H. OKONOGI, B. SAKITA and S. ONEDA: *Prog. Theor. Phys.*, **13**, 19 (1955).

generalized weak Fermi interaction: such as ⁽¹⁴⁾

$$(19) \quad \left\{ \begin{array}{l} \pi \rightarrow e + \nu \\ K \rightarrow e + \nu \end{array} \right. \quad (15).$$

These are not yet established too and they seem to be highly forbidden. So far as we take the strong and the generalized weak Fermi interactions as the elementary ones, it may be difficult to forbid these processes by means of the selection rules only. Perhaps it may require the consideration of the dynamical structure of mutual interactions. The investigation along this line has been done by several authors ⁽¹⁶⁾ taking as the effective hamiltonian due to the strong and weak Fermi interaction

$$(20) \quad M'(\bar{\psi}_{(\mu \text{ or } e)} \gamma'_5 \gamma_\lambda \psi_\nu) \delta_\lambda \varphi_\pi + \text{c. c.},$$

where M' , the contribution from various intermediate states, is a function of momenta and masses of the intermediate particles and γ'_5 is γ_5 or I . They showed the ratio of the π -e-decay probability to that of π - μ -decay

$$R = \omega(\pi \rightarrow e + \nu) / \omega(\pi \rightarrow \mu + \nu) \sim 10^{-4},$$

which is consistent with the experimental results. Such a consideration may be applied to $K \rightarrow e + \nu$.

5. - Forbidden lepton processes.

In this section we shall discuss the lepton processes which are forbidden in our model, but allowed by the other conservation laws, which is one of the most interesting but delicate problems for lepton processes. Though this problem has been investigated by several authors, satisfactory results have not yet been obtained. The main lepton processes which should be forbidden by the experimental indication are as follows (limited to two- and three-body decays):

⁽¹⁴⁾ To forbid these processes, SHIMAZU tried to assign the lepton number to the Bose particles (π , K). H. SHIMAZU: *Soryushiron-Kenkyu* (Mimeographed circular in Japanese), **13**, 194 (1956).

⁽¹⁵⁾ Though this mode has been inferred by CRUSSARD, it has not definite evidence. J. CRUSSARD: *Proc. 6th Rochester Conf.*, V-19.

⁽¹⁶⁾ See, for example, S. ONEDA and A. WAKASA: *Nucl. Phys.*, **1**, 445 (1956).

1) three-body decay of heavy meson

$$(21) \quad \left\{ \begin{array}{l} K^+ \rightarrow \pi^- + e^+ + \mu^+ \\ K^+ \rightarrow \pi^+ + e^+ + e^- \\ K^+ \rightarrow \pi^+ + \mu^+ + \mu^- \\ K^+ \rightarrow \pi^+ + \nu + \bar{\nu} \\ \dots \end{array} \right.$$

$$(22) \quad \left\{ \begin{array}{l} K^+ \rightarrow \pi^+ + \mu^+ + e^- \\ K^+ \rightarrow \pi^+ + \mu^- + e^+ \\ \dots \end{array} \right.$$

2) three-body decay of baryon

$$(23) \quad \left\{ \begin{array}{l} \Lambda_0 \rightarrow N + \nu + \bar{\nu} \\ \Sigma^0 \rightarrow N + \nu + \bar{\nu} \\ \Sigma^0 \rightarrow \Lambda^0 + \nu + \bar{\nu} \\ \dots \end{array} \right.$$

3) two-body decay

$$(24) \quad \left\{ \begin{array}{l} K^0 \rightarrow \mu^+ + \mu^- \\ K^0 \rightarrow e^+ + e^- \\ \dots \end{array} \right.$$

Among these processes, Konopinski-Mahmoud, by the conservation of the lepton number, could prohibit (22) and $\mu \rightarrow e + e^+ + e^-$, but not (21), (23) and (24).

For the reaction $\Lambda^0 \rightarrow N + \nu + \bar{\nu}$, we get the life-time

$$(25) \quad \tau(\Lambda^0 \rightarrow N + \nu + \bar{\nu}) \sim 10^{-8} \text{ s}$$

and its ratio to the main decay mode of Λ^0 , $\Lambda^0 \rightarrow p + \pi^-$ is

$$(26) \quad \frac{\omega(\Lambda^0 \rightarrow N + \nu + \bar{\nu})}{\omega(\Lambda^0 \rightarrow p + \pi^-)} \sim 10^{-2}$$

so the processes (23) can be rejected by dynamical considerations, though they are allowed by conservation laws.

On the other hand, for the reaction $K^+ \rightarrow \pi^+ + \nu + \tilde{\nu}$, we get the following life-time

$$(27) \quad \tau(K \rightarrow \pi + \nu + \tilde{\nu}) \sim 10^{-8} \text{ s},$$

which is comparable with $\tau(K_{\mu 3} \rightarrow \pi^0 + \mu + \nu)$ and $\tau(K_{e 3} \rightarrow \pi^0 + e + \nu)$. And its ratio to the decay probability of $K_{\pi 2}$, the main decay mode of the K -particle is,

$$(28) \quad \frac{\omega(K \rightarrow \pi + \nu + \tilde{\nu})}{\omega(K \rightarrow \pi^0 + \pi)} \sim 1.$$

Thus, as for the processes (21), we cannot reject them dynamically, too. With our model, all these processes, (21), (23) and (24), can be ruled out by the η_i -charge conservation rule.

6. - Concluding remarks.

In this paper we have discussed mainly the lepton processes based on the hypothesis that the Fermi interaction is an elementary weak one, and « universality » exists among the interactions concerned with the fundamental particles. We have clarified how K-M's attempt to prohibit the unwanted processes concerning leptons fails to explain the fact that processes such as $K \rightarrow \pi + \nu + \tilde{\nu}$ are not observed in nature. By introducing a new quantum number η_i for leptons, minimizing reasonable assumptions we have tried to forbid the unwanted processes and succeeded in prohibiting all the unwanted processes including those which were impossible to be forbidden by the K-M model.

But there remain some defects in our model, that is; the reaction $\pi \rightarrow e + \nu$ which is indicated experimentally to be highly forbidden could not be excluded by our selection rules, and we were also forced to put some unnatural assumption for the η_i -selection rule to get good coincidence with experimental facts.

Nevertheless, as is noted in the introduction, whatever standpoint we may take, it is necessary to keep in mind that the weak interactions have the coupling constant of the same order of magnitude ($\sim 10^{-14}$) for both hyperon and lepton. So it may be still worthwhile to seek some scheme to explain all the processes concerned with fundamental particles on the same footing, though our model has some defects.

As for these defects, they may be due to the peculiar dynamical structure of interaction of leptons, or they may depend on the form of the interaction taken as elementary one. So it seems to be important to enter into the details of dynamical structure of the interaction.

* * *

The author would like to thank Prof. K. SAKUMA, Drs. S. OGAWA, T. OUCHI and M. YONEZAWA for helpful discussions.

Notes added in proof.

1. — A similar analysis in which a Konopinski-Uhlenbeck type of weak interaction is assumed instead of the Fermi interaction taken in this paper has been performed by Y. MIYACHI (*Progr. Theor. Phys.*, in press).

2. — Recently J. J. SAKURAI and J. WERLE independently have proposed a possible way to check directly the validity of time reversal invariance in the $K_{\mu 3}^+$ decay process. It can be done by measuring the muon polarization perpendicular to the decay plane. If the polarization along this direction is observed the condition (A.5) is violated in this process. It is noted that the conditions for the coupling constants used by J. WERLE (*Nucl. Phys.*, 4, 171 (1957)) are not correct. The correct one is (A.5). The author would like to thank Dr. J. J. SAKURAI and Dr. J. WERLE for sending him preprints.

RIASSUNTO (*)

Si sviluppa un modello di prova, modificazione del modello di Konopinski-Mahmoud riguardante i leptoni, per la classificazione dei processi cui partecipano leptoni. Per mezzo di questo modello si ottiene una buona regola di selezione, senza dover introdurre la particella neutra sovrabbondante che sempre appare nei modelli basati sulla ipotesi dell'indipendenza della carica applicata ai leptoni. Si fa in breve riferimento alla relazione tra il modello N-G e il nostro schema e si discute al lume di tale schema la struttura dell'interazione. E per quanto si ottenga una buona regola di selezione per processi leptonici, si conclude che per una classificazione dei leptoni si deve sempre tener conto della loro struttura di interazione.

(*) Traduzione a cura della Redazione

On the Threshold Behavior of the Negative to Positive Ratio in Pion Photoproduction.

M. J. MORAVCSIK (*)

Brookhaven National Laboratory - Upton, N.Y.

(ricevuto il 31 Maggio 1957)

Summary. — It is shown that the extrapolation used by BENEVENTANO *et al.* to obtain the negative to positive ratio at threshold is very sensitive to small alterations which can be made due to the approximate nature of the procedure. Such small alterations bring about very substantial changes in the energy dependence of the ratio near threshold and hence the extrapolation is quite ambiguous in the absence of extensive experimental data on the ratio in this energy region. Since such extensive set of data does not exist at the present time, it is concluded that there is no good reason to believe that the ratio at threshold is in disagreement with the theoretical predictions.

1. — Introduction.

The value of the negative to positive ratio in pion photoproduction and its relationship to other experimental quantities has been somewhat of a puzzle for some time. This quantity is an important clue to the *S* wave part of the pion-nucleon interaction, which is considerably less well known than the *P* wave part. In fact, a consistent scheme which includes the interpretation of the threshold ratio in photoproduction, the *S* wave scattering phase shifts, the Panofsky ratio, and perhaps even other quantities, has been the aim of numerous investigators during the past few years.

(*) Work carried out under the auspices of the U.S. Atomic Energy Commission.

One of the important papers in this field has been that of BENEVENTANO *et al.* ⁽¹⁾. This paper, besides presenting some new experimental data, attempted an over-all analysis of photoproduction data in the energy region between threshold and about 240 MeV photon energy in the laboratory system. In particular, it derived a semi-empirical equation (reference ⁽¹⁾ Eq. (21)) for the energy dependence of the ratio near threshold and used the coefficients of the angular distribution of positive photopions in conjunction with four pieces of data on the ratio itself to extrapolate and determine the ratio at threshold. The resulting ratio turned out to be 1.85 or even higher. It was remarked that this value strongly disagrees with the value predicted by the threshold theorems and the dispersion approach, which claim that the result of the perturbation theory (about 1.4) should be correct. Similarly, the pion-nucleon coupling constant obtained by the usual extrapolating procedure also turns out peculiarly low when we utilize this high value of the ratio. The value of the coupling constant has been determined with great apparent reliability by several procedures, all agreeing very well, while the coupling constant obtained from this high threshold ratio is more than 20% lower than the commonly accepted value. On the other hand, it was also remarked that the high ratio can be correlated more easily with the latest value of the difference in the slopes of the two *S* wave scattering phase shifts and with the latest value of the Panofsky ratio. The implication of BBCST is that the real discrepancy is between the theoretical prediction of the ratio and the «experimental» value of the ratio as obtained by BBCST, and that this «experimental» value is in reasonable agreement with other clues to the *S* wave pion-nucleon interaction.

The purpose of this paper is *not* to solve this discrepancy and to give a unified scheme for the *S* wave interaction. Instead, the aim is to show that if one alters slightly the approximations used by BBCST one can obtain a quite different and considerably lower result for the threshold ratio. It is not claimed that the new ratio is *a priori* a more reliable value than the old one. It is claimed however, that our modification of the BBCST analysis is equally in agreement with the general principles used and with the experimental data which go into the numerical evaluation.

The important criterion for the choice of the extrapolating formula is of course the experimental material on the ratio itself. BBCST used four pieces of data at 90° (see reference ⁽¹⁾, Fig. 5). It has been pointed out ⁽²⁾ that apart from the quantitative inadequacy of these data they also fall at higher energies below, and at lower energies above, the value one obtains when inter-

⁽¹⁾ M. BENEVENTANO, G. BERNARDINI, D. CARLSON-LEE, G. STOPPINI and L. TAU: *Nuovo Cimento*, **4**, 323 (1956). This paper will be referred to as BBCST.

⁽²⁾ M. J. MORAVCSIK: *Phys. Rev.*, **105**, 267 (1957).

polating the measured values of the ratio at angles other than 90° . In other words, the data used by BBCST give a steeper energy dependence of the ratio at 90° than one would deduce from using *all* data on the ratio. This contention is supported by the new preliminary data of DUDZIAK ⁽³⁾ on the energy dependence of the ratio near threshold. These data, which are considerably more extensive than those used by BBCST, fit much better into the angular distribution curves of the ratio ⁽²⁾ which have been measured previously. The new data seem to give a considerably gentler energy dependence and if extrapolated «by eye» to threshold they give a considerably lower ratio, a value around 1.6. The purpose of this paper is to show that such a low threshold value and gentle energy dependence (if confirmed by the final version of Dudziak's data) is by no means incompatible with a semiempirical analysis which is of the same general type and of equal reliability as the one worked out by BBCST.

Such a lower ratio, if yielded by the experiments and supported by a semi-phenomenological scheme, might easily be in agreement with the theoretical prediction of 1.4. The difference, now only about 10%, could perhaps be explained by the deuterium correction which is yet to be given a really reliable treatment, but which could certainly amount to that much.

Of course, on the other end we made things even worse, and the disagreement with the Panofsky ratio and the *S* wave scattering phase shifts now replaces the disagreement we just eliminated. It should be noted, however, that the experimental values of the Panofsky ratio and of the *S* wave phase shifts are still subject to large changes, and that the connection between these quantities and the threshold ratio might also be subject to modifications ⁽⁴⁾ Thus, without offering an over-all solution of the general problem of the *S* wave interaction, we will restrict ourselves to pointing out a way to a consistent picture of the special problem of the threshold value of the negative to positive ratio in photoproduction.

2. - The analysis of Beneventano *et al.*

Let us first review the assumptions and the derivation of the BBCST analysis. The relevant formula giving the energy dependence of the ratio near threshold is Eq. (21) of reference ⁽¹⁾. We will follow the notation used in that paper. The derivation which leads to the above equation can be sum-

⁽³⁾ W. F. DUDZIAK: private communication. I am greatly indebted to Dr. DUDZIAK for sending me his preliminary data which aroused my interest in this problem.

⁽⁴⁾ See e.g. H. P. NOYES: *Phys. Rev.*, **101**, 320 (1956).

marized as follows:

$$(2.1) \quad \frac{\sigma^-}{\sigma^+} = \frac{a_0^- + a_1^- \cos \theta + a_2^- \cos^2 \theta}{a_0^+ + a_1^+ \cos \theta + a_2^+ \cos^2 \theta},$$

$$(2.2) \quad \frac{a_0^-}{a_0^+} \equiv r = \text{ratio at } 90^\circ,$$

$$(2.3) \quad \begin{cases} a_0^\pm = (S \mp R)^2 + a_{\text{op}} \\ a_1^\pm = -2(S \mp R)K, \\ a_2 = K^2 - a_{\text{op}} \approx -a_{\text{op}}, \end{cases}$$

$$(2.4) \quad r = \frac{ra_0}{a_0} = \frac{(S+R)^2 - a_2}{(S-R)^2 - a_2},$$

where $a_0 \equiv a_0^+$

$$(2.5) \quad \begin{cases} 2S = (ra_0 + a_2)^{\frac{1}{2}} + (a_0 + a_2)^{\frac{1}{2}}, \\ 2R = (ra_0 + a_2)^{\frac{1}{2}} - (a_0 + a_2)^{\frac{1}{2}}, \end{cases}$$

$$(2.6) \quad S(\nu, \omega) = \frac{g_{\text{os}}}{\sqrt{\nu\omega}} + \varrho \approx \frac{g_{\text{os}}}{\sqrt{\nu\omega}},$$

$$(2.7) \quad S(\nu_0, 1) = \frac{1}{2}\sqrt{a_0}(\sqrt{r_0} + 1),$$

where r_0 is the threshold value of the ratio and ν_0 is the photon energy at threshold.

$$(2.8) \quad (ra_0 + a_2)^{\frac{1}{2}} + (a_0 + a_2)^{\frac{1}{2}} = \left(\frac{a_0\nu_0}{\nu\omega}\right)^{\frac{1}{2}}(\sqrt{r_0} + 1),$$

$$(2.9) \quad r = \left(\frac{\nu_0}{\nu\omega}\right)(1 + \sqrt{r_0})^2 - 2\left(\frac{\nu_0}{\nu\omega}\right)^{\frac{1}{2}}(1 + \sqrt{r_0})\left(1 + \frac{a_2}{a_0}\right) + 1,$$

which is identical with Eq. (21) of BBCST.

Next let us list all the assumptions which enter the above derivation. Eq. (2.1) implies that the angular distribution for photoproduction can be represented to a good approximation by a quadratic expression in $\cos \theta$. We know ⁽⁵⁾ that this might not be so, depending on what feature of the angular

⁽⁵⁾ M. J. MORAVCSIK: *Phys. Rev.*, **104**, 1451 (1956).

distribution we are interested in. For instance, BBCST state that a_0^+ (which gives the cross-section at 90°) is constant in the energy region we are considering, namely, from threshold to 260 MeV photon energy in the laboratory system. The more accurate quartic analysis ⁽⁶⁾ gives a 10% change in the same energy range. Since our analysis as well as that of BBCST utilizes only the ratio a_2/a_0 , which is small in any case, the assumption of Eq. (2.1) will probably not cause any drastic errors. Nevertheless this is one possible source of small corrections which, as we will see, have a very substantial influence on the conclusions.

Eq. (2.2) is the definition of r which, granting Eq. (2.1), is precisely the ratio at 90° .

Eq. (2.3) is based on several assumptions beside the one underlying (2.1).

a) It is assumed that the quantities on the right hand side are real. In view of the fact that at 240 MeV the $P_{\frac{3}{2}}$ phase shift is around 15° , this assumption might easily introduce an error up to 5% in the P wave parameters on the right hand side.

b) It is assumed that the so-called «spin flip» amplitude is negligible compared to the «no-spin-flip» amplitude. Using Table V and Eq. (A-5) of BBCST we can see that this assumption might introduce another error up to 8% in the magnitude of a_2 .

c) It is assumed that the S - D interference term can be neglected. Actually BBCST considered the S - D interference but, since they found that it could not resolve entirely what they considered was a discrepancy between theory and experiment, they omitted it in their subsequent analysis. The inclusion of such term might again contribute a change of about 10%.

d) It is assumed that a_2 is the same for positive and negative pion, or in other words, that the P wave negative to positive ratio (a not too well defined quantity) is unity. This is clearly not so, as we know ⁽²⁾ from the behavior of the ratio at higher energies. The effect of the P wave ratio at lower energies is something which is not too easy to estimate, but another 10% is not an unreasonable guess.

We see, therefore, that Eq. (2.3) is contingent on several assumptions which hold only approximately. We will consider below what happens to Eq. (2.9) if we use slightly different values for the parameters, values which are equally possible within the approximations we made.

Eq. (2.4) follows from the previous equations without further assumptions, and so does Eq. (2.5).

⁽⁶⁾ M. J. MORAVCSIK: *Phys. Rev.* **107**, 600 (1957).

Eq. (2.6) is discussed in detail by BBCST and so we will not repeat the arguments which lead to this form of S . It is important to notice, however, that BBCST use the approximation in which ϱ is neglected. It is pointed out by BBCST that the leading term in the expansion of ϱ into powers of ω is of the order of $(\mu/M)^2$. We will consider below how the inclusion of such a term affects the energy dependence of Eq. (2.9).

Eq. (2.7) follows from Eq. (2.5) without further assumptions, and Eq. (2.8) and (2.9) follow from the previous ones without further assumptions.

Summarizing, we see that all assumptions are introduced in Eqs. (2.1), (2.3) and (2.8).

Before we proceed to illustrate the effect of these approximations on Eq. (2.9) let us rewrite this equation so that all dependence on ν and ω is explicit. In doing so we will introduce the following notation

$$(2.10) \quad (\nu\omega)^{-\frac{1}{2}} \equiv y$$

$$(2.11) \quad 1 + \sqrt{r_0} \equiv \Phi,$$

and we know from kinematics that $\nu_0 = 0.944$. Using these we can write

$$(2.1) \quad r = 0.944\Phi^2 y^2 - 1.944\Phi y(1 + a_2/a_0)^{\frac{1}{2}} + 1.$$

Now let us write out the y dependence of a_2 . BBCST give the following empirical and approximate expression for it

$$(2.13) \quad a_2/a_0 = (-0.62 \pm 0.10)\eta^2/\nu^2.$$

One can easily convince oneself that it is a good kinematical approximation to write

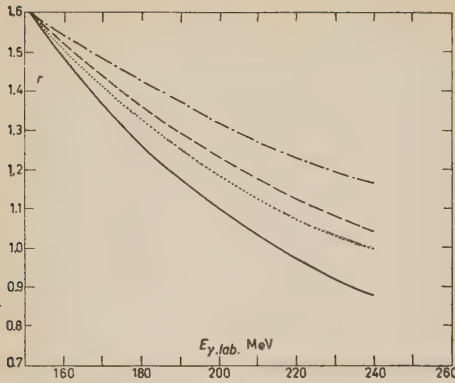
$$(2.14) \quad \eta^2/\nu^2 = 1 - 0.944y^2.$$

To approximate $(1 + a_2/a_0)^{\frac{1}{2}}$ we can use the expression

$$(2.15) \quad [1 - 0.62(1 - 0.944y^2)]^{\frac{1}{2}} \approx 0.65 + 0.33y^2.$$

Both of these kinematical approximations are accurate to 2% or so. In addition, our conclusions do not depend at all on these approximations which are given only to present Eq. (2.9) in a more transparent form. This form is

$$(2.16) \quad r = -0.642\Phi y^3 + 0.944\Phi^2 y^2 - 1.264\Phi y + 1.$$



This type of formula was used by BBCST to obtain the curve in their Fig. 5. In our Fig. 1 we show Eq. (2.16) for $r_0 = 1.60$. It is marked by the solid line.

Fig. 1. — The energy dependence of the negative to positive ratio r near threshold. All four curves are plotted using $r_0 = 1.60$. The solid curve is the form given in reference (1). The dotted line

includes the correction of a_2 , the dashed line includes the correction of ρ , while the dash-dot line includes both corrections. For quantitative details see the text.

3. — Possible modifications of the analysis.

We will consider two ways of modifying Eq. (2.16). These two ways by no means exhaust the possibilities, but since our aim is mostly illustrative these two examples which, we believe, are particularly realistic, will suffice to prove the point we want to make.

A) The first method is to make an allowance for the approximations made in connection with Eq. (2.3). As a consequence of these approximations, the first formula in Eq. (23.) is not necessarily

$$(3.1) \quad a_0^\pm = (S \mp R)^2 - a_2,$$

but rather

$$(3.2) \quad a_0^\pm = (S \mp R)^2 - a_2'^\pm,$$

where the $a_2'^\pm$ is made up of a_2 , K , a_{sd} , and of the effect of the P ratio. In fact, for the sake of simplicity, we will consider the example when

$$(3.3) \quad a_2'^+ = a_2'^- \equiv a_2'.$$

We will also assume that the energy dependence of a_2' is the same as that of a_2 , which is quite plausible anyway. In this case the only change we have to make is in Eq. (2.15). Let us assume, for instance, that Eq. (2.15) changes to

$$(3.4) \quad 0.550 + 0.425y^2,$$

which means that we change the value of a_2 by about 25% — quite a conservative assumption in view of our estimates of the approximations involved and in view of the experimental error on a_2 itself, which is more than 15%. In this case we have

$$(3.5) \quad r = -0.826 \Phi y^3 + 0.944 \Phi^2 y^2 - 1.069 \Phi y + 1.$$

This formula is also shown in our Fig. 1 for the case of $r_0 = 1.60$. It is marked by the dotted line.

B) The second way of modifying our formula for r consists of the inclusion of an appropriately small ϱ in Eq. (2.6). In particular, the ϱ we include will be, in accordance with BBCST's Eq. (16), of the form

$$(3.6) \quad \varrho = \varrho_1 \left(\frac{\mu}{M} \right)^2 \omega \approx \frac{\lambda}{y},$$

where $\lambda = \varrho_1 (\mu/M)^2$, that is, of the order of $(2 \div 5)\%$.

The derivation of the expression for r must be modified somewhat in this case. Eqs. (2.1)–(2.5) hold unchanged, and so does Eq. (2.7). On the other hand, Eq. (2.8) reads now

$$(3.7) \quad (ra_0 + a_2)^{\frac{1}{2}} + (a_0 + a_2)^{\frac{1}{2}} - \frac{2\lambda}{y} = \left(\frac{a_0 v_0}{v\omega} \right)^{\frac{1}{2}} \left[(1 + \sqrt{r_0}) - \frac{2\lambda}{\sqrt{a_0 y_0}} \right],$$

which leads to

$$(3.8) \quad \left(\frac{v_0}{v\omega} \right)^{\frac{1}{2}} \left[\sqrt{r_0} + 1 - \frac{2\lambda}{\sqrt{a_0 y_0}} \right] + \frac{2\lambda}{\sqrt{a_0 y}} - \left(1 + \frac{a_2}{a_0} \right)^{\frac{1}{2}} = \left(r + \frac{a_2}{a_0} \right)^{\frac{1}{2}},$$

and finally we get

$$(3.9) \quad r = \left[0.972 \Phi y - \frac{2\lambda}{\sqrt{a_0}} \left(0.944 y - \frac{1}{y} \right) \right]^2 - 2 \left[0.972 \Phi y - \frac{2\lambda}{\sqrt{a_0}} \left(0.944 y - \frac{1}{y} \right) \right] \left(1 + \frac{a_2}{a_0} \right)^{\frac{1}{2}} + 1,$$

where in the last three equations the threshold value of y was denoted by y_0 . Using for $(1 + a_2/a_0)^{\frac{1}{2}}$ the *unmodified* form, that is, Eq. (2.15), we obtain the effect of the inclusion of ϱ alone. This is shown in Fig. 1 by the dashed line. The values of the parameters are $r_0 = 1.60$ and $\lambda/\sqrt{a_0} = 0.05$. The combined effect of the two independent corrections we have considered is shown in Fig. 1 by the dash-dot line.

4. - Conclusions.

As we see from Fig. 1, the small and quite conservative corrections we made bring about a very substantial changes in the ratio. The reason for this sensitivity to small changes lies simply in the analytic form of the expression for r . The value of the function is the algebraic sum of several terms most of which are several times larger than the final result.

It is also evident, however, from the above discussion that good experimental data will be able to determine the slope of the energy dependence and thereby tell not only the threshold value of the ratio but also the value and sign of the corrections which we discussed above. In the meantime, however, while we lack such data, there is no reason to believe that the threshold value of the ratio is very large and that it is in disagreement with theoretical predictions, even if indirect and uncertain indications from the Panofsky ratio and the S wave scattering phase shifts seem to point in that direction.

RIASSUNTO (*)

Si dimostra che l'estrapolazione usata da BENEVENTANO *et al.* per ottenere il rapporto negativo a positivo alla soglia è molto sensibile a piccole modificazioni rese possibili dalla approssimazione adottata nel procedimento. Tali piccole modificazioni portano con sé variazioni sostanziali nella dipendenza dall'energia del rapporto vicino alla soglia e pertanto l'estrapolazione risulta ambigua in assenza di estesi dati sperimentali sul rapporto in questo intervallo di energia. Poichè queste estese serie di dati per il momento non esistono, si conclude che non esistono buone ragioni di ritenere che il rapporto alla soglia sia in disaccordo con le predizioni teoriche.

(*) Traduzione a cura della Redazione.

The Diffusion Coefficient of Thermal Neutrons.

I. KUŠČER

Institute of Physics, University of Ljubljana

M. RIBARIČ

J. Stefan Institute - Ljubljana, Yugoslavia

(ricevuto il 12 Giugno 1957)

Summary. — Diffusion of slow neutrons in an extended uniform medium is treated by a method which accounts for the thermal motion of the medium. If neutron capture is absent, a single integral equation has to be solved, in order to determine the velocity distribution and the diffusion coefficient. A system of such equations is obtained for a capturing medium. For the case of a non-capturing monoatomic gaseous medium several approximations are discussed, which express the diffusion coefficient as a function of the atomic weight.

1. — Introduction.

Calculations of neutron diffusion coefficients are usually based upon investigations of stationary neutron distributions in media which are macroscopically isotropic and uniform, and free of neutron sources. For such cases Boltzmann's transport equation ^(1,2), in the notation of DAVISON ⁽¹⁾, reads as follows

$$\begin{aligned} (1) \quad v\boldsymbol{\Omega} \cdot \text{grad } N(\mathbf{r}, v\boldsymbol{\Omega}) + v[l_s^{-1}(v) + l_c^{-1}(v)]N(\mathbf{r}, v\boldsymbol{\Omega}) = \\ = \iint \int v' l_s^{-1}(v') N(\mathbf{r}, v'\boldsymbol{\Omega}') f(v'\boldsymbol{\Omega}' \rightarrow v\boldsymbol{\Omega}) dv' d\boldsymbol{\Omega}' . \end{aligned}$$

⁽¹⁾ B. DAVISON: *Neutron Transport Theory* (Oxford, 1957).

⁽²⁾ J. H. TAIT: *Rep. Prog. Phys.*, **19**, 268 (1956).

Herein $l_s(v)$ and $l_c(v)$ denote the scattering and the capture mean free paths for neutrons having the velocity v . The neutron distribution function N depends upon the position vector \mathbf{r} and the velocity vector $v\mathbf{\Omega}$, with $\mathbf{\Omega}$ being the respective unit vector. $d\Omega'$ represents the element of solid angle, pertaining to the velocity vector $v'\mathbf{\Omega}'$ before scattering.

The scattering function f , which is normalized to unity,

$$\iiint f(v'\mathbf{\Omega}' \rightarrow v\mathbf{\Omega}) dv d\Omega = 1,$$

depends upon v , v' and $\mathbf{\Omega} \cdot \mathbf{\Omega}'$ (the cosine of the scattering angle), and may be expressed by the Legendre series

$$(2) \quad f(v'\mathbf{\Omega}' \rightarrow v\mathbf{\Omega}) = \frac{1}{4\pi} \sum_{l=0}^{\infty} (2l+1) f_l(v' \rightarrow v) P_l(\mathbf{\Omega} \cdot \mathbf{\Omega}').$$

The first two coefficients (f_0 and f_1) are of special interest. f_0 is used in the theory of the slowing down of neutrons if only their energy distribution has to be determined (^{3,6a}), whereas f_1 is of importance for the determination of the diffusion coefficient.

If the neutrons are fast, the atoms can be assumed to be free and at rest before encounter. In this case, and if scattering is elastic, f involves a δ function (^{1,2}). With slow neutrons, however, the thermal motion of the atoms must be taken into account, whereby the function f is more or less smeared out (^{5,7}).

The mean cosine of the scattering angle and the transport mean free path for neutrons of the initial velocity v' are

$$(3) \quad b(v') = \iiint f(v'\mathbf{\Omega}' \rightarrow v\mathbf{\Omega}) \mathbf{\Omega} \cdot \mathbf{\Omega}' dv d\Omega = \int_0^{\infty} f_1(v' \rightarrow v) dv,$$

$$(4) \quad l_{tr}(v') = l_s(v')/[1 - b(v')].$$

For an infinite non-capturing medium the Maxwellian distribution, i.e. $N \propto v^2 \exp[-\beta^2 v^2]$, with $\beta = \sqrt{m/2kT}$, represents a solution of Eq. (1). The

(³) G. PLACZEK: *Phys. Rev.*, **69**, 423 (1946).

(⁴) E. P. WIGNER and J. E. WILKINS, JR.: *U.S. AEC Document* 2275 (1948).

(⁵) C. C. GROSJEAN: *Mededelingen Nat. Lab. Univ. Gent* (1955).

(⁶) E. R. COHEN: *Proc. Int. Conf. on the Peaceful Uses of Atomic Energy* (Geneva, 1955), Vol. 5, p. 405.

(^{6a}) H. HURWITZ, JR., M. S. NELKIN, and G. J. HABETLER: *Nuclear Sci. and Engr.*, **1**, 280 (1956).

(⁷) G. JAFFÉ: *Phys. Rev.*, **88**, 603 (1952), equation (56).

principle of detailed balance then asserts that (4)

$$(5) \quad l_s^{-1}(v')f(v'\Omega' \rightarrow v\Omega)v'^3 \exp[-\beta^2 v'^2] = \\ = l_s^{-1}(v)f(v\Omega \rightarrow v'\Omega')v^3 \exp[-\beta^2 v^2],$$

with relations of the same form holding for $f_i(v' \rightarrow v)$.

Multiplying both sides of Eq. (1) by $dv d\Omega$ and integrating we obtain the equation of continuity

$$(6) \quad \text{div } \mathbf{j} = -\tau^{-1}(\mathbf{r})n(\mathbf{r}).$$

n , \mathbf{j} and τ denote the neutron density, the neutron current, and the mean life time of the neutrons, respectively, i.e.

$$(7) \quad n(\mathbf{r}) = \iiint N(\mathbf{r}, v\Omega) dv d\Omega,$$

$$(8) \quad \mathbf{j}(\mathbf{r}) = \iiint v\Omega N(\mathbf{r}, v\Omega) dv d\Omega,$$

$$(9) \quad \tau^{-1}(\mathbf{r}) = n^{-1}(\mathbf{r}) \iiint v l_c^{-1}(v) N(\mathbf{r}, v\Omega) dv d\Omega.$$

In general τ depends upon the velocity distribution, and therefore may vary from place to place, as indicated. For a Maxwellian neutron distribution Eq. (9) leads to the particular value

$$(10) \quad \tau_0 = \langle l_c \rangle / \bar{v},$$

where \bar{v} is the average neutron velocity ($\bar{v} = \sqrt{8kT/\pi m}$), and $\langle l_c \rangle$ the average capture mean free path. The latter average is defined in analogy with Maxwell's mean free path in the kinetic theory of gases (8,9):

$$(11) \quad \langle l_c \rangle^{-1} = 2\beta^4 \int_0^\infty l_c^{-1}(v) v^3 \exp[-\beta^2 v^2] dv.$$

If $l_c(v)$ is proportional to the neutron velocity, τ is independent of the neutron velocity distribution, viz.

$$(12) \quad \tau = l_c(v)/v.$$

(8) J. JEANS: *Kinetic Theory of Gases* (Cambridge, 1952), § 108.

(9) B. DAVISON: l. c., p. 44.

$\langle l_c \rangle$ is then equal to the capture mean free path for neutrons having the velocity \bar{v} .

In general the variations of the capture mean free path with the neutron velocity will be represented by a function $\varphi_c(v) = \langle l_c \rangle / l_c(v)$. Similarly we introduce the ratio $\varphi_s(v) = l_0 / l_s(v)$, where l_0 denotes some standard value or average of $l_s(v)$. The Maxwellian average $\langle l_s \rangle$ defined in analogy with Eq. (11), could be substituted for l_0 ; in the special case, discussed in Sect. 3, it will however be more convenient to take $l_0 = l_s(\infty) = \sqrt{(M+1)/M} \cdot \langle l_s \rangle$.

2. - Diffusion in a non-capturing medium.

In order to determine the diffusion coefficient of thermal neutrons in a non-capturing medium ($l_c^{-1} = 0$), we look for solutions of Eq. (1) which have the special form ^(10,11)

$$(13) \quad N = v^2 \exp[-\beta^2 v^2] \{C_1 - C_2[x/l_0 - \mu U_{11}(v)]\}.$$

Herein C_1 and C_2 are arbitrary constants; $\arccos \mu$ is the angle between the velocity vector and the positive x -axis. The following equation for $U_{11}(v)$ is obtained from (1):

$$(14) \quad \varphi_c(v) \left[U_{11}(v) - \int_0^\infty f_1(v \rightarrow v') U_{11}(v') dv' \right] = 1.$$

For a neutron distribution like (13) the proportionality

$$(15) \quad \mathbf{j} = -D \text{grad } n$$

holds. The above equations show that

$$(16) \quad D = \frac{1}{3} \kappa l_0 \bar{v},$$

with

$$(17) \quad \kappa = 2\beta^4 \int_0^\infty U_{11}(v) v^3 \exp[-\beta^2 v^2] dv.$$

⁽¹⁰⁾ L. BOLTZMANN: *Sitzber. Akad. Wien*, **88**, 835 (1883); *Wiss. Abh.*, III (Leipzig, 1909), p. 39.

⁽¹¹⁾ Compare also S. CHANDRASEKHAR: *Radiative Transfer* (Oxford, 1950), p. 14, Eq. (80).

Hence, in order to determine the diffusion coefficient D , it appears necessary to solve Eq. (14). For a specified kernel f_1 this could be done by numerical iteration.

The following approximate solution of Eq. (14) is obtained if $U_{11}(v)$ is substituted for $U_{11}(v')$ into the integrand

$$(18) \quad U_{11}(v) = \{\varphi_s(v)[1 - b(v)]\}^{-1} = l_{tr}(v)/l_0.$$

When this is introduced into Eqs. (17) and (16) an approximation for D follows which can be expressed in the conventional form

$$(19) \quad D = \frac{1}{3} \bar{l}_{tr} \bar{v},$$

if the average transport mean free path \bar{l}_{tr} is defined by

$$(20) \quad \bar{l}_r = 2\beta^4 \int_0^\infty l_{tr}(v) v^3 \exp[-\beta^2 v^2] dv.$$

3. - Diffusion in a non-capturing monoatomic gas.

As an example the case of a monoatomic gas, where scattering of slow neutrons is isotropic in the center-of-mass system, will be treated in more detail. We assume furthermore that the scattering cross-section (σ_s) is constant and that capture is absent. These assumptions make the problem equivalent to that with smooth hard spherical molecules in the classical kinetic theory of gases⁽¹²⁾. It can be expected that the results valid for this idealized case approximately apply also to some non-gaseous media⁽⁶⁾.

The only essential parameter of this problem is the ratio $M = m_1/m$ of the mass of the atoms to the neutron mass; κ (Eq. (17)) is a function of this parameter. The following auxiliary quantities will be useful:

$$\begin{aligned} \theta &= \beta(M+1)/(2\sqrt{M}), & \zeta &= \beta(M-1)/(2\sqrt{M}), & v''\Omega'' &= v\Omega - v'\Omega', \\ \xi &= (\theta v\Omega + \zeta v'\Omega') \cdot \Omega'' = \frac{1}{2} (\beta\sqrt{M}/v'') (v^2 - v'^2 + v''^2/M). \end{aligned}$$

$\sqrt{2kT/Mm} \cdot \xi$ is the projection of the velocity which the atom had before collision, upon the vector $v''\Omega''$, which represents the change of the neutron velocity.

⁽¹²⁾ S. CHAPMAN and T. G. COWLING: *The Mathematical Theory of Non-Uniform Gases* (Cambridge, 1939).

In the present case simple expressions exist for the functions $f(v'\Omega' \rightarrow v\Omega)$ and $\varphi_s(v)$, namely

$$(21) \quad f(v'\Omega' \rightarrow v\Omega) = \theta^2 v^2 [\sqrt{M\pi^3} \beta v' v'' \varphi_s(v')]^{-1} e^{-\xi^2},$$

$$(22) \quad \varphi_s(v) = [1 + (2M\beta^2 v^2)^{-1}] \operatorname{erf}(\sqrt{M}\beta v) + \exp[-M\beta^2 v^2]/(\sqrt{\pi M}\beta v),$$

with $\operatorname{erf}(x) = (2/\sqrt{\pi}) \int_0^x e^{-t^2} dt$. We have chosen $l_0 = l_s(\infty) = 1/n_1 \sigma_s$, with n_1 being the number of atoms per unit volume, so that $\varphi_s(\infty) = 1$.

JAFFÉ⁽⁷⁾ derived the expression (21) by starting with the original form of the Boltzmann equation for a binary gas mixture, and by carrying out some of the integrations. The same result can also be achieved by geometric reasoning, based upon the vector diagram for binary encounters⁽¹³⁾. This way has been followed (for $M=1$) by HIBY and PAHL⁽¹⁴⁾. Also a quantum mechanical deduction is known^(6a).

Fortunately the Legendre coefficients $f_l(v' \rightarrow v)$ of (21) can be expressed in closed forms by the error function and elementary functions. We find

$$(23) \quad f_0(v' \rightarrow v) = \theta^2 v [\beta^2 v'^2 \varphi_s(v')]^{-1} \{ [\operatorname{erf}(\theta v - \zeta v') \pm \operatorname{erf}(\theta v + \zeta v')] + \\ + \exp[\beta^2 v'^2 - \beta^2 v^2] [\operatorname{erf}(\theta v' - \zeta v) \mp \operatorname{erf}(\theta v' + \zeta v)] \},$$

$$(24) \quad f_1(v' \rightarrow v) = \theta^2 \sqrt{M} [\beta^4 v'^3 \varphi_s(v')]^{-1} \cdot \\ \cdot \{ (\beta \theta v^2 - \beta \zeta v'^2 - \sqrt{M}) [\operatorname{erf}(\theta v - \zeta v') \pm \operatorname{erf}(\theta v + \zeta v')] + \\ + (\beta \theta v'^2 - \beta \zeta v^2 - \sqrt{M}) \exp[\beta^2 v'^2 - \beta^2 v^2] [\operatorname{erf}(\theta v' - \zeta v) \mp \operatorname{erf}(\theta v' + \zeta v)] + \\ + (2/\sqrt{\pi}) \beta (v + v') \exp[-(\theta v - \zeta v')^2] - (2/\sqrt{\pi}) \beta |v - v'| \exp[-(\theta v + \zeta v')^2] \},$$

where the upper signs refer to $v < v'$, and the lower to $v > v'$. For $M=1$ both expressions become simpler and permit a reduction of the corresponding integral equations to second order differential equations^(4,6,10,15).

$f_1(v' \rightarrow v)$ can be approximated by simpler functions if v' is either large or small. Equation (14) then shows that $U_{11}(0) = 0$,

$$(25) \quad U'_{11}(0) = \frac{1}{2} \beta \sqrt{\pi M} + \frac{2}{3} \theta^2 \int_0^\infty U_{11}(v) (1 - 2\theta \zeta v^2) \exp[-\theta^2 v^2] dv,$$

$$(26) \quad U_{11}(\infty) = \left(1 - \frac{2}{3M}\right)^{-1}.$$

⁽¹³⁾ S. CHAPMAN and T. G. COWLING: l. c., p. 55.

⁽¹⁴⁾ J. W. HIBY and M. PAHL: *Zeits. f. Phys.*, **129**, 517 (1951), Eq. (13).

⁽¹⁵⁾ C. L. PEKERIS: *Proc. Nat. Acad. Sci. USA*, **41**, 661 (1955).

This supplements the picture of $U_{11}(v)$, which is obtained with the approximate solution (18). The figure below represents a few cases, and also shows the function $2(\beta v)^3 \exp[-\beta^2 v^2]$, by which the function $U_{11}(v)$ has to be multiplied and then integrated, according to Eq. (17), in order to obtain $\kappa(M)$.

Some special values and approximations of D are known from the kinetic theory of gases ⁽¹²⁾. If $M \gg 1$, scattering becomes isotropic in the laboratory system, and therefore $D = \frac{1}{3} l_0 \bar{v}$. This means that $\kappa(\infty) = 1$. If $M = 1$, D is equal to the coefficient of self-diffusion of gases with smooth hard spherical molecules ^(12,15,16). According to PEKERIS ⁽¹⁵⁾ the value of this coefficient is $D = 1.01896 \cdot (3/32) \pi \sqrt{2} l_0 \bar{v}$, so that

$$(27) \quad \kappa(1) = \frac{9}{32} \pi \sqrt{2} \cdot 1.01896 = 1.27325.$$

The behaviour of the functions occurring in Eq. (14) permits the conclusion that the approximation (19), viz. $\kappa = \bar{l}_{tr}/l_0$, should be satisfactory for $M \gg 1$.

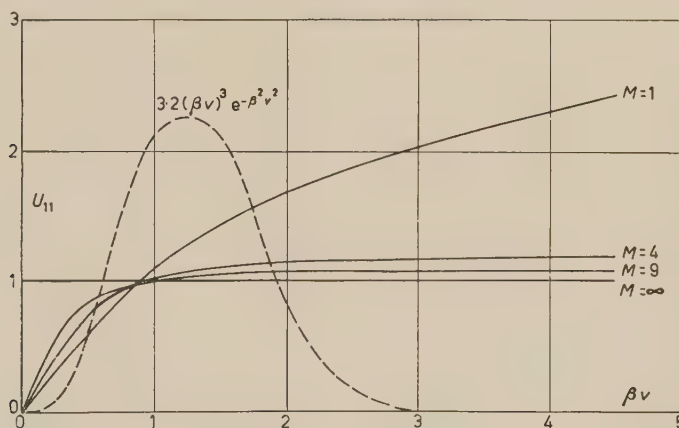


Fig. 1. — Graphs showing $U_{11}(v)$ for some values of M . The curve for $M=1$ represents the data of PEKERIS ⁽¹⁵⁾.

(Even for $M=1$ we find the value $\kappa = 1.29$ which is only by 2% too high.) When terms of smaller order than M^{-1} are neglected an asymptotic approximation follows:

$$(28) \quad \kappa = 1 + 1/6M.$$

Some remarks may be added concerning the one-group treatment of the diffusion of thermal neutrons. The neutron spectrum is assumed to be Maxwellian. If both the thermal motion of the atoms and the anisotropy of the scattering (in the laboratory system) are neglected, the already mentioned

⁽¹⁶⁾ F. B. PIDDUCK: *Proc. London Math. Soc.*, **15**, 89 (1916).

result $\kappa = 1$, i.e. $D = \frac{1}{3}l_0\bar{v}$, follows, which is correct for very heavy atoms. No improvement is achieved if only the anisotropy of scattering is taken into account, while the atoms are still assumed to be at rest before encounter. This treatment is equivalent to the substitution of $U_{11}(\infty)$ (Eq.(26)) for $U_{11}(v)$ into (17). The figure explains why the formula so obtained, $\kappa = 1 - b(\infty)$, i.e.

$$(29) \quad D = \frac{1}{3}l_{tr}(\infty)\bar{v} = \frac{1}{3} \cdot \frac{l_0\bar{v}}{1 - b(\infty)},$$

with $b(\infty) = 2/3M$, gives the correct limit $\kappa(\infty) = 1$, but much too high values for small M (e.g. $\kappa(1) = 3$ instead of 1.273). In order to account for the thermal motion of the atoms we may substitute for l_0 , $b(\infty)$ or $l_{tr}(\infty)$, into (29) some reasonable averages of $l_s(v)$, $b(v)$ or $l_{tr}(v)$, respectively. Equation (19), with (20), represents an example. A simpler but less satisfactory way would be to keep the denominator in (29), but to use Maxwell's mean free path $\langle l_s \rangle = l_0\sqrt{M/(M+1)}$ instead of l_0 . The result, though in accord with (28), is again too high for small M .

The method of Chapman and Enskog consists in approximating $U_{11}(v)$ by an odd polynomial, the coefficients of which are determined by a variational principle⁽¹⁷⁾. The result obtained by a cubic polynomial, when specialized to the present case, can be written as

$$(30) \quad \kappa = \frac{9\pi}{32} \sqrt{\frac{M+1}{M}} \cdot \frac{13M^2 + 16M + 30}{12M^2 + 16M + 30}.$$

This formula is very good for small M (it gives $\kappa(1) = 1.271$ instead of 1.273), but not so good for large M (it leads to $\kappa(\infty) = 0.96$ instead of $\kappa(\infty) = 1$). This is understandable as the polynomial approximation cannot be satisfactory for large M , when $U_{11}(v)$ approaches a step function (see the figure).

By a modification, which is insignificant for small M , formula (30) can be made to agree asymptotically with (28) and to assume the correct value (27) for $M=1$. A graphical comparison of the various approximations seems to support the hope that the modified formula

$$(31) \quad \kappa = \sqrt{\frac{M+1}{M}} \cdot \frac{M^2 + 2.530M + 2.727}{M^2 + 2.863M + 3.087},$$

is correct to within a few tenths of a percent for the whole range of M .

⁽¹⁷⁾ S. CHAPMAN and T. G. COWLING: l. c. It should be noted that if the medium is a monoatomic gas the above equation (14) is a reduced form of a special case of Chapman and Cowling's equation (5a) on p. 141, with D_1 corresponding to U_{11} .

4. - Diffusion with capture.

When capture of neutrons occurs we may look for solutions which are proportional to $\exp[-x/L]$, where L is an unknown parameter, called the diffusion length. Obviously also for neutron distributions of this kind the proportionality (15) remains valid. With (6) the well known relation

$$(32) \quad L^2 = D\tau$$

follows.

If capture is very weak the diffusion length is large ($L \gg l_0$). If moreover the energy exchange with the atoms is not too weak (i.e. if the atoms are not too heavy) the wanted distribution is almost Maxwellian. More exactly, this distribution but little differs from a certain distribution of the type given by Eq. (13). The results of Sect. 2 are therefore still applicable and Eq. (16) is still valid. In this case τ_0 can be substituted for τ in Eq. (32), so that

$$(33) \quad L^2 = \frac{1}{3}\kappa l_0 \langle l_c \rangle$$

(or approximately $L^2 = \frac{1}{3}l_{tr} \langle l_c \rangle$). The ratio $\nu = l_0/L$ is therefore related to the ratio $\varepsilon = l_0/\langle l_c \rangle$ by $\nu^2 = 3\varepsilon/\kappa$.

For stronger capture equations (16) and (33) become invalid. For such cases a possible method will be indicated, which aims at the development

$$(34) \quad \nu^2 = \sum_{n=1}^{\infty} A_n \varepsilon^n,$$

where in particular $A_1 = 3/\kappa$. According to what has been said before a good convergence of this development can be expected if capture is not too strong and if all the atoms are not too heavy. (It is easy to see that also the second condition is necessary. In a capturing medium with only extremely heavy atoms the exchange between different velocity groups of neutrons is so weak, that at great distance from the sources by capture an almost monokinetic group is selected, which approximately corresponds to some maximum value of $l_c(v)$. The corresponding diffusion length is not necessarily anything near the value $\frac{1}{3}\kappa l_0 \langle l_c \rangle$.)

In order to determine the coefficients A_2 etc., we start with an inverse series

$$(35) \quad \varepsilon = \sum_{n=1}^{\infty} B_n \nu^{2n},$$

and try to solve the problem by a perturbation method, using the development

$$(36) \quad N \propto \exp[-x/L] \cdot v^2 \exp[-\beta^2 v^2] \sum_{n=0}^{\infty} \sum_{i=0}^{[\frac{1}{2}n]} \nu^n U_{n,n-2i}(v) P_{n-2i}(\mu).$$

Herein $[\frac{1}{2}n]$ stands for $\frac{1}{2}n$ or $\frac{1}{2}(n-1)$, according to whether n is even or odd. A system of integral equations for the functions $U_{nl}(v)$ ($n=0, 1, 2, \dots$; $l \leq n$; l and n both even or both odd) follows from (1):

$$(37) \quad \varphi_s(v) \left[U_{ni}(v) - \int_0^\infty f_i(v \rightarrow v') \dot{U}_{ni}(v') dv' \right] = \\ = \frac{l}{2l-1} U_{n-1, l-1}(v) + \frac{l+1}{2l+3} U_{n-1, l+1}(v) - \varphi_c(v) \sum_{i=1}^{\frac{1}{2}(n-l)} B_i U_{n-2i, l}(v).$$

These equations can be solved in succession.

The first equation ($n=0$, $l=0$) is homogeneous and is solved by $U_{00} = \text{const}$. We take $U_{00}=1$, whereby the next equation ($n=1$, $l=1$), becomes identical with (14). The equations with $l=0$, $n=2, 4, 6, \dots$, require special attention because they are inhomogeneous and have the same kernel f_0 as the mentioned homogeneous equation. These equations therefore have non-trivial solutions only if the orthogonality conditions

$$(38) \quad \int_0^\infty \left[\frac{1}{3} U_{n-1,1}(v) - \varphi_c(v) \sum_{i=1}^{\frac{1}{2}n} B_i U_{n-2i,0}(v) \right] v^3 \exp[-\beta^2 v^2] dv = 0$$

are satisfied. These conditions determine the coefficients B_i . We find

$$(39) \quad \begin{cases} B_1 = \kappa/3, \\ B_2 = \frac{2}{3} \beta^4 \int_0^\infty [U_{31}(v) - \kappa \varphi_c(v) U_{20}(v)] v^3 \exp[-\beta^2 v^2] dv, \text{ etc.} \end{cases}$$

Then we have $A_1 = B_1^{-1} = 3/\kappa$, $A_2 = -B_2/B_1^3$ etc.

No attempts have as yet been made to apply this method to any particular case.

RIASSUNTO

La diffusione dei neutroni lenti in un mezzo esteso omogeneo viene trattata con un metodo che tiene conto del moto termico del mezzo. Se l'assorbimento dei neutroni è nullo, per determinare la distribuzione di velocità dei neutroni ed il coefficiente di diffusione deve essere risolta una sola equazione integrale. Un sistema di tali equazioni è ottenuto per un mezzo assorbente. Per un mezzo gassoso monoatomico non-assorbente vengono discusse alcune approssimazioni, che esprimono il coefficiente di diffusione in funzione del peso atomico.

One-particle Levels with Spin-orbit Interaction According to the Shell Model for Nuclei.

A. SCHRÖDER (*)

Istituto di Fisica dell'Università - Padova

Istituto Nazionale di Fisica Nucleare - Sezione di Padova

(ricevuto il 6 Agosto 1957)

Summary. — The shell model of nuclei is considered, and the average potentials for protons and neutrons are calculated on a phenomenological basis. Different assumptions about the types of spin-orbit coupling and their magnitudes are treated in the one-particle picture. Their relative influence on the one-particle levels is discussed for almost the greatest part of the periodic system (above $A \approx 40$). Calculations show that a spin-orbit interaction $-\lambda(\hbar/m_\pi c)^2(1/r)(d/dr)V(r) \cdot (\mathbf{Ls}/\hbar^2)$ with only one fixed parameter λ leads to consistent results in one-particle levels: magic numbers are reproduced. The diffuse boundary potentials $V(r)$ derived for neutrons and protons separately are in agreement with those derivable from elastic scattering experiments in the lowest energy limit.

1. — Introduction.

The purpose of this paper is to investigate how far the simple suppositions on which the shell model for nuclei are based, can yield improved predictions as to the energy levels of atomic nuclei available, particularly as regards the field of the heavier nuclei (from $A \approx 40$ to $A \approx 250$), which can be linked up with the so-called one-particle structure (in the widest sense of the word). Of special interest here is the problem, of whether spin-orbit level spacing must be linked in its main part with a overall quality (average potential) of the nuclei. To this end the one-particle levels were calculated on the basis of several assumptions about the spin-orbit interaction for neutrons.

(*) A greater part of this work was carried out while the author was at the University of Zurich.

Therefore average central potentials felt by a considered nucleon were set up on a phenomenological basis for a sequence of only one ideal isotope for a given A , along the domain of stable nuclei in the valley of the total energy surface. The nuclear radii parameters found for the potential wells are in good agreement with known data.

It has been demonstrated that a coupling law, which is directly connected to the average potential; leads to the right magic numbers and, where applicable, to the probably correct size of the energy jumps of the undisturbed one-particle ionization energies.

The same is also obtained for the protons by using an average nuclear potential which, for the case of zero neutron excess, has the same shape and depth as that for neutrons (Coulomb-potential excluded). Its depth has to be monotonically increased with the increasing of the neutron excess.

The results are listed in a form which is suggested by the sequence of the average potentials and their spin-orbit interaction ⁽¹⁾.

2. - The shell model.

Although the concept of the shell model is well known the basic idea will be reviewed.

The quantum mechanical treatment of an atomic nucleus requires the solution of a complicated wave mechanical many-body problem the crux of which is the calculation of the wave function (the limits of a non-relativistic treatment of the system are hereby reached). The difficulties in managing such a problem are made even greater by the fact that the Hamilton operator for a nucleus, because of the rather scarcely known nature of the nuclear forces, cannot be explicitly set up. Experimentally known data about nuclear forces and the nuclei themselves must be used in trying to construct the Hamilton operator of the system and therefore it is of very great importance to get simple visual interpretations of its constructing elements.

The predictions which can be obtained from such a Hamilton operator, depend for their validity and absence of contradictory elements, on the degree to which the lowest approach agrees with the real circumstances.

In the shell model this lowest approach is established by the fact that the total wave function of the system, like those of a Fermi gas, is built up on a total anti-symmetrical product of single eigenfunctions of a Hamilton

⁽¹⁾ A similar type of diagram was first used by K. BLEULER and CH. TERREAUX: *Helv. Phys. Acta*, **28**, 245 (1955).

operator, whose potential is a well of finite domain and represents the average of all the force effects in the system.

This procedure makes it possible (*) to define a particle within the corresponding system with simple quantum numbers as in the Hartree-Fock approach to the many particle problem (2).

It is supposed that this average potential of all the forces acting within the system on a particle at the point \mathbf{r} represents the average value which may be described by a spatial isotropic one-particle force (central field), and further acts strongly on the spin. This leads to particle states with the quantum numbers $nljm$ for one nucleon. A high degeneracy occurs (because the energy of a configuration belongs only to nlj with the half integer quantum number $j = l \pm \frac{1}{2}$ for orbit and spin) specially for energy levels with greater j . Levels which are energetically separated from others by large amounts lead to shell formation.

From the radial part of the eigenfunctions associated with a certain j , a strong ring formed density distribution is produced (n gives the number of ring structures).

A weak self-consistency condition has however to be introduced, namely that the part of the potential which only depends on the position is not in contrast with its total radial density distribution. The potential is fixed in advance and guarantees the stability of the system.

Although the particles in such a field are treated as formally independent, their behavior depends on the nature of the origin of their potentials, and their properties are closely connected one with the other. In particular, the excitation of one particle must considerably alter the energetic conditions of all the others and therefore its potential. Such an effect is neglected in the simplest approach of the Hartree-Fock theory. Another difference is that the individual interactions between the particles are not yet specified (two — and many — body forces) so that the calculation of the total binding energy of the system will depend on the special convention adopted. A direct fixing of the energy zero-point of the system would give rise to a strong self consistency condition and would base the model on a theory or experimental data about the individual interactions.

The physical existence of an average potential is certainly linked with the fact that strong individual interactions between the nucleons may be considered as perturbations, so that the wave-function of a nucleus, before and after the perturbation has been introduced, may be made up of the one-particle

(*) This possibility is only approximative because the total linear momentum of the whole system must be conserved. The neglect of the proper center-of-mass motion results in this case in errors of order $1/A$ in the binding energies, levels, etc.

(2) P. O. LÖWDIN: *Phys. Rev.*, **97**, 1475 (1955).

eigenfunctions of this potential or at least may be made up of products of stable core wave functions and one-particle eigenfunctions produced from the average potential given by the core. Strong admixtures from other levels are thereby not excluded.

The shell model concept arises from modern experimental knowledge of the behaviour of the nuclei at low energy ⁽³⁾. It has, however, considerable theoretical difficulties on account of the strong interaction between nucleons, which the Hartree-Fock method does not seem to be sufficient to overcome. Recently, as a result of the knowledge obtained from the description of highly energetic scattering experiments with nucleons, methods have been developed which attempt to explain theoretically the correlation and saturation phenomena in the nuclear matter with two-body forces ⁽⁴⁾. In this way an attempt has been made to solve the problem in the sense of a hypothesis as to the very important part played by the Pauli-principle in the matter of the nucleus. But by this method the important influence of shell formation is not directly taken into account.

Characteristic alterations in the meaning of the simple average potential in the shell model have been made (velocity dependence) by the generalization of known methods of the perturbation theory and by further specific development on the basis of allowed individual interactions.

But till now the simple one-particle concept, which is still free of additional hypotheses, has not been sufficiently investigated quantitatively.

The following shows that the results for the one-particle levels produced by a spin-orbit interaction in strict connection with the average potential obtained with the simplest model are good, and do not require to be substantially modified by invoking a more complicated model.

3. - The one-particle Schrödinger equation.

According to the problem we are considering we have to treat the one-particle wave functions which are solutions of the equation:

$$(1) \quad (H + H')\Psi = E\Psi.$$

The most general form of a central force acting on a particle is given by a potential

$$(2) \quad V(r) = V_1(r) + f(r) \cdot (\mathbf{l}\mathbf{s}).$$

⁽³⁾ M. G. MAYER: *Phys. Rev.*, **75**, 1969 (1949); O. HAXEL, J. H. D. JENSEN and H. E. SUSS: *Phys. Rev.*, **75**, 1766 (1949); M. G. MAYER and J. H. D. JENSEN: *Elementary Theory of Nucl. Shell Structure* (New York).

⁽⁴⁾ H. A. BETHE: *Phys. Rev.*, **103**, 1353 (1956) and references.

Invariance of (1) against rotation and reflection in the configuration space is assumed. Let us take

$$(3) \quad H = T + V_1(r), \quad \text{where} \quad T = -\frac{\hbar^2}{2M} \Delta,$$

and

$$(4) \quad H' = f(r) \cdot (\mathbf{L}\mathbf{s}).$$

According to (2) it is sufficient after separation of the angular part, to represent E as eigenvalues of the radial equation

$$(5) \quad \left\{ \frac{d^2}{dr^2} + \frac{2}{r} \frac{d}{dr} - \frac{l(l+1)}{r^2} + \frac{2M}{\hbar^2} (E_{n,l} - V(r)) \right\} R_{n,l}(r) = 0,$$

with the conditions for bound states

$$(6) \quad \begin{aligned} &R(0): \text{ regular} \\ &\text{so that } \int_0^\infty R^2(r) r^2 dr: \text{ converges,} \\ &R(\infty): \text{ vanishes.} \end{aligned}$$

4. - The empirical data for the determination of $V_1(r)$.

The task now arises of establishing as exactly as possible the potential function $V_1(r)$. We represent the well $V_1(r)$ in the first place by a reasonable physical assumption and determine its parameter in the light of the experimentally well known properties of the stable nuclei. Let $V_1(r)$ be the average potential that acts on a particle situated at r while all the other particles are in their normal positions inside the nucleus, so that their energy levels are completely filled with nucleons. The gradient of this function — $\text{grad } V_1(r)$ is the effective force felt by the particle. By this definition, the potential $V_1(r)$ contains also an energy shift produced by all the other nucleons due to the change in radius after the evaporation of the considered particle. A static description of $V_1(r)$ is an acceptable approximation only if the influence of its (virtual) part occurring from the contraction on the eigenfunction of the considered particle is small. It seems to be so here.

As empirical data for the determination of $V_1(r)$ we chose the mean ionization (separation) energy for a nucleon and the suitably defined density radius of the nuclei proportional to $A^{1/3}$. Both are in close connection with the saturation phenomenon of nuclear forces. We do not consider a special $V_1(r)$ alone,

but always a selected sequence $V_1(r; A)$ and we try to determine them indirectly by the above mentioned empirical properties.

These empirical properties can be represented for a selection of idealized nuclei, by a smooth mean value curve provided one does not take into account

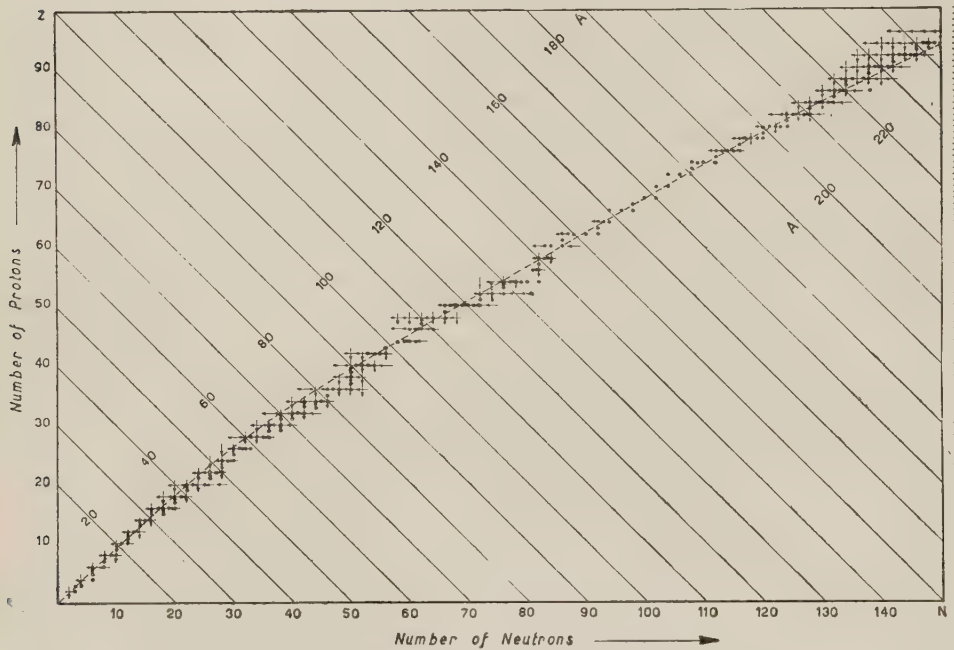


Fig. 1. — The chosen mean value curve $A = \bar{N} + \bar{Z}$ in the N, Z -plane (corresponding roughly to the valley on the energy surface for the most stable odd nuclei). \leftarrow . Separation of a neutron pair from a nucleus with even Z and odd N . \downarrow . Separation of a proton pair from a nucleus with even N and odd Z (contains all cases which can be built up from known binding energies). \circ : Known isobar with greatest total binding energy (note the difference between the chosen curve for the most stable odd nuclei).

their subjective differences. They are simple functions of the particle number A for the whole periodical system. Especially in the case of the strongly varying separation energy τ suitable mean values $\bar{\tau}(A)$ must be built up.

As we want to calculate typical one particle effects later on, only data from nuclei with odd A are taken into consideration. For the determination of the neutron separation energy we take nuclei with an odd N and an even Z and the opposite for the proton.

We must notice here, that the resulting «even A » nucleus, does not have the same one-particle properties (assignments). This comes from the pairing-effect in even A nuclei. In order to remain in the connect with odd nuclei

we remove a pair of nucleons but form

$$(7) \quad \tau_N = \frac{1}{2} \left\{ B_{\text{exp}} \left(\begin{smallmatrix} N \\ Z \end{smallmatrix} \right) - B_{\text{exp}} \left(\begin{smallmatrix} N-2 \\ Z \end{smallmatrix} \right) \right\} \text{ for the neutrons ,}$$

and respectively

$$(8) \quad \tau_Z = \frac{1}{2} \left\{ B_{\text{exp}} \left(\begin{smallmatrix} N \\ Z \end{smallmatrix} \right) - B_{\text{exp}} \left(\begin{smallmatrix} N \\ Z-2 \end{smallmatrix} \right) \right\} \text{ for the protons (*),}$$

where $B_{\text{exp}} \left(\begin{smallmatrix} N \\ Z \end{smallmatrix} \right)$ is the experimentally known total binding energy of the nucleus in question ⁽⁵⁾ (see Fig. 2).

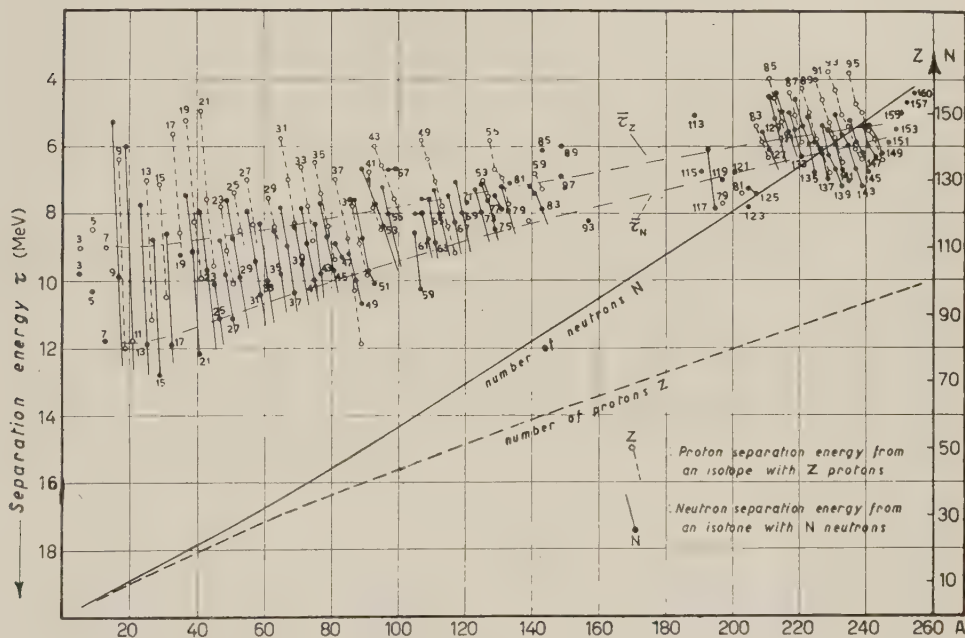


Fig. 2. - The experimentally known values of the separation energy of one nucleon, given by the formulae

$$\tau_N = \frac{1}{2} \left\{ B \left(\begin{smallmatrix} N \\ Z \end{smallmatrix} \right) - B \left(\begin{smallmatrix} N-2 \\ Z \end{smallmatrix} \right) \right\}, \quad \tau_Z = \frac{1}{2} \left\{ B \left(\begin{smallmatrix} N \\ Z \end{smallmatrix} \right) - B \left(\begin{smallmatrix} N \\ Z-2 \end{smallmatrix} \right) \right\},$$

and the determination of the mean values $\bar{\tau}_N(A)$ and $\bar{\tau}_Z(A)$ by means of the chosen mean value curve $A = N + Z$. (The smooth curves τ_N from an isotope with N -neutrons and τ_Z from an isotope with Z protons are extrapolated for some cases, in agreement with the eliminated effects). From every curve τ only one point is taken into account in order to fix the shell model parameters.

(*) I am indebted for this important idea to Dr. CH. TERREAUX (see also ⁽¹⁰⁾).

⁽⁵⁾ A. H. WAPSTRA: *Physica*, **21**, 367, 385 (1955); I. R. HUIZENGA: *Physica*, **21**, 410 (1955).

In this way through successive ionization of a nucleus one also attains its binding energy B_{exp} without destroying the pure one-particle picture which is needed for the lowest approximation of the model.

From these values τ_N and τ_Z we determine the mean value given by smooth functions $\bar{\tau}_N(A)$ and $\bar{\tau}_Z(A)$ on the periodic system from a smooth curve for the mean values N and Z of N and Z (not necessarily integral) chosen from the flow of all stable odd nuclei in the (N, Z) -plane.

For the total density distribution of the nuclear matter, of the idealized nuclei (belonging to \bar{N} and \bar{Z}) we make the following assumption in order to give a clear picture of the different radius definitions.

$$(9) \quad \varrho(r) = \begin{cases} \varrho^0 & \text{for } 0 \leq r \leq C - t/2, \\ \varrho^0 \frac{(C + t/2) - r}{t} & \text{» } C - t/2 \leq r \leq C + t/2, \\ 0 & \text{» } C + t/2 \leq r \leq \infty, \end{cases}$$

which approximately corresponds to the relations derived from electron scattering experiments.

If one considers the distribution of the charge only, then (8) must be somewhat generalized in view of the electrostatic potential that is to be calculated from it. (Experimentally such a distribution is only tested in the case of ^{197}Au).

$$(9a) \quad \varrho_Z(r) = \begin{cases} \varrho^0 \left[1 + \delta \left(\frac{r}{C' - t'/2} \right)^2 \right] & \text{for } 0 \leq r \leq C' - t'/2, \\ \varrho^0 [1 + \delta] \left[\frac{C' + t'/2 - r}{t'} \right] & \text{» } C' - t'/2 \leq r \leq C' + t'/2, \\ 0 & \text{» } C' + t'/2 \leq r \leq \infty. \end{cases}$$

By means of the moments

$$(10) \quad J^{(n)} = 4\pi \int_0^\infty \varrho(r) r^{n+2} dr \quad \text{with } n = 0, 2, \dots,$$

the « half density radius »

$$(11) \quad C = \int_0^\infty \varrho(r) dr / \varrho^0,$$

and the « skin thickness » t , with

$$J^{(0)} = 4\pi \varrho^0 \left\{ \frac{1}{3} C^3 + \frac{1}{12} C t^2 \right\},$$

$$J^{(2)} = 4\pi \varrho^0 \left\{ \frac{1}{5} C^5 + \frac{1}{6} C^3 t^2 + \frac{1}{80} C t^4 \right\},$$

the «root mean square radius»

$$(12) \quad R_{(\text{msq})} = \sqrt{r^2} = C \left(\frac{3/5 + (1/2)(t/C)^2 + (3/80)(t/C)^4}{1 + (1/4)(t/C)^2} \right)^{\frac{1}{2}} \\ = C \left(\frac{3}{5} + \frac{7}{20} \left(\frac{t}{C} \right)^2 - \frac{1}{20} \left(\frac{t}{C} \right)^4 + \dots \right)^{\frac{1}{2}},$$

as well as the radius of an equivalent equiform density

$$(13) \quad R_{\Pi} = \left(\frac{5}{3} \right)^{\frac{1}{2}} R_{(\text{msq})}, \\ = C \left(1 + \frac{7}{12} \left(\frac{t}{C} \right)^2 - \frac{1}{12} \left(\frac{t}{C} \right)^4 + \dots \right)^{\frac{1}{2}},$$

the following constants can now be determinated:

$$(14) \quad r_0 = R_{\Pi} A^{-\frac{1}{3}},$$

$$(15) \quad r_1 = C A^{-\frac{1}{3}},$$

$$(16) \quad r_2 = R_{(\text{msq})} A^{-\frac{1}{3}}.$$

From (11) and (14) it follows that

$$(17) \quad r_0 = r_1 F(t/C).$$

Only in the case of a proportionality between t and C , if r_1 were constant, would r_0 also be constant. Experimental evidence contradicts this ⁽⁶⁾.

5. - The neutron potential.

Now a potential $V_1(r)$ is built up which should be in agreement with the distribution of the density (9) by taking into account a finite range for the nuclear forces. (But no assumption about the forces has been made).

⁽⁶⁾ B. HAHN, D. G. RAVENHALL and R. HOFSTADTER: *Phys. Rev.*, **101**, 1131 (1956); R. HOFSTADTER: *Rev. Mod. Phys.*, **28**, 214 (1956).

We simply put:

$$(18) \quad V_1(r) = \begin{cases} -V_N & \text{for } 0 \leq r \leq R-a, \\ -V_N(R-r)/a & \text{» } R-a \leq r \leq R, \\ 0 & \text{» } R \leq r \leq \infty. \end{cases}$$

(One could certainly give a more analytical description, however this more schematical form is most suitable for the applied calculation method without

any particular auxiliary calculatory devices). « a » determines a diffuseness of the potential boundary. Let R be defined as follows (see Fig. 3).

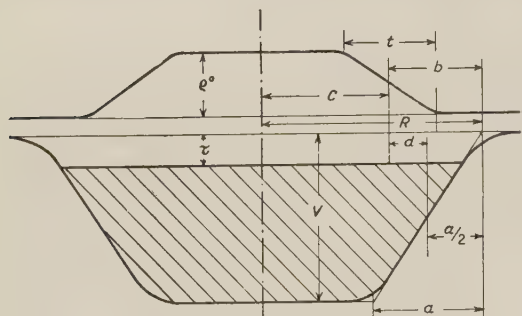


Fig. 3. - Density distribution and potential.
(Definition of the parameters).

$$(19) \quad R = r_1 A^{\frac{1}{3}} + b = C + b.$$

The parameters r_1 , b , a , V_N must now be chosen so that the above average separation energies $\bar{\epsilon}_N(A)$ can be reproduced by the solutions E of (5) with $f(r)=0$ and completely filled energy levels (with

$\bar{N}(A)$ particles). This determination of the parameters is a rather sensitive one.

By the application of the procedures described in Appendices I and II, this problem can be solved by means of a lengthy and extensive calculation. We attempt to take r_1 , b , a and V_N to be constant.

Results: the given values $\bar{\epsilon}_N(A)$, $\bar{N}(A)$ and the conditions

$$r_1 = \text{const},$$

$$b = \text{const},$$

$$V_N = \text{const},$$

$$a = \text{const},$$

where chosen. It therefore follows that

$$r_1 = 1.18 \cdot 10^{-13} \text{ cm},$$

$$b = 2.05 \cdot 10^{-13} \text{ cm},$$

$$V_N = 44.5 \text{ MeV},$$

$$a = 2.83 \cdot 10^{-13} \text{ cm}.$$

6. — The spin-orbit interaction.

A satisfactory theoretical explanation of the high doublet splitting of the one particle energy levels which would lead to a specific shell structure for nuclei, and to the formation of the so-called magic particle numbers, has not yet been given. It is therefore important to establish if the operator H' contained in (1) in the form (4), like $V_1(r)$, possesses a significance which covers the periodic system of the nuclei. i.e. whether $f(r)$ is connected with an overall property of the nucleus in question (the nuclear field), or if H' undergoes notable modifications as a function of the particle number. (In the latter case H' could in a certain way, represent rather a caricature of an effect produced by an individual two body tensor force interaction between the nucleons in the shells in question similar, for instance, to the behavior of the eliminated pairing energies). This second hypothesis would however make the simplest approach to the shell model very doubtful and would make senseless the level representation given later as continuous functions of A .

In order to test this, we again consider the case of neutrons in the nucleus. Making the assumption suggested by the determination of $V_1(r)$, namely, that it is not considerably modified by the addition of H' to the one particle operator H (average separation energies are approximately equal with H' added), the adaptation of $V_1(r)$ by means of $\bar{\tau}_N$ would otherwise be useless. Next, the angular momentum j resulting from the spin-orbit coupling of a particle is to be diagonalized with respect to $H+H'$ (which leads to the jj -coupling scheme).

For the case $l \neq 0$ this will be reached by means of the well known complete reduced product representation of the rotating group

$$D_l \times D_{\frac{1}{2}} = D_{j=l+\frac{1}{2}} + D_{j=l-\frac{1}{2}}.$$

The matrix of Clebsch-Gordan coefficients, which performs the reduction is

$$(20) \quad (G) = \frac{1}{\sqrt{2l+1}} \cdot \begin{pmatrix} \sqrt{l+m+1} & \sqrt{l-m} \\ \sqrt{l-m} & -\sqrt{l+m+1} \end{pmatrix}.$$

For both directions of the angular momenta it follows that

$$(21) \quad H' = f(r) \frac{\hbar^2}{2} \begin{cases} l & \text{for } j = l + \frac{1}{2}, \\ -(l+1) & \text{» } j = l - \frac{1}{2} \end{cases} \quad \text{with } l \neq 0,$$

and the eigenfunctions of H are then:

$$(22) \quad \begin{pmatrix} \Psi_{nj=l+1/2}^{m+1/2}(r, \vartheta, \varphi) \\ \Psi_{nj=l-1/2}^{m+1/2}(r, \vartheta, \varphi) \end{pmatrix} = \begin{pmatrix} R_{n,l}^{j=l+1/2}(r) & 0 \\ 0 & R_{n,l}^{j=l-1/2}(r) \end{pmatrix} (G) \begin{pmatrix} Y_l^m(\vartheta, \varphi) \\ Y_l^{m+1}(\vartheta, \varphi) \end{pmatrix}.$$

From (21) it follows that the radial eigenfunctions $R_{n,l}^j(r)$ for larger l depend closely on j .

For the sake of simplicity the assumption is frequently made that

$$(23) \quad f(r) = -|\text{const}|,$$

where the minus sign is required in order to split the level with $j = l + \frac{1}{2}$ down, according to the empirical facts. The centre point of the occupied doublet lies in this case exactly on the level formed without splitting, so that the determination of $V_1(r)$ is not in any way influenced.

$$H' = -0.38 \left(\frac{\hbar}{m_\pi c} \right)^2 \frac{1}{r} \frac{dV_N(r)}{dr} \cdot \frac{(\mathbf{l}\mathbf{s})}{\hbar^2} \text{ MeV}$$

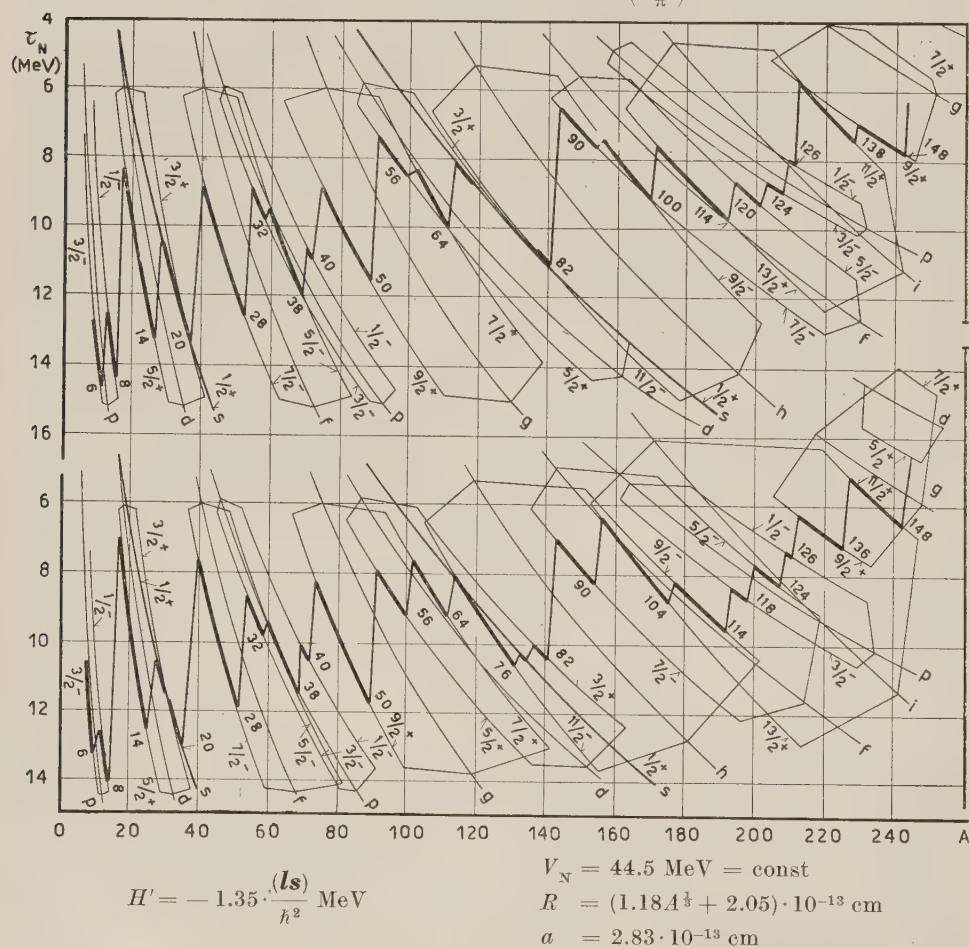


Fig. 4. — Energy levels corresponding to the shell model according to two different assumptions about the spin-orbit interaction for a single neutron. (Potential wells determined by neglecting spin-orbit splitting).

In the lower part of Fig. 4 this coupling is represented with the special value

$$(24) \quad f(r) = -1.35/\hbar^2,$$

(corresponding to an approximate adaptation to the level splitting of experimental values for $A = 40$ up to $A = 50$).

We can see here that the magic numbers cannot be employed satisfactorily for the heavier nuclei: the splitting of levels for greater A is much too large. The assumptions (23) and (24) are not realistic. Closely linked and employed by many authors is an assumption which binds $f(r)$ with $V_1(r)$ in a simple way and also satisfies the invariance condition for spatial inversion:

$$(25) \quad f(r) = -|\text{const}| \frac{1}{r} \frac{d}{dr} V_1(r).$$

This corresponds formally to the well known Thomas-term for the magnetic « doublet splitting » in the structure of atomic alkali spectra. H' is here proportional to

$$\sim s(\text{grad } V_1(r) \times p).$$

It must be noted that such a coupling term, because of the magnitude of the coupling energy in question, can no longer be taken into consideration by means of the application in the usual manner of an ordinary perturbation calculation. Therefore, for every coupling parameter involved, a new calculation of the whole level scheme for $l \neq 0$ is necessary. The conditions are such that the corresponding method, described in the Appendix II, can suitably be used.

Results: the result of the calculation is given for three different values of the dimensionless coupling parameter λ in Fig. 5 (also for the case with good adaptation in Fig. 4 above). With

$$(26) \quad H' = -\lambda \left(\frac{\hbar}{m_\pi c} \right)^2 \frac{1}{r} \frac{d}{dr} V_1(r) \begin{cases} l/2 & \text{for } j = l + \frac{1}{2}, \\ -(l+1)/2 & \text{» } j = l - \frac{1}{2} \end{cases} \quad \text{with } l \neq 0,$$

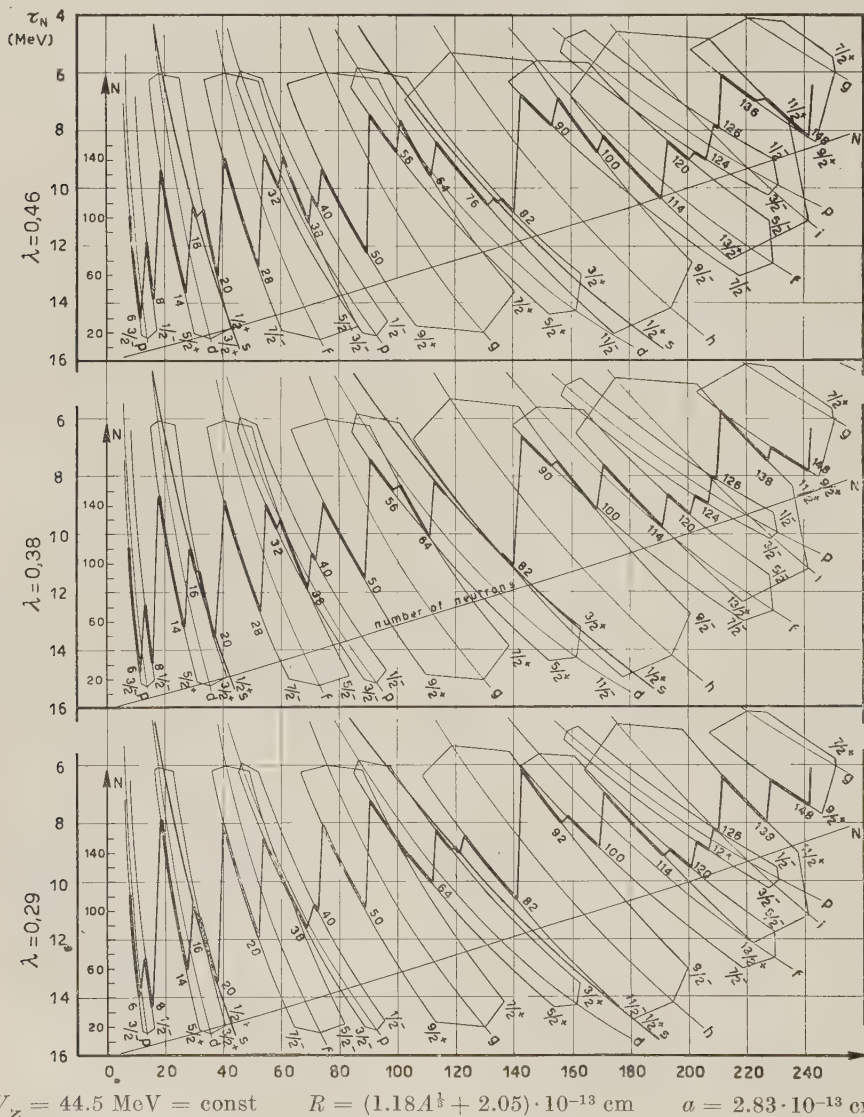
and

$$\lambda = 0.46, \quad \lambda = 0.38, \quad \lambda = 0.29,$$

and applying $V_1(r)$ from Sect. 5 (*).

(*) The Compton wave length of the π -meson is introduced for dimensional reasons. With the Compton wave length of the nucleon the best adaptation gives $\lambda = 18.4$.

The best agreement with the average of the experimental data can be seen for $\lambda = 0.38$. Fig. 5 shows that by comparison over the domain of A already λ can be relatively exactly determined only from known experimental level assignments and spacing in a few cases. The applied coupling law represents the experimental facts relative to the one particle attribute of nuclei with shell structure. Only in the field of the nuclei from $A \approx 160$ upwards, (the



lightest nuclei have not been taken into account because the structure of their core seems to be more complicated) is the agreement less good. But in the calculation made, it has not been taken into consideration that in this domain the more rapidly increasing coupling energy between spin and orbit alters the value of the mean separation energy (Fermi energy) somewhat to the value of $\bar{\tau}_N(A)$ respectively.

Therefore a new determination for $V_1(r)$ is necessary. Further, a rounding off of the potential well certainly brings a notable raising of the level having a high orbital momentum.

Taking these arguments into account a new adaptation of the potentials $V_1(r)$ (now $V_N(r)$) was set up with the direct employment of H' with the same grad $V_1(r)$ on the surface and $\lambda = 0.38$ where the « corners » of the potential boundary in the region of $1.2 \cdot 10^{-13}$ cm were rounded off.

Results: the given values now are $\bar{\tau}_N(A)$, $\bar{N}(A)$, grad $V_N(r)$ on the surface and the conditions $b^0 = \text{const}$, $r_1^0 = \text{const}$, the final parameter values for the neutron potential.

For $A > 60$ are:

$$r_1^0 = 1.08 \cdot 10^{-13} \text{ cm},$$

$$b^0 = 2.40 \cdot 10^{-13} \text{ cm},$$

$$V_N^0 \approx 46 \text{ MeV},$$

$$a^0 = 2.93 \cdot 10^{-13} \text{ cm}.$$

These results are given in graphical form in Fig. 6, and in Table I, also for values below $A = 60$.

7. - The proton potential.

If the given spin-orbit interaction has a universal significance, this fact ought also to lead to reasonable results in the case of the protons: this will be demonstrated in the following. If in the first place we consider the potential $V_1(r)$ to which, according to its definition there is a small contribution of electric energy formed by the closing up of the charges in the nucleus when a nucleon is eliminated (this contribution appears also in the neutron potential), then this would have to be completed with the Coulomb potential of the proton charge distribution. If in order to do this by means of the electrostatic potential (the influence of the electric exchange effect ought not to be big, as a statistic estimate shows) it follows that the condition for which the limiting energies of the $\bar{Z}(A)$ protons must agree in the mean with $\bar{\tau}_Z(A)$ can be obtained with V_N^0 only in the field of the nuclei with $\bar{N}(A) \approx \bar{Z}(A)$. In nuclei with an increasing excess of neutrons the protons would however find too little space within the nucleus.

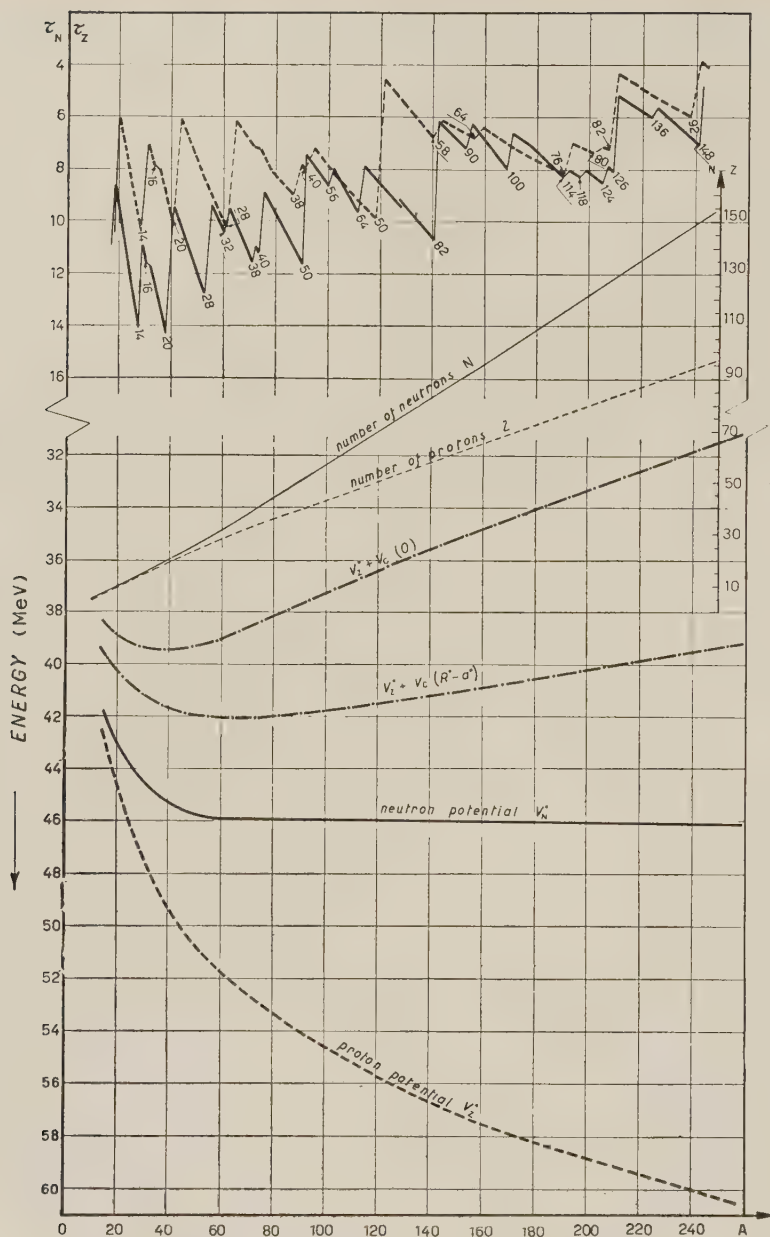


Fig. 6. — Pure one-particle separation-energies for the most stable nuclei derived from the shell model. The energy jumps corresponding to neutrons and protons for equal A are of the same order of magnitude. A β -stability condition between neutron and proton levels brings irregularities in the total energy valley just in those places where the differences between corresponding neutron and proton levels are great (but then we must take into account pairing effects). The calculated potential parameters are drawn below.

TABLE I.

| A | Z | \bar{N} | $\bar{\tau}_Z$ | $\bar{\tau}_N$ | V_Z^0 | $V_Z^0 + V_c(0)$ | $V_Z^0 + V_c(R - a)$ | $V_c(0)$ | $V_c(R - a)$ | $V_c(R)$ | V_N^0 | C | $E - a$ | a | $R - \frac{a}{2}$ | R |
|-----|------|-----------|----------------|----------------|---------|------------------|----------------------|----------|--------------|----------|---------|------|---------|------|-------------------|-----|
| 20 | 9.5 | 10.5 | 9.00 | 11.85 | 44.25 | 38.9 | 40.20 | 5.35 | 4.05 | 2.31 | 43 | 2.75 | 2.40 | 3.75 | 5.14 | |
| 40 | 19 | 21 | 8.79 | 11.37 | 49.35 | 39.47 | 41.70 | 9.88 | 8.25 | 4.15 | 45.35 | 3.65 | 3.16 | 4.56 | 6.00 | |
| 60 | 28 | 32 | 8.48 | 10.68 | 51.77 | 39.00 | 42.08 | 12.77 | 9.69 | 5.70 | 45.90 | 4.23 | 3.70 | 5.16 | 6.63 | |
| 80 | 36 | 44 | 8.13 | 10.02 | 53.36 | 38.12 | 42.04 | 15.24 | 11.32 | 7.02 | 45.94 | 4.65 | 4.12 | 5.59 | 7.05 | |
| 100 | 43.4 | 56.6 | 7.80 | 9.42 | 54.60 | 37.20 | 41.78 | 17.40 | 12.82 | 8.20 | 45.99 | 5.01 | 4.48 | 5.95 | 7.41 | |
| 120 | 50.7 | 69.3 | 7.44 | 8.82 | 55.70 | 36.35 | 41.50 | 19.35 | 14.20 | 9.27 | 46.00 | 5.34 | 4.81 | 6.27 | 7.74 | |
| 140 | 58 | 82 | 7.10 | 8.30 | 56.67 | 35.57 | 41.20 | 21.10 | 15.47 | 10.27 | 46.00 | 5.61 | 5.08 | 6.54 | 8.01 | |
| 160 | 65.2 | 94.8 | 6.76 | 7.76 | 57.52 | 34.78 | 40.90 | 22.74 | 16.62 | 11.20 | 46.02 | 5.86 | 5.33 | 6.80 | 8.26 | |
| 180 | 72.5 | 107.5 | 6.39 | 7.29 | 58.18 | 34.08 | 40.56 | 24.10 | 17.62 | 12.09 | 46.04 | 6.09 | 5.56 | 7.02 | 8.49 | |
| 200 | 79.7 | 120.3 | 6.05 | 6.82 | 58.79 | 33.35 | 40.19 | 25.44 | 18.60 | 12.91 | 46.06 | 6.32 | 5.79 | 7.25 | 8.72 | |
| 220 | 86.2 | 133.8 | 5.71 | 6.32 | 59.38 | 32.63 | 39.87 | 26.75 | 19.51 | 13.73 | 46.08 | 6.51 | 5.98 | 7.45 | 8.91 | |
| 240 | 92.5 | 147.5 | 5.40 | 5.88 | 60.00 | 31.94 | 39.50 | 28.06 | 20.50 | 14.50 | 46.10 | 6.71 | 6.18 | 7.65 | 9.11 | |

The mean values \bar{N} , \bar{Z} ; $\bar{\tau}_N$, $\bar{\tau}_Z$ with the calculated potential parameters for a number of idealized nuclei corresponding to the smoothed out mean of the valley on the total energy surface for the most stable odd nuclei).

The parameter $V^0 = V_z^0$ has therefore been treated as a variable in order to take this into account. For R^0 and a the values obtained for the neutron potential were maintained. The Coulomb potential

$$V_c(r) = e^2 \int \frac{\varrho_z(\mathbf{r}')}{|\mathbf{r} - \mathbf{r}'|} d\mathbf{r}',$$

is to be added to $V_z(r)$. For spherical symmetry $\varrho_z(r)$ from (9) or (9a) gives, as is known

$$(27) \quad \Phi_j(r)/e = 4\pi \left(\frac{1}{r} \int_0^r \varrho_z(x) x^2 dx + \int_r^{x \rightarrow \infty} \varrho_z(x) x dx \right),$$

within the charge distribution

$$\Phi_A(r)/e = 4\pi \frac{1}{r} \int_0^{x \rightarrow \infty} \varrho_z(x) x^2 dx,$$

outside the charge distribution and must be normalized by

$$(28) \quad Z - 1 = 4\pi \int_0^{x \rightarrow \infty} \varrho_z(x) x^2 dx.$$

For the charge distribution (9a) it follows:

$$V_c(r) = e \begin{cases} \Phi_j^I(r) + \Phi_j^{II}(C' - t'/2) & \text{for } 0 \leq r \leq C' - t'/2 & \text{I} \\ \Phi_A^I(r) + \Phi_j^{II}(r) & \text{» } C' - t'/2 \leq r \leq C' + t'/2 & \text{II} \\ \Phi_A^I(r) + \Phi_A^{II}(r) & \text{» } C' + t'/2 \leq r \leq \infty, \end{cases}$$

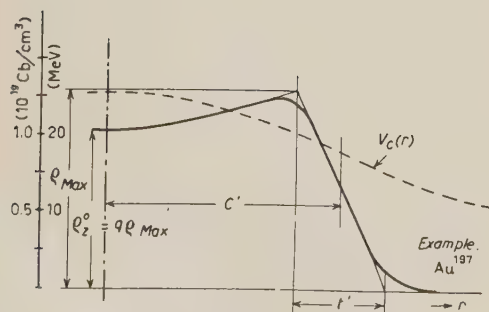


Fig. 7. — Charge distribution and potential. (Definition of the parameters).

where I and II refer to the given integration limits. Because of the simple form of (9a), only elementary integrals result. In these $\delta = (1 - q)/q$ ($\varrho_z^0 = q\varrho_{\max}$) with the linear function of A , $q(0) = 1 \geq q(A) \geq q(250) = 0.72$, $C' = 1.07 A^{\frac{1}{3}} \cdot 10^{-13}$ cm and $t' = 2.4 \cdot 10^{-13}$ cm were used to take into account at least approximately the central depression of the charge density affecting the Coulomb potential.

The depression within the nucleus has a distinct influence on the situation of the proton levels in heavier nuclei, as the calculations have shown. $V_c(r)$ can very well be substituted by a Coulomb potential created from a uniform density distribution with a slightly variable r_{0e} between 1.11 and 1.13 (10^{-13} cm).

We can therefore simply take

$$(27b) \quad V_c(r) = e^2 \frac{Z-1}{r_{0e}A} \begin{cases} (r_{0e}^3 A)/r & \text{for } r > r_{0e}A^{\frac{1}{3}} \\ (3r_{0e}^3 A^{\frac{2}{3}} - r^2)/2 & \text{» } r < r_{0e}A^{\frac{1}{3}} \end{cases}$$

The parameter V_z^0 was then chosen so that the mean separation energy for the protons (taking into account the spin-orbit interaction (26) with $V_1(r) = V_z(r) + V_c(r)$ and $\lambda = 0.38$) was satisfied.

While for the calculation of the levels in case $l \neq 0$, the calculation procedure, according to Appendix II, was very suitable, an ordinary perturbation calculation for the s -levels was carried out in order to take into account the « wine bottle » effect of the potential well.

Results: the parameter values for the proton potential are given in Table I, and a graphical representation of the result in Fig. 6. It can be seen here that the same spin-orbit coupling in the proton case gives reasonable results when the potential $V_z(r) + V_c(r)$ is set up in the given way.

8. - Comparison with experimental facts.

In order to obtain a direct comparison of nuclear spin and parity (measured from the ground and lowest excited energy levels, which might be interpreted as one particle levels in the widest sense of the word) with the calculated level schemes, these, have been drawn separately for neutrons and protons together with all measured assignments (assignments have been taken from the « Nuclear Data » (*)). Care was taken to plot only such excited levels which might be considered as certain. Doubtful assignments were excluded (see Fig. 8 and Fig. 9).

A glance at the measured values shows clearly the appearance of magic numbers, especially when spin and parity change (?). On the basis of the calculated pure one-particle ionization energies, we are here able to distinguish between magic and half-magic particle numbers. The magic numbers appear

(*) I am indebted to Dr. CH. TERREAUX who put a compilation at my disposal.

(?) This type of assignments diagram was first used by R. LATHAM: *Proc. Phys. Soc.*, 59, 979 (1947).

in cases when the energetic change in the calculated ionization energy after the filling of a sub-shell is greater than about 2.5 (MeV) in the model.

$$H' = -0.38 \left(\frac{\hbar}{m_{\pi} c} \right)^2 \frac{1}{r} \frac{dV_N(r)}{dr} \frac{(\mathbf{l}\mathbf{s})}{\hbar^2}$$

$$V_N^0 \sim 46 \text{ MeV}$$

$$a^0 = 2.93 \cdot 10^{-13} \text{ cm}$$

$$R^0 = (1.08 A^{\frac{1}{3}} + 2.4) \cdot 10^{-13} \text{ cm}$$

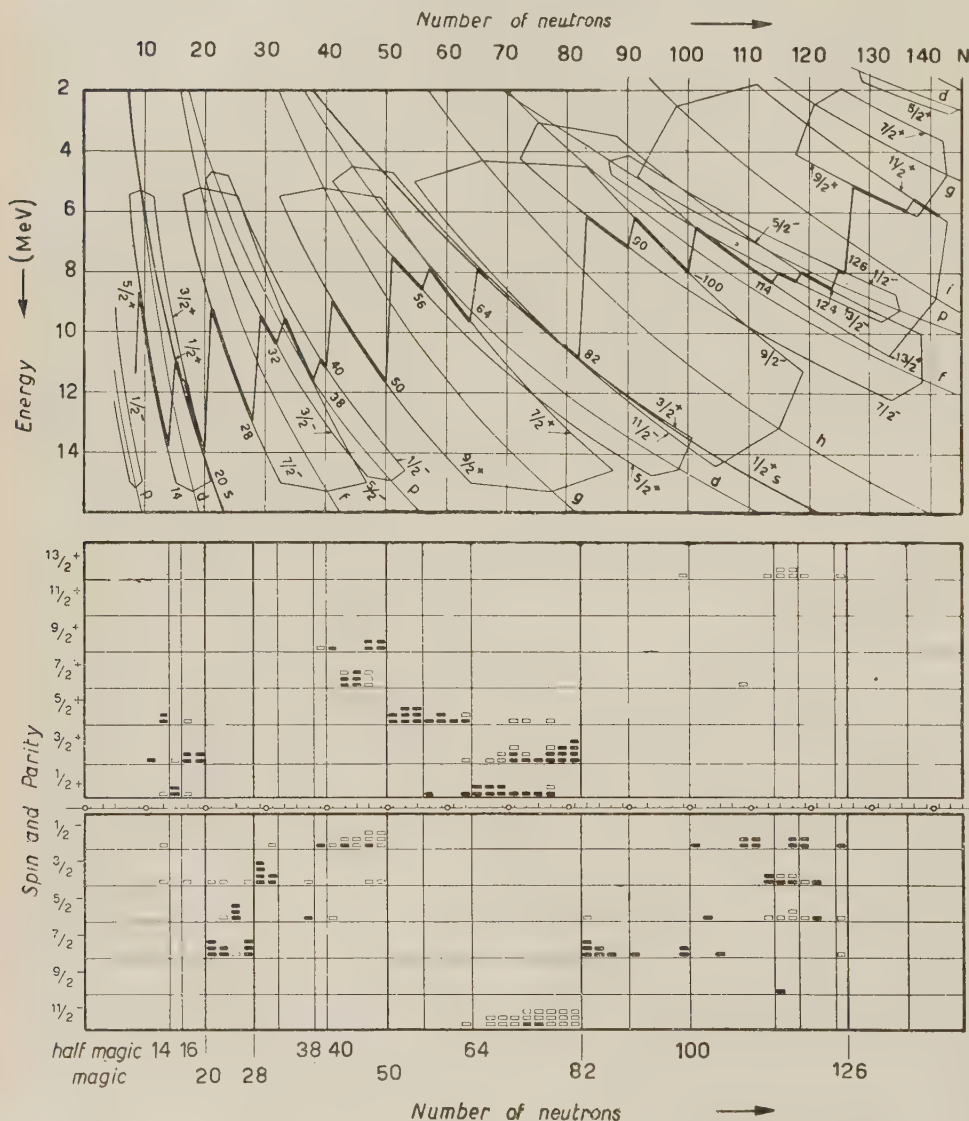


Fig. 8. — Shell model level scheme for neutrons together with the measured values for spin and parity from odd A nuclei: ■ ground states; □ excited states.

$$H' = -0.38 \left(\frac{\hbar}{m_{\pi} c} \right)^2 \frac{1}{r} \frac{d(V_z + V_c)}{dr} \cdot \frac{(\mathbf{l}\mathbf{s})}{\hbar^2}$$

$$R^0 = (1.08A^{\frac{1}{3}} + 2.4) \cdot 10^{-13} \text{ cm}$$

$$a^0 = 2.93 \cdot 10^{-13} \text{ cm}$$

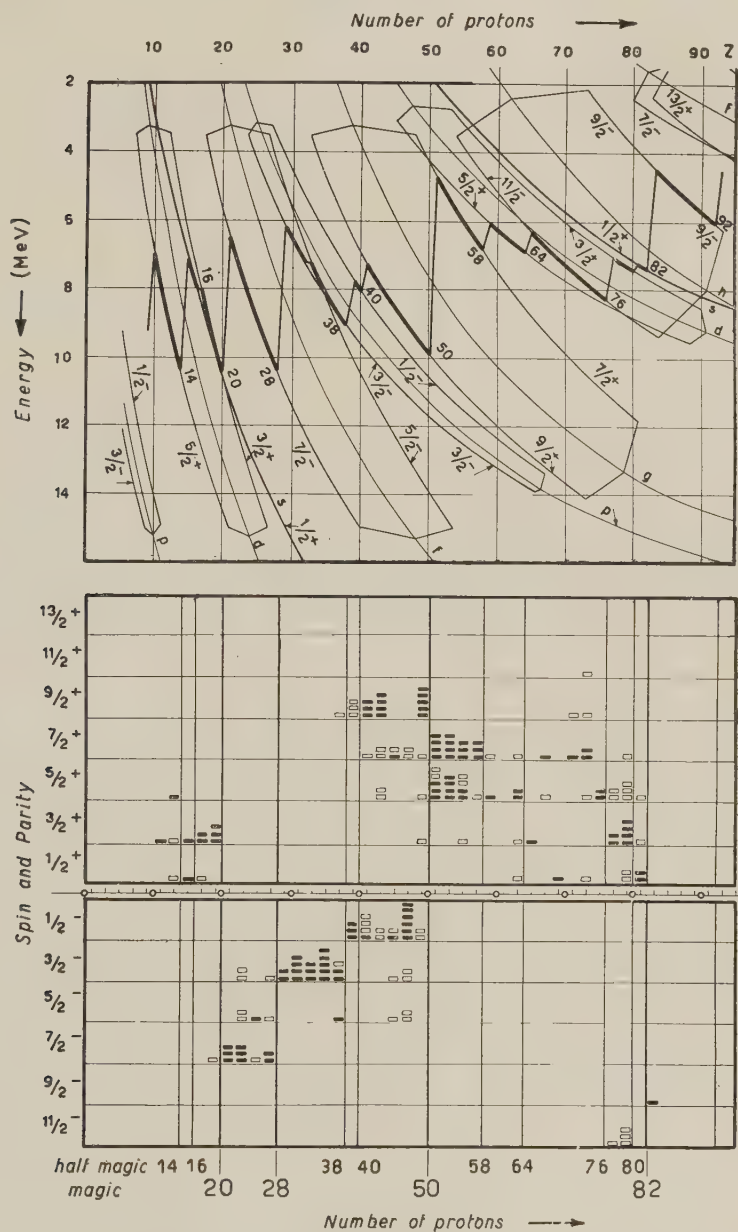


Fig. 9. - Shell model level scheme for protons together with the measured values for spin and parity from odd A nuclei: ■ ground states; □ excited states.

Results: the following magic numbers result:

| Neutron numbers (theoretical) | | | | | | | | | | | | | | |
|--|----|----|----|----|----|----|----|----|------|-----|-----|------|-----|---------------------|
| M | | 20 | 28 | | 40 | 50 | | 82 | | | | | 126 | |
| hM | 14 | 16 | | 32 | 38 | | 56 | 64 | 90 | 100 | 114 | 118 | 124 | 136 |
| Neutron numbers (from known experimental data for spin and parity) | | | | | | | | | | | | | | |
| M | 14 | 16 | 20 | 28 | 32 | 38 | 40 | 50 | 56 | 64 | 82 | (90) | 100 | (114) (118) 124 126 |
| Proton numbers (theoretical) | | | | | | | | | | | | | | |
| M | | 20 | 28 | | 50 | | | 82 | | | | | | |
| hM | 14 | 16 | | 38 | 40 | 58 | 64 | 76 | 80 | 92 | | | | |
| Proton numbers (from known experimental data for spin and parity) | | | | | | | | | | | | | | |
| M | 14 | 16 | 20 | 28 | 38 | 40 | 50 | 58 | (64) | 76 | 80 | 82 | | |

The numbers in brackets () are those for which the evidence from Fig. 8 or Fig. 9 for the appearance of a magic number is very small and uncertain.

An extensive comparison between the measured values for spin and parity of the observed odd nuclei shows that nearly all the low lying energy levels may be assigned as one particle states of the given central potentials $V(r)$. This is also valid for the highly degenerate half-filled sub-shells (the known break-down of the normal structure in the shells $7/2^-$ and $9/2^+$ with $I=j-1$ for neutrons and protons separately by their first occurring in the periodic system being excluded).

From the point of view of a perturbation theory, in which individual interactions occur (deviations from the average central potential) not only the degeneration is annulled but the perturbations will lead to strong admixtures to the unperturbed wave function from energy states in the close neighbourhood of the last occupied state (from neutrons and protons) in the one-particle picture.

Excited hole states occur after a sub-shell is filled, and arise from the displacement of a particle from the occupied state to the first unoccupied state. These holes therefore lie energetically below the separation energy.

Only in a few cases where admixtures are expected to be small one can test the calculated levels directly (closed shells plus or minus one nucleon) ⁽⁸⁾.

⁽⁸⁾ Levels in the neighbourhood of $1f7/2$ and Ca isotopes: R. H. NUSSBAUM: *Rev. Mod. Phys.*, **28**, 423 (1956); C. M. BRAAMS: *Phys. Rev.*, **103**, 1310 (1956). — Levels of ^{207}Pb : I. A. HARVEY: *Can. Journ. Phys.*, **31**, 278 (1953); D. E. ALBURGER and A. W. SUNYAR: *Phys. Rev.*, **99**, 695 (1955). — Levels of ^{209}Bi : M. J. POOLE: *Phil. Mag.*, **44**, 1298 (1953); E. A. ELIOT, D. HICKS, L. E. BEGHIAN and H. HALBAN: *Phys. Rev.*, **94**, 144 (1954); R. B. DAY: *Phys. Rev.*, **102**, 767 (1956).

TABLE II.

| ⁴¹ Ca (particle) 20 21 | | ⁴⁹ Ca (particle) 20 29 | | ²⁰⁷ Pb (hole) 82 125 | |
|--------------------------------------|------------------------|--------------------------------------|------------------------|--|-------------------------|
| exp. | theor. | exp. | theor. | exp. | theor. |
| 7/2 ⁻ 0 | f 7/2 ⁻ 0 | 3/2 ⁻ 0 | p 3/2 ⁻ 0 | 1/2 ⁻ 0 | p 1/2 ⁻ 0 |
| 3/2 ⁻ 1.95 | p 3/2 ⁻ 3.8 | (1/2 ⁻) 2.02 | p 1/2 ⁻ 2.0 | 5/2 ⁻ 0.569 | f 5/2 ⁻ 0.8 |
| (1/2 ⁻) 3.7 | p 1/2 ⁻ 6 | | f 5/2 ⁻ 1.7 | 3/2 0.894 | p 3/2 ⁻ 1.1 |
| 5/2 ≥ 4 | f 5/2 ⁻ 6.7 | | | 13/2 ⁺ 1.633 | i 13/2 ⁺ 1.9 |
| | | | | 7/2 ⁻ 2.338 | f 7/2 ⁻ 3.6 |
| ⁴¹ Sc (particle) 21 20 | | ⁴⁹ Sc (particle) 21 28 | | ²⁰⁹ Bi (particle) 83 126 | |
| 7/2 ⁻ 0 | f 7/2 ⁻ 0 | 7/2 ⁻ 0 | f 7/2 ⁻ 0 | 0 | h 9/2 ⁻ 0 |
| 3/2 ⁻ ≈ 1.9 | p 3/2 ⁻ 4.1 | 3/2 ⁻ 3.1 | p 3/2 ⁻ 4.2 | (7/2 ⁻) 0.9 | f 7/2 ⁻ 1.4 |
| | | (5/2 ⁻) ≥ 4 | f 5/2 ⁻ 6.4 | 1.61 | i 13/2 ⁺ 1.8 |
| | | | | 2.6 | f 5/2 ⁻ 3.6 |

Measured and calculated levels for spherical nuclei with closed shells plus or minus one nucleon.

(Note: for the given Ca and Sc isotopes the discrepancies between the calculated levels are great, but we are near the top of the wells and in this domain small variations of the shape have a great influence on the levels because centrifugal — and Coulomb — forces are not high. For ²⁰⁷Pb and ²⁰⁹Bi this situation is completely reversed).

In particular for those parts of the periodic system where marked deformations on the nuclei are observed, the given shell model spin-orbit interaction together with the central field potentials $V(r)$ predicts precisely a high degeneration in the unperturbed one-particle levels and a very large level density. If this is the case for neutrons together ($N = 90 \div 114$; $Z = 60 \div 75$), one can not longer expect that central field shell-structure in the perturbed case is a useful approximation (strong perturbations between the shells and therefore polarization of the core). Here the simplifying Bohr-Mottelson collective particle movement description leads to good results ⁽⁹⁾ but even the shell model situation suggests this.

A detailed analysis of the experimentally known shell structure for odd neutron nuclei related in a new way to the shell model is given recently by K. BLEULER and CH. TERREAUX ⁽¹⁰⁾.

⁽⁹⁾ A. BOHR: *Dan. Mat. Fys. Medd.*, **26**, No. 14 (1952); A. BOHR and B. R. MOTTELSON: *Dan. Mat. Fys. Medd.*, **27**, No. 16 (1953); K. GOTTFRIED: *Phys. Rev.*, **103**, 1087 (1956); S. A. MOSZKOWSKI: *Phys. Rev.*, **103**, 1328 (1956).

⁽¹⁰⁾ K. BLEULER and CH. TERREAUX: *Helv. Phys. Acta*, **30**, 183 (1957).

symmetry of the total wave function and can give information about the character of the forces (ordinary and exchange) between nucleons in nuclei.

The potential wells correspond in a good manner to the real part of the optical-model potential ⁽¹¹⁾ for the limiting cases in which the energy of the incoming nucleons tends towards zero. This can be tested for example with the positions of the *s*- (size) resonances for neutron scattering.

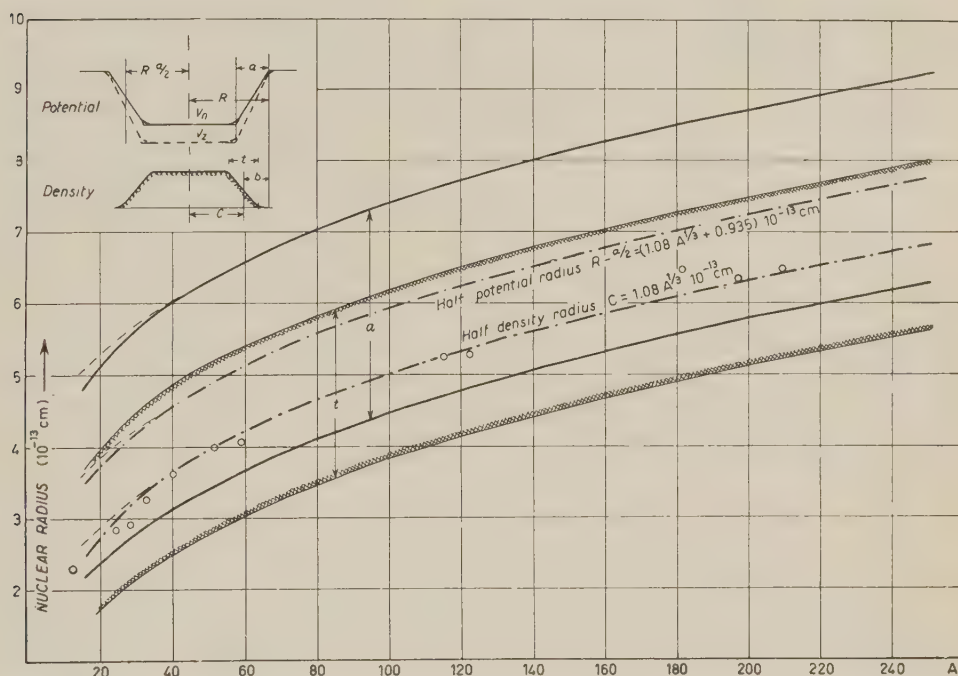


Fig. 11. — Nuclear radii consistent with the mean separation energies $\bar{\epsilon}_N(A)$ and $\bar{\epsilon}_Z(A)$. (Potential wells determined by taking into account spin-orbit splitting). \circ : Stanford results from high energy electron scattering experiments (with the assumption of a Fermi charge density shape).

For the potentials $V_N(r)$ the calculation gives

3s: at $A \approx 60$,

4s: at $A \approx 176$,

and the experiments.

3s: at $A \approx 57$,

4s: at $A \approx 160$,

⁽¹¹⁾ H. FESHBACH, C. PORTER and V. WEISSKOPF: *Phys. Rev.*, **96**, 448 (1954).

(but it should be born in mind, that the determination of the s -levels near the top of the wells gives values for A which are somewhat too high). The

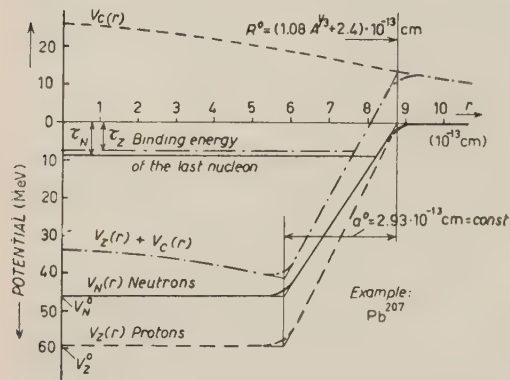


Fig. 12. — Mean potentials calculated for the heavy nucleus ^{207}Pb . (Note the Johnson-Teller effect, caused by Coulomb potential on protons).

spin-orbit coupling parameter determined by the analysis of proton polarization data ⁽¹²⁾, possesses, within the limits of error, the same value as that reached here by other methods.

It must here be remembered that when comparing this paper with others on the same subject, the nucleon mass M is not reduced inside the nucleus; nevertheless it represents the experimentally known low-lying spectra with half integer spin satisfactorily (*).

The proof of self consistency between the average potentials and the zero-order radial density distributions, will be given in a later paper, together with a study about the nuclear core.

* * *

I am very grateful to Prof. Dr. K. BLEULER for having encouraged me to undertake this research, also to Dr. CH. TERREAUX for many encouraging discussions, and to Prof. Dr. W. HEITLER for the helpful interest he has taken. I would like to thank the « Martha Selve-Gerdtsen-Stiftung » for the grant of a scholarship which has made it possible for me to carry on the greater part of the calculations. I am also much indebted to Professors A. ROSTAGNI, N. DALLAPORTA and A. KIND for their kind interest and the INFN for a support to finish the work.

⁽¹²⁾ T. ERIKSSON: *Nuovo Cimento*, **2**, 907 (1955); S. KÖHLER: *Nuovo Cimento*, **2**, 911 (1955) (with different energy), see also L. VAN HOVE: *Physica*, **22**, 979 (1956).

(*) A velocity dependence of the average potential $V(r, p)$ represented in a one, particle picture starting approximation, is the result of an enlargement of the shell model discussed in Sect. 2. Here we have to symmetrize $V(r, p)$ in order to obtain a hermitian operator, but the results will depend on the method used, since there is not a unique solution. A result of the present work is, that we cannot prove the effect of a mass reduction in the now formal kinetic energy operator $T(r)$ [which is the first approximation of the velocity dependence of $V(r)$] on the low lying one-particle levels. The energetic differences between the normal occupied shells inside the potential wells would give better information about the effective mass problem, but there is so far no direct experimental information in nuclear spectroscopy.

APPENDIX I

The adaptation of the potential well (schematically).

For this purpose it is best to transform (22) by $rR_{n,l}(r) = \chi_{n,l}(r)$ with the new limiting conditions $\chi(0) = \chi(\infty) = 0$ to form a one-dimensional Schrödinger equation and then use the approximation procedure for the solution which is given in Appendix II.

In order to adapt the parameters we make use of the properties of the Schrödinger equation for which the relative eigenvalues ε are invariable with respect to the following transformation:

$$(29) \quad \frac{E}{V^0} = \varepsilon,$$

$$(30) \quad \frac{V(r)}{V^0} = v(\xi) \quad \text{with} \quad \xi = \frac{r}{R^0}.$$

It follows that

$$(31) \quad \chi''(\xi) + \left[X^2(\varepsilon - v(\xi)) - \frac{l(l+1)}{\xi^2} \right] \chi(\xi) = 0,$$

with

$$(32) \quad X = \sqrt{\frac{2M}{\hbar^2}} \sqrt{V^0} R^0 = \mu^0 R^0 (V^0)^{-\frac{1}{2}},$$

and by means of (18), where in particular:

$$(33) \quad v(\xi) = \begin{cases} -1 & \text{for } 0 \leq \xi \leq 1-y, \\ -\frac{1}{y}(1-\xi) & \text{» } 1-y \leq \xi \leq 1, \\ 0 & \text{» } 1 \leq \xi \leq \infty, \end{cases}$$

with

$$(34) \quad y = a^0/R^0.$$

The parameters responsible for the essential physical properties of the system appear together in X , whereas the behaviour at the potential limits is represented by y .

Potentials with the same X and y are therefore equivalent to their relative eigenvalues ε and one can in this way, by calculating (31) for a suitable domain of X and y , adapt the parameter so that the conditions necessary for the mean value of the last fully occupied level (according to the Pauli principle) are

satisfied. However, for this purpose a three-dimensional representation $\varepsilon(X, y)$ is necessary, the calculation of which demands an excessive effort. An approximation procedure was therefore resorted to.

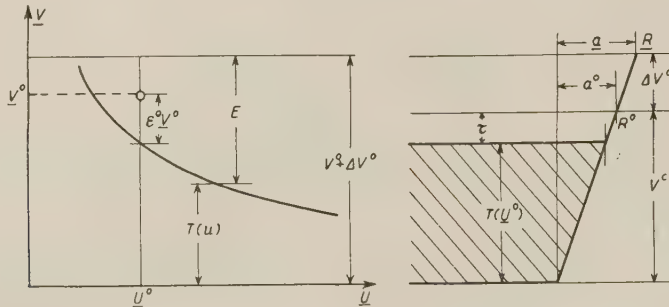


Fig. 13. - Approximation method for the determination of the potential parameters.

We next substitute all the parameters r, b, a^0, V^0 with constant upper limits $\underline{r}, \underline{b}, \underline{a}, \underline{V}$: they can be reached in a relatively easy way by means of experimental data. We then have:

$$(35) \quad \begin{cases} \underline{R} = R^0 + \Delta R^0, \\ \underline{V}^0 = V^0 + \Delta V^0, \\ \underline{a} = a^0 + \Delta a^0, \end{cases}$$

and the level scheme is calculated over a domain of A . If by means of the present relations one now sets up the suitably fulfilled condition that if

$$(36) \quad \frac{\underline{V}}{\underline{a}} = \frac{V^0}{a^0} = \frac{1}{k} = \text{const}, \quad \text{then} \quad E(\underline{V}, \underline{a}) \approx E^0(V^0, a^0) - \Delta V^0,$$

and consequently

$$(37) \quad \underline{R} = (R^0 - a^0) + \underline{a} = \underline{U} + k\underline{V},$$

$$(38) \quad \varepsilon = (\underline{V} + T(\underline{U}))/\underline{V}.$$

In particular however

$$(39) \quad X = \mu\sqrt{\underline{V}}R = \mu\underline{V}^{\frac{1}{2}}(\underline{U} + k\underline{V}),$$

$$(40) \quad y = \frac{\underline{a}}{\underline{R}} = \frac{\underline{a}}{\underline{U} + k\underline{V}} = \frac{k\underline{V}}{\underline{U} + k\underline{V}},$$

and this leads to the solution

$$(41) \quad \underline{U} = k\underline{V}\left(\frac{1}{y} - 1\right),$$

$$(42) \quad \underline{V} = (Xy/\mu k)^{\frac{2}{3}}.$$

Whereas for the adapted values

$$(43) \quad X^0 = \mu^0 (V^0)^{\frac{1}{2}} R^0,$$

$$(44) \quad y^0 = \frac{a^0}{R^0},$$

ought to be valid. Inserting (43) and (44) in (41) and (42) (for $X^0 = X$, $y^0 = y$) leads to

$$(45) \quad \underline{U}^0 = k \left(\frac{\mu^0 a^0}{\mu k} \sqrt{V^0} \right)^{\frac{2}{3}} \left(\frac{R^0 - a^0}{a^0} \right) = k V^0 \left(\frac{r_1}{a^0} A^{\frac{1}{3}} + b - 1 \right),$$

$$(46) \quad \underline{V}^0 = \left(\frac{\mu^0 a^0}{\mu k} \sqrt{V^0} \right)^{\frac{2}{3}},$$

and according to (38) it follows for one energy level that

$$(47) \quad E^0 \approx (\underline{V}^0 - T(\underline{U}^0)) \frac{V^0}{\underline{V}^0}.$$

When one sets up this levels in the right way with $\bar{N} = f(A)$ particles for the nuclei in the trough of the energy surface, its mean limiting curve may be made to agree with $\bar{\tau}_N(A)$ for a certain parameter combination over the whole periodical system. Then the level scheme can be recalculated, and so on.

APPENDIX II

The approximation method for the solution of the Schrödinger equation for a potential well.

The solution for the Schrödinger equation

$$-\frac{\hbar^2}{2M} \chi''(r) + (W_l(r) - E) \chi(r) = 0,$$

with

$$W_l(r) = V(r) + \frac{\hbar^2}{2M} \frac{l(l+1)}{r^2},$$

are required for the potential (18) (*).

For the s -states with $l=0$ it can be solved with analytical eigenfunctions. In the case of $l \neq 0$ we replace the potential which appears in the one dimensional Schrödinger equation as $W_1(r)$ with a suitable approach potential, for

(*) The spin-orbit potential is excluded here for simplicity, because the method for the solution remains the same. Only the parameters u, v, w are then functions of n, l, j .

which there are analytical, and therefore easily manageable eigenfunctions. In the case of the potentials used in this work, the following are particularly suitable:

oscillator potential:

$$-u_1 \left[1 - \left(\frac{r-v_1}{w_1} \right)^2 \right] = W_{n,l}^{(1)}(r).$$

Morse potential:

$$-u_2 \left[2 \exp \left(\frac{r-v_2}{w_2} \right) - \exp \left\{ -2 \left(\frac{r-v_2}{w_2} \right) \right\} \right] = W_{n,l}^{(2)}(r).$$

The parameters $u_i(n, l)$, $v_i(n, l)$, $w_i(n, l)$ with $i = 1$ or 2 must be chosen so that the approximate eigenfunctions obtained with them, have the same turning point on the potential boundary as the exact eigenfunctions. They must satisfy the condition

$$\int (W_l - W_{n,l}) \chi_{n,l}^{(i)2}(r) dr = 0,$$

with $(W_l - W_{n,l})$: small in the domain of $\chi_{n,l}^{(i)}(r)$. This adaptation was carried out graphically (*). The results for the approximate eigenvalues are then

$$E_{n,l}^{(1)} = -u_1 + \frac{\hbar}{w_1} \sqrt{\frac{2u_1}{M}} \left(n - \frac{1}{2} \right),$$

$$E_{n,l}^{(2)} = -u_2 + \frac{\hbar}{w_2} \sqrt{\frac{2u_2}{M}} \left(n - \frac{1}{2} \right) \left[1 - \frac{\hbar}{4u_2 w_2} \sqrt{\frac{2u_2}{M}} \left(n - \frac{1}{2} \right) \right],$$

and the exact eigenfunction $\chi_{n,l}(r)$ is analytically approximated by $\chi_{n,l}^{(i)}(r)$. Only the values $n = 1, 2, 3$ are necessary for the radial quantum number.

(*) See for a special case without spin-orbit interaction: K. BLEULER and CH. TERREAUX: *Helv. Phys. Acta*, **28**, 260 (1955).

RIASSUNTO

Si calcola fenomenologicamente, considerando il modello a shell, il potenziale medio dei protoni e dei neutroni. Si discutono diversi tipi di accoppiamento spin-orbita e i relativi ordini di grandezza; si analizza la loro influenza sui livelli ad una particella, per la maggior parte del sistema periodico (da $A \approx 40$). I calcoli dimostrano che una interazione spin-orbita del tipo $-\lambda(\hbar/m_{\pi}c)^2(1/r)(d/dr)V(r) \cdot (\mathbf{l}s/\hbar^2)$ è un parametro fisso, porta a risultati consistenti per la determinazione dei livelli ad una particella: sono riprodotti i numeri magici. Si ottengono inoltre dei potenziali diffusi per protoni e neutroni, in accordo con quelli derivabili dalla diffusione elastica elettrone-nucleo a bassa energia.

On the Creation Operators of Physical Particles.

G. MOHAN

Department of Physics, University of Nebraska - Lincoln, Nebraska

(ricevuto il 28 Agosto 1957)

Summary. — The conventional annihilation and creation operators of free particles are modified in view of the fact that all measurements require non-vanishing duration of time. The modified operators create and annihilate physical particles. Asymptotic assumption or adiabatic hypothesis are not invoked so that the renormalized S -matrix can be obtained without their help. The analysis of certain functions that occur in the definitions of the modified operators is incomplete.

1. — Introduction.

The renormalization procedure in the theory of the S -matrix is a process of converting the transition probability amplitudes between non-physical bare-particle states to those between physical particle states. However, it is desirable to develop a theory which avoids introducing non-physical states even in the intermediate stages. It is possible to write down neat expressions for renormalized S -matrix elements directly, but their derivation is always based on either some sort of asymptotic assumption ^(2,1) or on a switching technique ⁽³⁾ which has not been completely established and which looks quite non-physical. Our approach to the problem is entirely different. We attempt to improve the technique of construction of the in- and out-states. The conventional annihilation and creation operators are modified on the basis of the fact that no measurements are instantaneous. The modified operators refer to an ex-

⁽¹⁾ H. LEHMANN, K. SYMANZIK and W. ZIMMERMANN: *Nuovo Cimento*, **1**, 205 (1955).

⁽²⁾ K. NISHIJIMA: *Prog. Theor. Phys.*, **17**, 765 (1957). Other references are listed in this paper.

⁽³⁾ G. KÄLLÉN: *Physica*, **19**, 850 (1953).

tended time which should correspond to the duration of measurements (+). It is shown that these operators are the «renormalized» creation annihilation operators. Starting from them one can directly obtain the renormalized S -matrix by the usual methods.

2. - Instantaneous creation and annihilation operators.

We shall confine our attention on a system with pseudoscalar interaction between fermion field $\Psi(x)$ and boson field $\Phi(x)$. The method developed is applicable to other renormalizable theories also. The field equations and commutation relations are

$$(1) \quad \begin{cases} \left(\frac{\partial^2}{\partial x_\mu \partial x^\mu} - \kappa^2 \right) \Phi(x) = \delta \kappa^2 \Phi(x) + g \bar{\Psi}(x) \gamma_5 \Psi(x) + \lambda \Phi^3(x) \equiv -J(x), \\ \left(\gamma^\mu \frac{\partial}{\partial x^\mu} + m \right) \Psi(x) = \delta m \Psi(x) - g \gamma_5 \Psi(x) \Phi(x) \equiv I(x), \end{cases}$$

$$(2) \quad \begin{cases} [\Psi(x), \bar{\Psi}(x')]_+ \Big|_{x^0=x'^0} = i\gamma^0 \delta(\mathbf{x} - \mathbf{x}'), \\ \left[\Phi(x), \frac{\partial \Phi(x')}{\partial x'^0} \right]_- \Big|_{x^0=x'^0} = i \delta(\mathbf{x} - \mathbf{x}'). \end{cases}$$

Corresponding to every instant τ a set of annihilation and creation operators for the bosons and Fermi particles and antiparticles can be constructed from the Heisenberg fields. For example, the creation operators are (*)

$$(3) \quad \begin{cases} c_\tau^*(\mathbf{k}) = i \int_{x^0=\tau} d^3x \left[\frac{\partial}{\partial x^0}, f_{\mathbf{k}}(x) \right]_- \Phi(x), \\ a_\tau^*(\mathbf{p}\beta) = -i \int_{x^0=\tau} d^3x \bar{\Psi}(x) \gamma_0 u_\beta(\mathbf{p}; x), \\ b_\tau^*(\mathbf{p}\beta) = -i \int_{x^0=\tau} d^3x \bar{v}_\beta(\mathbf{p}; x) \gamma_0 \Psi(x), \end{cases}$$

where

$$f_{\mathbf{k}}(x) = \frac{(2\pi)^{-\frac{3}{2}}}{\sqrt{2k^0}} \exp[ikx]; \quad k^0 = \sqrt{\mathbf{k}^2 + \kappa^2},$$

$$u_\beta(\mathbf{p}; x) = (2\pi)^{-\frac{3}{2}} \sqrt{\frac{m}{p^0}} u_\beta(\mathbf{p}) \exp[ipx]; \quad p^0 = \sqrt{\mathbf{p}^2 + m^2}; \quad \text{etc.}$$

(+) E. C. G. STUECKELBERG has studied S -matrix with non-precise epoche of initial and final states separated by finite time interval; *Phys. Rev.*, **81**, 130 (1951).

(*) $\left[\frac{\partial}{\partial x^0}, f(x) \right]_- g(x) = \frac{\partial f}{\partial x^0} g - f \frac{\partial g}{\partial x^0}.$

These satisfy the typical commutation relations of creation and annihilation operators, for example,

$$(4) \quad \begin{cases} [a_\tau(\mathbf{p}'\beta'), a_\tau^*(\mathbf{p}\beta)]_+ = \delta_{\beta,\beta'} \delta(\mathbf{p} - \mathbf{p}'), \\ [a_\tau(\mathbf{p}'\beta'), a_\tau(\mathbf{p}\beta)]_+ = 0. \end{cases}$$

It cannot be asserted in general that c_τ^* , a_τ^* and b_τ^* create physical particles when acting on the physical vacuum state $|0\rangle$. In order that the state vectors $c_\tau^*|0\rangle$, $a_\tau^*|0\rangle$ and $b_\tau^*|0\rangle$ represent physical particles they must be eigenstates of $-P_\mu P^\mu$ with eigen-values κ^2 , m^2 and m^2 respectively, where P^μ is the *total* energy-momentum operator and κ and m are the masses of a physical boson and a physical fermion. For finite τ this condition is not satisfied, but if appropriate limit to remote future or to remote past can be taken, then, indeed, the above mentioned states represent physical particles ⁽⁴⁾ (the so-called outgoing and ingoing particles). Such a limiting process will be proposed in this paper.

In order to construct a complete orthonormal set of multiple physical particles by the repeated application of the creation operators it is obviously not enough to show that the proper limits of $c_\tau^*|0\rangle$, $a_\tau^*|0\rangle$ and $b_\tau^*|0\rangle$ are physical one-particle states. One also needs to establish commutation relations of the following type

$$(5) \quad \begin{cases} \lim_{\substack{\tau \rightarrow \infty \\ \tau' \rightarrow \infty}} z_3^{-1} [c_\tau(\mathbf{k}), c_{\tau'}^*(\mathbf{k})]_- = \delta(\mathbf{k} - \mathbf{k}'), \\ \lim_{\substack{\tau \rightarrow \infty \\ \tau' \rightarrow \infty}} z_3^{-1} [c_\tau(\mathbf{k}'), c_\tau(\mathbf{k})]_- = 0, \end{cases}$$

and similar ones for Fermi particles and antiparticle operators. The important point is that the limits to the remote future (or past) for each operator in a product have to be taken independently.

For the present work, before taking the limit to remote future or past we modify the instantaneous creation annihilation operators themselves in a way so as to conform more with the actual measuring technique. Such procedure yields the desired commutation relations also.

3. - Commutators of instantaneous operators.

Before introducing the modified creation and annihilation operators, we want to obtain in a convenient form the commutators between instantaneous

⁽⁴⁾ G. MOHAN: *Suppl. Nuovo Cimento*, **5**, 440 (1957).

operators that refer to different instant parameters τ and τ' . These relations will be used in the next section.

By means of the Gauss theorem we can relate the corresponding operators belonging to the two different instant parameters τ and τ' . For example,

$$\begin{aligned} -c_{\tau}^*(\mathbf{k}) + c_{\tau_0}^*(\mathbf{k}) &= i \int_{\tau_0}^{\tau} d^4x \frac{\partial}{\partial x_{\mu}} \left\{ \left[\frac{\partial}{\partial x^{\mu}}, f_{\mathbf{k}}(x) \right] \Phi(x) \right\} = \\ &= -i \int_{\tau_0}^{\tau} d^4x f_{\mathbf{k}}(x) \left(\frac{\partial^2}{\partial x_{\mu}^2} - \kappa^2 \right) \Phi(x), \end{aligned}$$

or

$$(6) \quad c_{\tau}^*(\mathbf{k}) = c_{\tau_0}^*(\mathbf{k}) - i \int_{\tau_0}^{\tau} d^4x f_{\mathbf{k}}(x) J(x).$$

Similarly we have

$$(7) \quad a_{\tau}^*(\mathbf{p}\beta) = a_{\tau_0}^*(\mathbf{p}\beta) - i \int_{\tau_0}^{\tau} d^4x \bar{I}(x) u_{\beta}(\mathbf{p}; x),$$

and other relations. The product $a_{\tau'}(\mathbf{p}'\beta') a_{\tau}^*(\mathbf{p}\beta)$ can now be expressed in a symmetrical fashion which will subsequently yield a simple expression for the anti-commutator of $a_{\tau'}(\mathbf{p}'\beta')$ and $a_{\tau}^*(\mathbf{p}\beta)$.

$$\begin{aligned} (8) \quad a_{\tau'}(\mathbf{p}'\beta') a_{\tau}^*(\mathbf{p}\beta) &= a_{\tau'}(\mathbf{p}'\beta') \left[a_{\tau_0}^*(\mathbf{p}\beta) - i \int_{\tau_0}^{\tau} d^4x \bar{I}(x) u_{\beta}(\mathbf{p}; x) \right] = \\ &= a_{\tau_0}(\mathbf{p}'\beta') a_{\tau_0}^*(\mathbf{p}\beta) - i a_{\tau'}(\mathbf{p}'\beta') \int_{\tau_0}^{\tau} d^4x \bar{I}(x) u_{\beta}(\mathbf{p}; x) + \\ &\quad + i \int_{\tau_0}^{\tau'} d^4y \bar{u}_{\beta'}(\mathbf{p}'; y) I(y) a_{\tau_0}^*(\mathbf{p}\beta). \end{aligned}$$

The product $I(y) a_{\tau_0}^*(\mathbf{p}\beta)$ in the last integral can be put in a different form:

$$\begin{aligned} (9) \quad I(y) a_{\tau_0}^*(\mathbf{p}\beta) &= I(y) a_y^*(\mathbf{p}\beta) + i I(y) \int_{\tau_0}^y d^4x \bar{I}(x) u_{\beta}(\mathbf{p}; x) = \\ &= [I(y), a_y^*(\mathbf{p}\beta)]_+ - a_{\tau}^*(\mathbf{p}\beta) I(y) - \\ &\quad - i \int_y^{\tau} d^4x \bar{I}(x) u_{\beta}(\mathbf{p}; x) I(y) + i I(y) \int_{\tau_0}^y d^4x \bar{I}(x) u_{\beta}(\mathbf{p}; x) = \\ &= [I(y), a_y^*(\mathbf{p}\beta)]_+ - a_{\tau}^*(\mathbf{p}\beta) I(y) + i \int_{\tau_0}^{\tau} d^4x T \{ I(y) \bar{I}(x) \} u_{\beta}(\mathbf{p}; x). \end{aligned}$$

Substituting eq. (9) into eq. (8) we obtain

$$\begin{aligned}
 (10) \quad a_{\tau'}(\mathbf{p}'\beta') a_{\tau}^*(\mathbf{p}\beta) &= a_{\tau_0}(\mathbf{p}'\beta') a_{\tau_0}^*(\mathbf{p}\beta) - \\
 &- i a_{\tau'}(\mathbf{p}'\beta') \int_{\tau_0}^{\tau} d^4x \bar{I}(x) u_{\beta}(\mathbf{p}; x) - i a_{\tau}^*(\mathbf{p}\beta) \int_{\tau_0}^{\tau'} d^4y u_{\beta'}(\mathbf{p}'; y) I(y) - \\
 &- \int_{\tau_0}^{\tau} d^4y \int_{\tau_0}^{\tau'} d^4x \bar{u}_{\beta'}(\mathbf{p}'; y) T \{I(y) \bar{I}(x)\} u_{\beta}(\mathbf{p}; x) + \\
 &+ i \int_{\tau_0}^{\tau'} d^4y \bar{u}_{\beta'}(\mathbf{p}'; y) [I(y), a_{\tau}^*(\mathbf{p}\beta)]_+.
 \end{aligned}$$

A similar expression can be derived for the product $a_{\tau}^*(\mathbf{p}\beta) a_{\tau'}(\mathbf{p}'\beta')$. Adding these two expressions we obtain

$$\begin{aligned}
 (11) \quad [a_{\tau'}(\mathbf{p}'\beta'), a_{\tau}^*(\mathbf{p}\beta)]_+ &= [a_{\tau_0}(\mathbf{p}'\beta'), a_{\tau_0}^*(\mathbf{p}\beta)]_+ + \\
 &+ i \int_{\tau_0}^{\tau'} d^4y \bar{u}_{\beta'}(\mathbf{p}'; y) [I(y), a_{\tau}^*(\mathbf{p}\beta)]_+ - i \int_{\tau_0}^{\tau} d^4x [\bar{I}(x), a_{\tau'}(\mathbf{p}'\beta')]_+ u_{\beta}(\mathbf{p}; x).
 \end{aligned}$$

All other commutators between various annihilation and creation operators can be derived by this method. Some of these are given below:

$$\begin{aligned}
 (12) \quad [a_{\tau'}(\mathbf{p}'\beta'), a_{\tau}(\mathbf{p}\beta)]_+ &= \\
 &= i \int_{\tau_0}^{\tau} d^4x \bar{u}(\mathbf{p}; x) [I(x), a_{\tau'}(\mathbf{p}'\beta')]_+ + i \int_{\tau_0}^{\tau'} d^4x \bar{u}(\mathbf{p}'; x) [I(x), a_{\tau}(\mathbf{p}\beta)]_+,
 \end{aligned}$$

$$\begin{aligned}
 (13) \quad [c_{\tau'}(\mathbf{k}'), c_{\tau}^*(\mathbf{k})]_- &= [c_{\tau_0}(\mathbf{k}'), c_{\tau_0}^*(\mathbf{k})]_- + \\
 &+ i \int_{\tau_0}^{\tau} d^4y f_{\mathbf{k}'}^*(y) [J(y), c_{\tau}^*(\mathbf{k})]_- + i \int_{\tau_0}^{\tau'} d^4x f_{\mathbf{k}}(x) [J(x), c_{\tau'}(\mathbf{k}')]_-.
 \end{aligned}$$

Expressions for other commutators have essentially the same structure. Substituting for $I(x)$ from eq. (1) into eqs. (11) and (13) we obtain

$$(14) \quad [a_{\tau'}(\mathbf{p}'\beta'), a_{\tau}^*(\mathbf{p}\beta)]_+ = [a_{\tau_0}(\mathbf{p}'\beta'), a_{\tau_0}^*(\mathbf{p}\beta)]_+ + i \int_{\tau'}^{\tau} d^4x N_{\mathbf{p}'\beta', \mathbf{p}\beta}(x),$$

$$(15) \quad [c_{\tau'}(\mathbf{k}), c_{\tau}^*(\mathbf{k})]_- = [c_{\tau_0}(\mathbf{k}'), c_{\tau}^*(\mathbf{k})]_- + i \int_{\tau'}^{\tau} d^4x G_{\mathbf{k}'\mathbf{k}}(x),$$

where

$$N_{\mathbf{p}'\beta, \mathbf{p}\beta}(x) = \bar{u}_{\beta}(\mathbf{p}'; x) \{ \delta m - g\gamma_5 \Phi(x) \} u_{\beta}(\mathbf{p}; x),$$

$$G_{\mathbf{k}\mathbf{k}}(x) = f_{\mathbf{k}}^*(x) f_{\mathbf{k}}(x) \{ \delta \mathcal{H}^2 + 3\lambda \Phi^2(x) \}.$$

A significant result that follows from these calculations is the vanishing of the following anticommutators for arbitrary τ and τ' :

$$(16) \quad \begin{cases} [a_{\tau'}, a_{\tau}]_+ = 0, \\ [b_{\tau'}, b_{\tau}]_+ = 0, \\ [a_{\tau'}, b_{\tau}^*]_+ = 0. \end{cases}$$

Now we are ready to introduce the modified operators and obtain their commutation properties by the help of the results of this section.

4. - Modified creation and annihilation operators.

It is generally believed that the creation operators of physical particles are obtained by taking suitable limits in the definitions (3) to remote future or past. In any expression involving product of such operators, such as the left hand side of eqs. (5), the limit for each operator must be taken independently. One might expect that this has the effect of making the reference to the instant parameter diffuse and thus, at least partially, take account of the non-vanishing duration of the measuring processes.

Our procedure is somewhat different. We first modify the definitions of the creation-annihilation operators themselves so as to be characterized by an extended time interval and then take the limit to remote past or future. The purpose of the limit is then only to avoid the insignificant transient effects. How exactly the time extension should be incorporated can be answered, in our opinion, only by a future well-developed quantum mechanical theory of measurements. Presently, we propose an extremely simple modification which undoubtedly can only be an idealization of completely realistic creation operators (*):

$$(17) \quad a^*(\mathbf{p}\beta) = \lim_{\frac{1}{2}(\tau_1 + \tau_2) \rightarrow \infty} \frac{1}{\tau_2 - \tau_1} \int_{\tau_1}^{\tau_2} d\tau \exp[i\alpha_1 \tau] a_{\tau}^*(\mathbf{p}\beta),$$

(*) We shall in the following study the limit to remote future alone. The case of remote past is very similar.

$$(18) \quad b^*(\mathbf{p}\beta) = \lim_{\frac{1}{2}(\tau_1 + \tau_2) \rightarrow \infty} \frac{1}{\tau_2 - \tau_1} \int_{\tau_1}^{\tau_2} d\tau \exp[i\alpha_1 \tau] b_\tau^*(\mathbf{p}\beta),$$

$$(19) \quad c^*(\mathbf{k}) = \lim_{\frac{1}{2}(\tau_1 + \tau_2) \rightarrow \infty} \frac{1}{\tau_2 - \tau_1} \int_{\tau_1}^{\tau_2} d\tau \exp[i\alpha_2 \tau] c_\tau^*(\mathbf{k}),$$

where α_1 and α_2 are real infinitesimal functions of the parameters of the theory and also of \mathbf{p} and \mathbf{k} respectively. These functions will be further specified presently. The interval $(\tau_2 - \tau_1)$ should be connected with the duration of measurement. The exponential factor in the integrands can be interpreted as altering the energy in the functions $u(\mathbf{p}; x)$, $v(\mathbf{p}; x)$ and $f_k(x)$ by real infinitesimal amount.

We now compute the anticommutator of $a(\mathbf{p}'\beta')$ and $a^*(\mathbf{p}\beta)$. From eq. (14) we have (*)

$$\begin{aligned} (20) \quad & [a(\mathbf{p}'\beta'), a^*(\mathbf{p}\beta)]_+ = \\ & = \lim_{\frac{1}{2}(\tau_1 + \tau_2) \rightarrow \infty} \frac{1}{(\tau_2 - \tau_1)^2} \int_{\tau_1}^{\tau_2} d\tau \int_{\tau_1}^{\tau_2} d\tau' \exp[i(\alpha_1 \tau - \alpha'_1 \tau')] [a_\tau(\mathbf{p}'\beta'), a_{\tau'}^*(\mathbf{p}\beta)]_+ = \\ & = \lim_{\frac{1}{2}(\tau_1 + \tau_2) \rightarrow \infty} \left\{ \frac{4 \exp[i\frac{1}{2}(\alpha_1 - \alpha'_1)(\tau_2 + \tau_1)] \sin \frac{1}{2}\alpha_1(\tau_2 - \tau_1) \sin \frac{1}{2}\alpha'_1(\tau_2 - \tau_1)}{\alpha_1 \alpha'_1 (\tau_2 - \tau_1)^2} \right. \\ & \quad \cdot [a_{\tau_0}(\mathbf{p}'\beta'), a_{\tau_0}^*(\mathbf{p}\beta)]_+ + \frac{i}{(\tau_2 - \tau_1)^2} \int_{\tau_1}^{\tau_2} d^4x N_{\mathbf{p}'\beta', \mathbf{p}\beta}(x) \frac{1}{\alpha_1 \alpha'_1} \cdot \\ & \quad \cdot \left. \left(\exp[-i(\alpha'_1 x^0 - \alpha \tau_2)] - \exp[-i(\alpha'_1 x^0 - \tau_1)] + \exp[i(\alpha_1 x^0 - \alpha_1 \tau_1)] - \right. \right. \\ & \quad \left. \left. - \exp[i(\alpha_1 x^0 - \alpha'_1 \tau_2)] + \exp[i(\alpha_1 \tau_1 - \alpha'_1 \tau_2)] - \exp[i(\alpha_1 \tau_2 - \alpha'_1 \tau_1)] \right) \right\}. \end{aligned}$$

Let $M(x^0)$ denote the quantity within the bracket in the integrand. An arbitrary matrix element of the anticommutator between energy momentum eigenstates will involve an integral of the type $\int_{\tau_1}^{\tau_2} d^4x \exp[iQx] M(x^0)$ which is easily evaluated. The $\frac{1}{2}(\tau_1 + \tau_2)$ dependence of the resulting expression is only through a factor

$$\exp[-i(Q^0 + \alpha'_1 - \alpha_1)\frac{1}{2}(\tau_1 + \tau_2)].$$

(*) $\alpha_1 = \alpha_1(\mathbf{p})$; $\alpha'_1 = \alpha_1(\mathbf{p}')$.

Now if we let $\frac{1}{2}(\tau_1 + \tau_2)$ go to $+\infty$, then unless there is a factor singular at $Q^0 = \alpha_1 - \alpha'_1$, we can replace the above factor by $\delta_{Q^0, \alpha_1 - \alpha'_1}$. Putting $Q^0 = \alpha_1 - \alpha'_1$ and retaining only the lowest order terms in α_1 and α'_1 we find that

$$(21) \quad \frac{i}{(\tau_2 - \tau_1)^2} \int_{\tau_1}^{\tau_2} d^4x \exp[iQx] M(x^0) = -\frac{(2\pi)^3}{12} \delta(Q)(\alpha_1 + \alpha'_1)(\tau_2 - \tau_1) \delta_{Q^0, \alpha_1 - \alpha'_1}.$$

From eq. (21) we find that to the lowest order in α_1 and α'_1 the matrix element of the anticommutator between any two energy-momentum eigenstates $|P'\gamma'\rangle$ and $|P''\gamma''\rangle$ is given by the following equation:

$$(22) \quad \begin{aligned} \langle P''\gamma'' | [a(\mathbf{p}'\beta'), a^*(\mathbf{p}\beta)]_+ | P'\gamma' \rangle &= [a_{\tau_0}(\mathbf{p}'\beta'), a_{\tau_0}^*(\mathbf{p}\beta)]_+ \langle P''\gamma'' | P'\gamma' \rangle - \\ &- \frac{m(\tau_2 - \tau_1)^2}{6p^0} \alpha_1 \delta m \delta_{\beta, \beta'} \delta(\mathbf{p} - \mathbf{p}') \langle P''\gamma'' | P'\gamma' \rangle + \\ &+ \frac{m(\tau_2 - \tau_1)^2}{12\sqrt{p^0 p'^0}} (\alpha_1 + \alpha'_1) \delta_{p^0 + p'^0 - p^0 - p'^0, \alpha_1 - \alpha'_1} \cdot \\ &\cdot \delta(\mathbf{p} + \mathbf{p}' - \mathbf{p} - \mathbf{p}') \cdot \bar{u}_{\beta'}(\mathbf{p}') \langle P''\gamma'' | g\gamma_5 \Phi(0) | P'\gamma' \rangle u_{\beta}(\mathbf{p}). \end{aligned}$$

So far we have made only one assumption; that is, α_1 is vanishingly small. Now the objective is to make it vanish in such a way that

$$z_2^{-1} [a(\mathbf{p}'\beta'), a^*(\mathbf{p}\beta)]_+ = \delta_{\beta, \beta'} \delta(\mathbf{p} - \mathbf{p}').$$

Consequently the last term on the right hand side of the eq. (22) must vanish. Further, since $0 \leq z_2 < 1$, the second term on the right hand side must not vanish. This means that for the applicability of this method δm , and similarly $\delta\kappa^2$ must necessarily be infinite. Following properties of α_1 can now be concluded:

$$(23) \quad \alpha_1(\mathbf{p}) = p^0 \eta_1,$$

where η_1 is independent of \mathbf{p} ,

$$(24) \quad z_2^{-1} \left\{ 1 - \frac{m(\tau_2 - \tau_1)^2}{6} \eta_1 \delta m \right\} = 1,$$

and

$$(25) \quad z_2^{-1} \eta_1 g\Phi = 0.$$

A similar consideration for the vanishing of the commutator $[a(\mathbf{p}\beta), c^*(\mathbf{k})]_-$

leads to the condition

$$(26) \quad z_2^{-\frac{1}{2}} z_3^{-\frac{1}{2}} \eta_1 g \Psi = 0.$$

The left hand sides of the eqs. (24), (25) and (26) are supposed to be defined through a limiting procedure in which η_1 goes to zero and δm goes to infinity.

With a better understanding of the magnitudes and relationships between the renormalization constants δm , $\delta \kappa^2$, z_1 , z_2 and z_3 it is hoped that an explicit expression for α_1 and also for α_2 will be obtainable. As it is, full implication of the eqs. (25) and (26) need to be further studied.

Similar relations for the function α_2 can be obtained from the commutators of boson creation annihilation operators.

Thus we find that functions α_1 and α_2 can possibly be so chosen that the operators $z_2^{-\frac{1}{2}} a^*(\mathbf{p}\beta)$, $z_2^{-\frac{1}{2}} a(\mathbf{p}\beta)$, $z_3^{-\frac{1}{2}} c^*(\mathbf{k})$, etc., have the typical commutation properties of annihilation and creation operators. In the next section we show that they annihilate or create physical particles.

5. - Physical particle states and S -matrix.

Let us consider as an example the state vector $z_2^{-\frac{1}{2}} a^*(\mathbf{p}\beta) |0\rangle$. If it represents a physical Fermi particle with momentum \mathbf{p} then we must have

$$(27) \quad P^\mu z_2^{-\frac{1}{2}} a^*(\mathbf{p}\beta) |0\rangle = p^\mu z_2^{-\frac{1}{2}} a^*(\mathbf{p}\beta) |0\rangle$$

so that

$$(28) \quad -P^\mu P_\mu z_2^{-\frac{1}{2}} a^*(\mathbf{p}\beta) |0\rangle = m^2 z_2^{-\frac{1}{2}} a^*(\mathbf{p}\beta) |0\rangle.$$

From the definition of $a^*(\mathbf{p}\beta)$ and noting that

$$\Psi(x) = \exp[-iPx] \Psi(0) \exp[iPx],$$

it is easily seen that $\langle P' \gamma' | z_2^{-\frac{1}{2}} a^*(\mathbf{p}\beta) |0\rangle$ vanishes unless $\mathbf{P}' = \mathbf{p}$ and $P'^0 = p^0 \equiv \sqrt{\mathbf{p}^2 + m^2}$. This implies the eqs. (27) and (28).

The renormalized S -matrix elements are constructed from the well known method of reduction formula (5).

(5) See reference (1).

6. - Conclusion.

We have introduced a set of modified creation and annihilation operators defined by the eqs. (17), (18) and (19). They differ from the conventional operators by incorporating a reference to extended time in their definitions, and thus there is a closer correspondence with actual measurements. It is shown, independently of asymptotic assumptions and provided certain consistency requirements can be met, that these obey the typical commutation relations of creation and annihilation operators, and they annihilate and create physical particles. There is no need for adiabatic hypotheses or asymptotic assumptions in the construction of multiple physical particle states or the renormalized S -matrix from these modified operators. However the analysis of the functions α_1 and α_2 which go to define the modified operators is incomplete. We expect that a study of α_1 and α_2 might be related with the renormalizability of the theory.

RIASSUNTO (*)

In vista del fatto che tutte le misure richiedono un tempo non scompaenente, si modificano gli usuali operatori di distruzione e di creazione. Gli operatori modificati creano e distruggono particelle fisiche. Non si invocano ipotesi asintotiche o adiabatiche, cosicchè si può ottenere la matrice S rinormalizzata senza il loro ausilio. L'analisi di talune funzioni che compaiono nelle definizioni degli operatori modificati è incompleta.

(*) Traduzione a cura della Redazione.

Decay of ^{152}Eu and the Unified Nuclear Model.

S. K. BHATTACHERJEE, T. D. NAINAN (*), SHREE RAMAN and BALDEV SAHAI

Tata Institute of Fundamental Research - Bombay

(ricevuto il 29 Agosto 1957)

Summary. — The radiations from ^{152}Eu ($t_{1/2}=13$ yrs) were investigated using an intermediate image spectrometer, a magnetic thin lens spectrometer and a coincidence scintillation spectrometer. Three β^- -groups are present with end-points (1450 ± 25) , (1040 ± 20) , (710 ± 20) keV; the highest energy group exhibits an α -shape. γ -ray investigations showed that the following γ -rays are present: 101 (5), 121 (88), 244 (30), 315 (4), 344 (100), 410 (9), 442 (4), 710 (13), 770 (77), 888 (14), 970 (89), 1090 (96), 1127 (96) and 1410 (135) keV. K -conversion coefficients were estimated for most of these transitions and multipole orders were assigned. X-ray- γ , γ - γ and β - γ coincidence experiments allow us to construct the decay scheme of ^{152}Eu . The difference in level structure in ^{152}Sm ($N=90$) and ^{152}Gd ($N=88$) is evident from the experimental results. The first three excited states at 121, 365 and 807 keV in ^{152}Sm are identified as the three members of the ground state rotational band ($K=0$); the levels at 1090 and 1248 keV having $I=2+$, and $3+$ respectively are shown to be the quadrupole γ -vibrational states corresponding to $K=2$. The highest excited state in ^{152}Sm is at 1417 keV and is most likely fed entirely by L -capture; this is the only odd-parity state in ^{152}Sm having the character $I=1-$. The levels in ^{152}Gd at 344 and 754 keV both with $I=2+$, reached by β^- -decay, are characteristic of the collective vibrations of the electric quadrupole type about a spherical equilibrium shape. The level at 1114 keV in ^{152}Gd has the character $I=3-$ and is interpreted as due to the octupole vibrations. The ground state of ^{152}Eu has been assigned the spin $I=4-$; the branching ratios and the transition probabilities for the β^- -groups and electron capture transitions have been calculated. The experimental results are consistent with the predictions of the Unified Nuclear Model.

(*) Present address: Department of Physics, University of Indiana, Bloomington, Indiana, U.S.A.

1. - Introduction.

The 13 year ^{152}Eu has been shown by several workers ⁽¹⁻⁴⁾ to decay by electron capture to ^{152}Sm and by β -emission to ^{152}Gd . The recent works of NATHAN and WAGGONER ⁽³⁾ and of BHATTACHERJEE and SHREE RAMAN ⁽³⁾ have clearly brought out the importance of the study of this isotope from the point of view of the Unified Nuclear Model ⁽⁵⁾. A change in the nuclear structure in the neighborhood of $N = 90$ has been indicated by anomalies in the isotopic shift ⁽⁶⁾, quadrupole moments ⁽⁷⁾ and Coulomb excitation energy levels ⁽⁸⁾. Several abnormalities ⁽⁹⁾ exist in the binding-energy data in the vicinity of the neutron number $N = 90$. MOTTELSON and NILSSON ⁽¹⁰⁾ employed an ellipsoidal potential with a spin-orbit force to calculate the individual-particle energy levels as a function of nuclear distortion. With these levels, the ground state equilibrium deformations were calculated for nuclei in the region $N = 82$ to $N = 126$. A sharp increase in nuclear deformation was predicted in going from $N = 88$ to $N = 90$. One encounters in the decay of ^{152}Eu different types of nuclear spectra as one crosses $N = 90$ at ^{152}Sm to $N = 88$ at ^{152}Gd . In ^{152}Sm well-developed low-lying rotational states exist corresponding to collective excitations of the strongly deformed nucleus; on the other hand, in ^{152}Gd the low-lying excited states can be classified as vibrational levels corresponding to the shape oscillations of a spherical nucleus ⁽⁵⁾. The recent works ^(3,4), as mentioned earlier, on this isotope were carried out with the mixed activities of 13 year ^{152}Eu and 16 year ^{153}Eu as obtained from the neutron irradiations of natural europium. Because of the similarity in the decays of these two isotopes it was found difficult to make proper isotopic assignments of some low-intensity γ -rays.

The present paper deals with the results of our work on the 13 year ^{152}Eu as obtained from the thermal neutron irradiations of 92 percent electromagnetically enriched isotope of ^{151}Eu . In this work attempt has been made to determine the relative intensities of the different γ -rays and the internal conversion lines; this enables us to estimate the K-conversion coefficients of

⁽¹⁾ R. E. SLATTERY, D. C. LU and M. L. WIEDENBECK: *Phys. Rev.*, **99**, 1615 (1955).

⁽²⁾ L. GRODZINS: *Bull. Am. Phys. Soc.*, **1**, 163 (1956).

⁽³⁾ O. NATHAN and M. A. WAGGONER: *Nuclear Phys.*, **2**, 548 (1957).

⁽⁴⁾ S. K. BHATTACHERJEE and S. RAMAN: *Nuclear Phys.*, **4**, 44 (1957).

⁽⁵⁾ K. ALDER, A. BOHR, T. HUUS, B. MOTTELSON and A. WINTHER: *Rev. Mod. Phys.*, **28**, 523 (1956).

⁽⁶⁾ P. BRIX and H. KOPFERMANN: *Phys. Rev.*, **85**, 1050 (1952).

⁽⁷⁾ P. BRIX: *Zeits. Phys.*, **132**, 579 (1952).

⁽⁸⁾ N. P. HEYDENBERG and G. M. TEMMER: *Phys. Rev.*, **100**, 150 (1955).

⁽⁹⁾ W. H. JOHNSON and A. O. NIER: *Phys. Rev.*, **105**, 1014 (1957).

⁽¹⁰⁾ B. R. MOTTELSON and S. G. NILSSON: *Phys. Rev.*, **99**, 1615 (1955).

most of the γ -rays and thus assign the multipole orders. The relative transition probabilities of electron capture and β^- -emission were calculated from the measured branching ratios and the experimental results were then compared with the predictions of the Unified Nuclear Model (⁵).

2. - Experimental procedure.

Electromagnetically enriched isotope of ^{151}Eu (92 per cent), obtained from the Stable Isotope Division, Oak Ridge, U.S.A., was bombarded by thermal neutrons for a period of 3 weeks at a flux of 10^{13} n/cm²/s in the Oak Ridge Reactor. Experiments were started after a month from the date of removal of the sample from the reactor. The whole experimental procedure consists of the following measurements:

- 1) Low energy electron spectrum with the Siegbahn-Slätis intermediate image spectrometer.
- 2) High energy electron spectrum with a thin magnetic lens spectrometer.
- 3) γ -rays energy and relative intensity measurements with a calibrated 2 in. thick \times 1 $\frac{3}{4}$ in. diameter NaI(Tl) crystal spectrometer.
- 4) X-ray- γ , γ - γ and β - γ coincidences with a coincidence scintillation spectrometer.

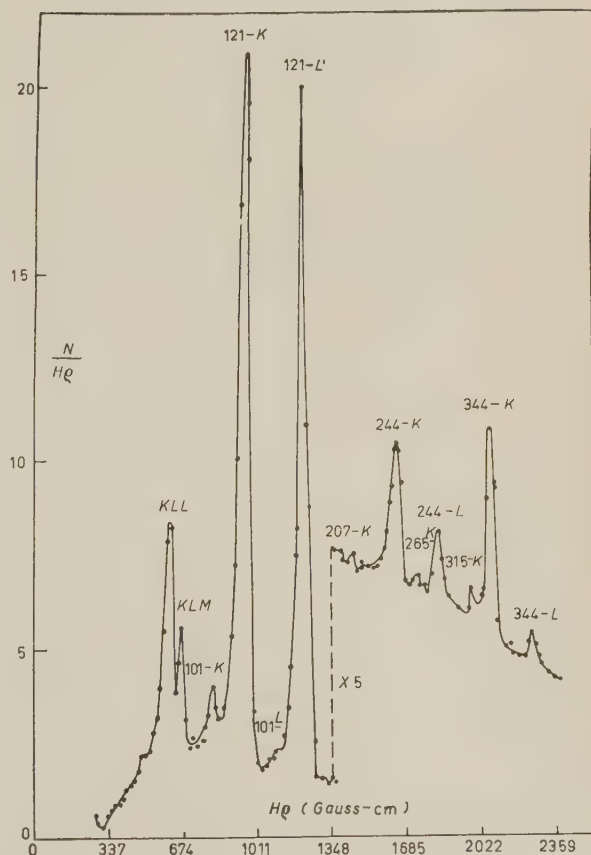


Fig. 1. - Low energy electron spectrum of ^{152}Eu taken with the intermediate image spectrometer. Energies, isotope assignments, and relative intensities are summarized in Table I.

2.1. *Low energy electron spectrum.* — The Siegbahn-Slätis Intermediate Image spectrometer of the Institute was employed for this measurement. The source was deposited on $150 \mu\text{g}/\text{cm}^2$ Al-foil, the Geiger-Müller counter window consisted of $75 \mu\text{g}/\text{cm}^2$ collodion film. The momentum resolution was about 4.5 per cent. The spectrum is reproduced in Fig. 1. For the low-energy electron lines the *KL* differences in Sm and Gd allow identification of the product nucleus.

In Table I these results are summarized along with those obtained with the Lens spectrometer. The isotopic assignments are made mainly on the basis of our coincidence results and our assignments agree well with those of CORK *et al.* ⁽¹¹⁾. The *L*-line of the 101 keV γ -rays falls at the low energy

TABLE I. — *Energies and relative intensities of internal conversion lines (*)*.

| Electron energy (keV) | Interpretation | Relative intensity | Isotope assignment | Corresponding γ -energy (keV) | <i>K/L</i> | Spectrometer employed |
|-----------------------|----------------|--------------------|--------------------|--------------------------------------|----------------|-----------------------|
| 33.1 | Auger-KLL | 700 | Sm | — | — | Intermediate image |
| 39.2 | Auger-KLM | 110 | Sm | — | — | » |
| 54.2 | K | 220 | Sm | 101 | ≈ 2.3 | » |
| 74.5 | K | 2355 | Sm | 121 | ≈ 1.25 | » |
| 95 | L | 95 | Sm | 101 | | » |
| 114 | L | 1900 | Sm | 121 | | » |
| 160 (+) | K | 16 | Sm | 207 | | » |
| 197 | K | 83 | Sm | 244 | ≈ 3.2 | Thin lens |
| 218 (+) | K | 2 | Sm | 265 | | » |
| 236 | L | 26 | Sm | 244 | | » |
| 243 (+) | M, N | 5 | Sm | 244 | | » |
| 268 | K | 4 | Sm | 315 | | » |
| 294 | K | 100 | Gd | 344 | ≈ 3.5 | » |
| 336 | L | 29 | Gd | 344 | | » |
| 362 | K | 4.5 | Gd | 412 | | » |
| 396 | K | 6 | Sm | 443 | | » |
| 656 | K | 4.5 | Sm | 703 | | » |
| 699 (+) | K | 1 | — | — | | » |
| 724 | K | 2.5 | Gd | 774 | | » |
| 926 | K | 5 | Sm | 973 | | » |
| 1047 | K | 6 | Sm | 1094 | | » |
| 1080 | K | 4 | Sm | 1127 | | » |
| 1370 | K | 2 | Sm | 1417 | | » |

(*) The energies are generally believed to be correct to within 1.5% and the intensities to within 15% except when otherwise stated.

(+) Since the lines are weak and broad, rather large errors must be assigned to their measurements.

⁽¹¹⁾ J. M. CORK, M. K. BRICE, R. G. HELMER and D. E. SARASON: *Bull. Am. Phys. Soc.*, 2, No. 1, E316 (1957).

tail of the L -line of 121 keV γ -rays because of poor resolution, this renders the intensity measurements of both these lines rather inaccurate. A conversion line corresponding to a γ -ray of 104 keV has been reported by CORK *et al.* ⁽¹¹⁾ and they have assigned it to ^{152}Gd ; our coincidence measurements, however, favour its origin in ^{152}Sm .

2.2. High energy electron spectrum. — Measurements were carried out with the thin Magnetic Lens Spectrometer ⁽¹²⁾ with a momentum resolution of about 2.4 per cent. Sources, were deposited (about 3 mm in diameter) on 0.6 mg/cm² rubber hydrochloride film with the source properly grounded by

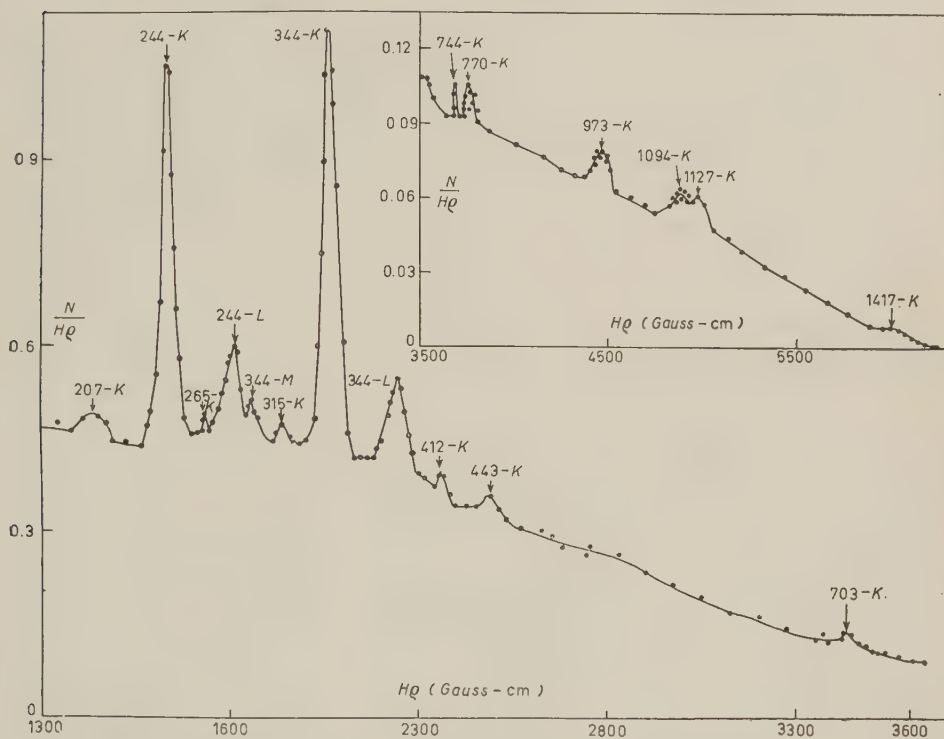


Fig. 2. — High energy electron spectrum of ^{152}Eu with the magnetic lens spectrometer. Energies, isotopic assignments and relative intensities are summarized in Table I.

aquadag lines. The Geiger-Müller counter window consisted of 1.6 mg/cm² mica foil. The spectrum is shown in Fig. 2, and the results are summarized in Table I. Besides the well resolved low-energy lines, some strong conversion

⁽¹²⁾ T. D. NAINAN, H. G. DEWARE and A. MUKERJI: *Proc. Ind. Acad. Sc.*, **44**, 111 (1956).

lines are present in the higher energy range. These higher energy lines are situated on a large continuous background and hence intensity measurements of these lines involve rather large errors due to this tailing.

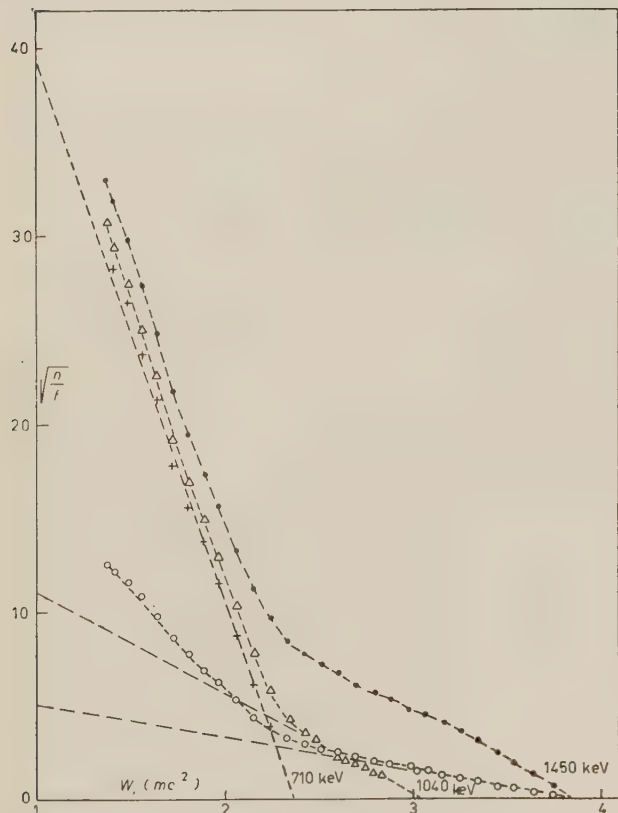


Fig. 3. - Kurie analysis of the β -spectrum. \bullet --- \bullet Gross Kurie plot. \circ ... \circ Corrected for the unique shape for the highest energy component. The correction factor employed: $S_w = (W^2 - 1) + (W_0 - W)^2$. Δ ... Δ The 710 and 1040 keV β -groups. +...+ The lowest energy β -component at 710 keV.

second β -group. This second Kurie plot starts to deviate from around 700 keV and subtracting from the second plot, we obtain the third β -group at end-point energy of 710 keV. The energy differences between the three β -groups indicate that the 770 and 410 keV γ -rays are associated with ^{152}Gd along with the 344 keV γ -ray. Our determination of the maximum energies of three β -groups agrees very well with that of CORK *et al.* ⁽¹¹⁾.

The area of the total β -spectrum was analysed into its three components by means of the Kurie plot analysis. The branching ratios of these three groups

The total β -spectrum was analysed by means of a Kurie plot and was found to be complex (Fig. 3). The upper energy portion of the uncorrected Kurie plot has a slight curvature concave towards the energy axis characteristic of a unique first forbidden spectrum. When the unique correction factor $S_w = (W^2 - 1) + (W_0 - W)^2$ is applied, the Kurie plot is straightened out, thereby giving the end-point of the highest energy β -group as (1450 ± 25) keV. The corrected Kurie plot starts to deviate from a linear plot near 1000 keV; when the highest energy unique forbidden spectrum is subtracted from the total spectrum, a second Kurie plot is obtained which gives the end-point energy of 1040 keV for the se-

are shown in Table II together with the results as obtained from the measured γ -ray intensities. The disagreement for the highest energy group is a little too large. However, considering the uncertainties involved in extracting the

TABLE II. - β -group maximum energies and branching ratios.

| β -energy (keV) | Branching ratio (from Kurie analysis) | Branching ratio from γ -intensities |
|--------------------------|--|---|
| 1450 | 27 | 18 |
| 1040 | 9 | 8 |
| 710 | 64 | 74 |

branching ratios from Kurie analysis, the intensities as derived from the γ -ray measurements are believed to be more reliable and hence these intensity values will be utilized in evaluating the transition probabilities in the β -branching

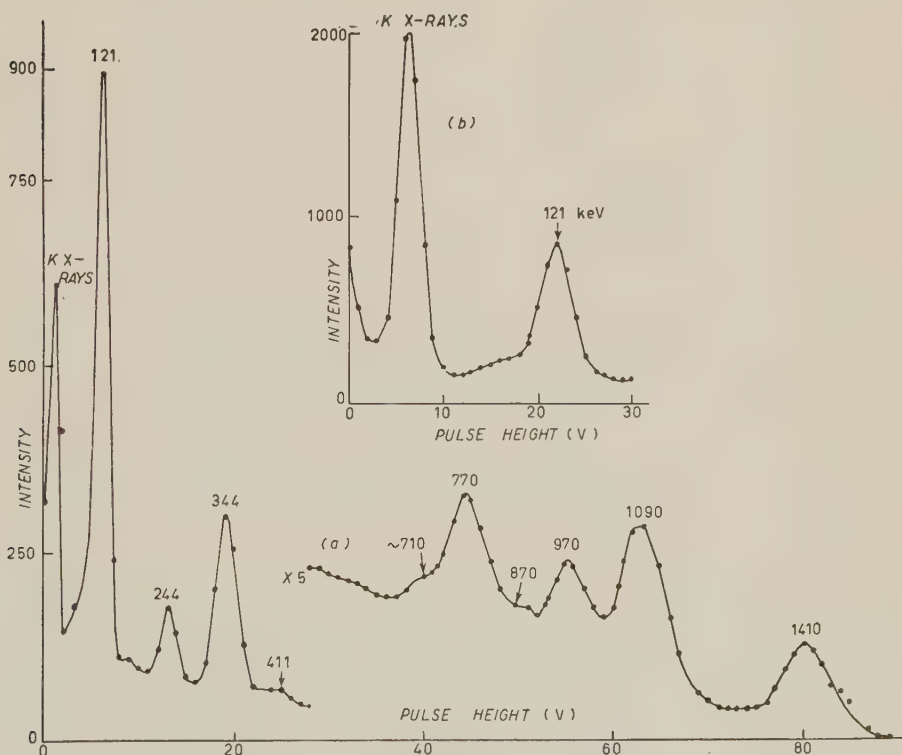


Fig. 4. - γ -spectrum of ^{152}Eu in 2 in. thick $\times 1\frac{3}{4}$ in. diam. NaI(Tl) crystal. The energies and relative intensities are summarized in Table III. Energies are in keV.

of ^{152}Eu . It has been established by HILL and SHEPHARD⁽¹³⁾ that ^{152}Eu does not emit positrons, as is also evidenced by the absence of any annihilation radiation in the observed γ -spectrum (Fig. 4).

2.3. Energies and relative intensities of the γ -rays. Singles spectrum analysis. — The single-channel spectrometer employed a 2 in. thick $\times 1\frac{3}{4}$ in. diameter NaI(Tl) crystal and a Dumont 6292 photomultiplier. The peak efficiency curve for this crystal at a source-to-crystal distance of 1 in. was determined (Fig. 1 of ref. (4)) for various monoenergetic γ sources. The resolution was about 9 per cent for the 661 keV line of ^{137}Cs . The pulse height distribution generated by the ^{152}Eu γ -rays is shown in Fig. 4, and the γ -ray energies and their relative intensities are summarized in Table III.

TABLE III. — Observed γ -ray energies and their relative unconverted intensities (*).

| γ -ray Energies | Relative Intensities |
|------------------------|----------------------|
| 121 | 74 |
| 244 | 24 |
| 344 | 100 |
| 410 (+) | 9 |
| 710 (+) | 10 |
| 770 | 62 |
| 870 (+) | 11 |
| 970 | 71 |
| 1090 | 154 |
| 1410 | 108 |

(*) The energies are believed to be correct to 2 % and intensities within 15 % unless otherwise stated. From the considerations of thermal neutron absorption cross-sections of ^{151}Eu and ^{153}Eu , the isotopic enrichment ratios (92 % of ^{151}Eu), and their lifetimes one can conclude that the interference due to the radiations from ^{154}Eu present is practically negligible.

(+) These lines are not well resolved in the single spectrum and hence their energies and relative intensity measurements are subject to larger errors.

2.4. X-ray- γ and γ - γ coincidences. — The coincidence experiments were carried out with a Coincidence Scintillation Spectrometer which is described elsewhere⁽⁴⁾. It utilizes the «fast-slow» principle, the fast coincidence resolving time was $6 \cdot 10^{-8}$ s. For the γ - γ coincidences both the detecting crystals were 2 in. thick $\times 1\frac{3}{4}$ in. diameter and 6292 photomultipliers were employed.

(13) J. M. HILL and L. R. SHEPHARD: *Proc. Phys. Soc.*, A **63**, 126 (1950).

All the coincidence experiments were carried out with the counter axes oriented at 90° with a view to avoid spurious coincidences; an anti-scattering shield was used in the usual ray. The ratio of the accidental coincidence rate to the genuine coincidence rate in the region of the true coincidence peaks was usually small. The results are summarized in Table IV and a few representative coincidence spectra are shown in Fig. 5, 6 and 7.

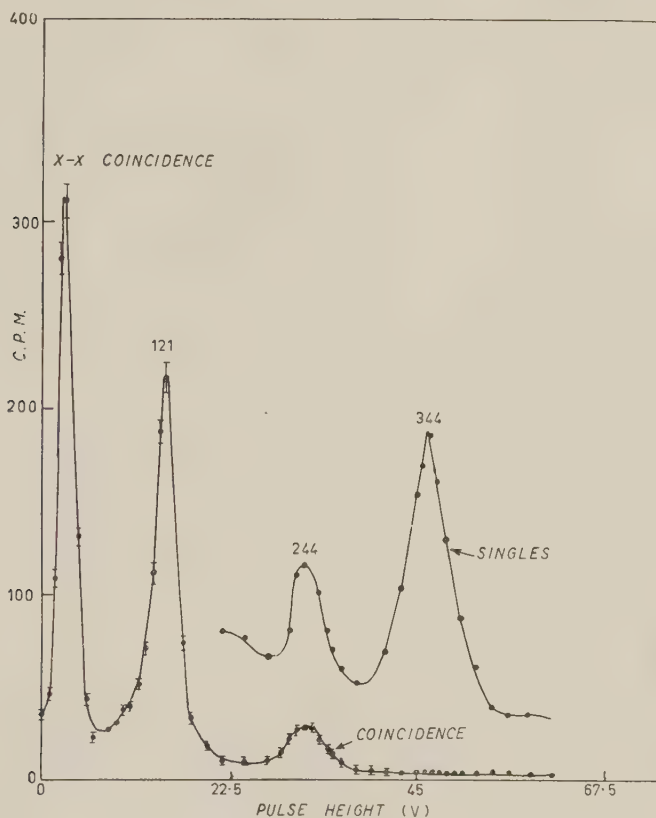


Fig. 5. — KX -ray coincidences with the low energy γ -rays in ^{152}Eu .

One of the features of our coincidence results is the presence of weak γ -rays of energies (in keV) $\approx 108, 315, 410$ and 442 ; all these lines are also shown up as weak conversion lines in the β -spectrum (Fig. 2). These low-energy coincidence peaks cannot be explained as spurious coincidences in view of the geometry used in these experiments. The relative intensities of these lines could be roughly estimated from the coincidence data; the energies quoted above are appropriate to the observed conversion lines (Table I). Within the limits of experimental errors the energies of the coincidences peaks as shown

in Fig. 5, 6 and 7 agree well with the above-mentioned energies for these γ -rays. Such an observation was also made in our earlier work (4) with the mixed activity. In coincidence with the 121 keV γ -ray, the relative intensity of the

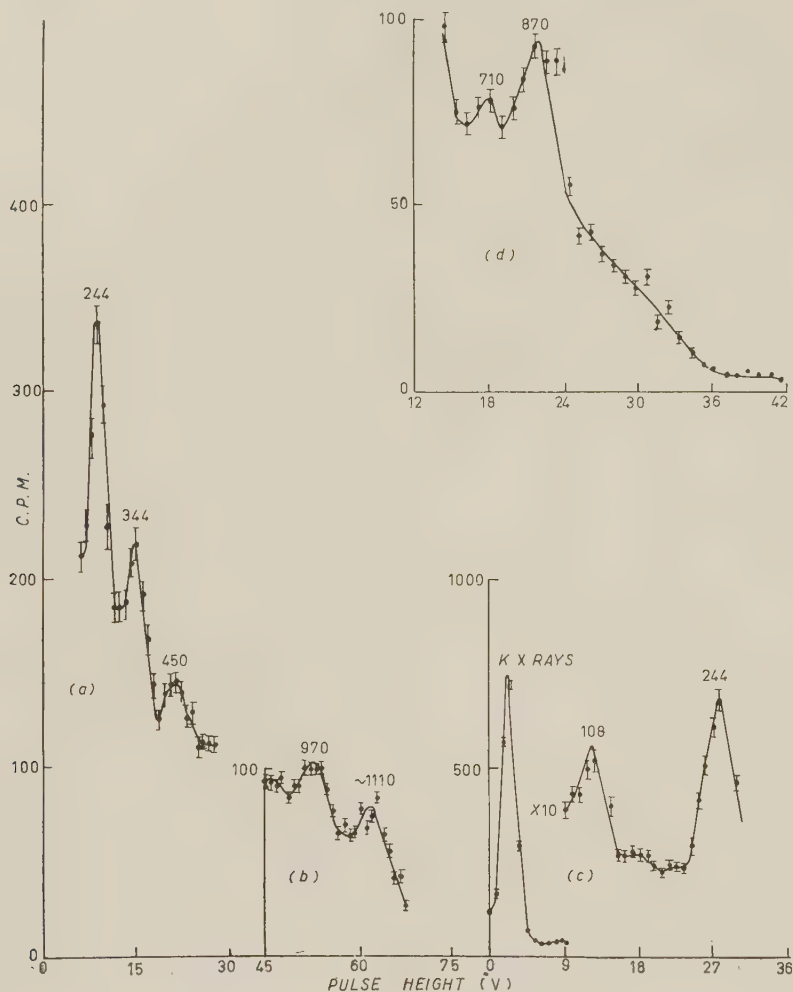


Fig. 6. — (a), (b), (c) show the coincidences of ^{152}Eu γ -rays with 121 keV photopeak. (d) represents a portion of the spectrum in coincidence with 244 keV photopeak. Note that the unresolved peaks in the single spectrum at 710 and 870 keV are completely resolved here.

1090 keV γ -ray is reduced by 50 per cent as compared to that of 970 keV, if the relative intensity ratio of these two γ -rays from the singles spectrum is taken as standard. This establishes the presence of the γ -ray of energy 1127 keV which is of equal intensity as that of 1090 keV; these two lines were

not resolved in the singles spectrum, the former is in coincidence with the 121 keV γ -ray, while the latter goes directly to the ground state from the 1090 keV level in ^{152}Sm .

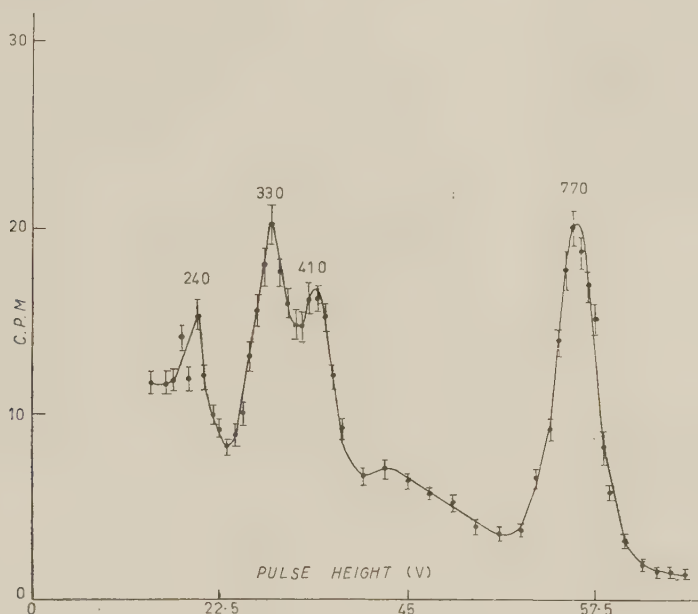


Fig. 7. — The γ -spectrum in coincidence with 344 keV photopeak. Note that the unresolved line at 410 keV is completely resolved here. No appreciable coincidences were observed for γ energies higher than 770 keV.

It is significant to note that no KX -ray or 121 keV coincidences were observed with the 1417 keV γ -ray. In the earlier works ^(3,4) with the mixed activity the coincidences with the 121 keV γ -ray attributed to the 1410 keV γ -ray are most probably due to ^{154}Eu . This fact has been verified ⁽¹⁴⁾ with an enriched activity (95%) of ^{154}Eu and we have found coincidences between 123 keV and the higher energy γ -rays present in this isotope.

2.4.B β - γ coincidences. — An anthracene crystal of $\frac{1}{4}$ in. thickness and $1\frac{1}{2}$ in. diameter was used to detect the β -particles. This crystal was covered on the top by $150 \mu\text{g}/\text{cm}^2$ Al-reflector to ensure efficient light collection; the resolution obtained was about 18 per cent for the 624 keV K -conversion line of the ^{137}Cs γ -ray. The full photopeak at 344 keV was accepted in the γ -ray detecting gate channel and the coincidences β -spectrum was obtained by

⁽¹⁴⁾ Work on 16 yr ^{154}Eu decay is in progress and will be reported in due course.

TABLE IV. - *Summary of X- γ and γ - γ coincidences.*

| Gating radiation (keV) | Coincident radiations (keV) | Remarks |
|------------------------|--|--|
| 39 K-X-rays | K-X-rays, 121, 121, 244, 710, 870, 970, 1090 | Strong X-ray coincidences indicate that in the capture branch (^{152}Sm) some low-lying states de-excite by highly converted γ -rays. No coincidences were observed with 344 keV indicating that this γ -ray is in bulk in the β -branch. |
| 121 | K-X-rays, ≈ 108 , 244, 340, 450, 970, 1110 | Weak coincidences at ≈ 108 keV confirm our earlier observation that the 121 keV γ line is composed of a γ -ray of energy close to 108 keV and must be present in the capture branch. Similar arguments hold for weak 340 keV coincidences. No appreciable coincidences were observed near the 770 keV photo peak. The relative intensity of 1090 keV photons per 121 keV photons is about 50% of that in singles spectrum showing that the 1090 keV peak is composed of two γ -rays, each of equal intensity. |
| 244 | K-X-rays, 121, ≈ 240 , 340, 450, 710 and 870 | The unresolved peaks near 770 keV in singles spectrum are completely resolved in coincidence spectrum showing that the 244 keV γ -ray is in coincidence with the 710 keV and 870 keV γ -rays but not with the 770 keV γ -rays. The existence of a weak γ -ray ≈ 340 keV in the capture branch is also confirmed. |
| 344 | 108, 240, 330, 410 and 770 | The 410 keV unresolved peak in the singles spectrum is clearly resolved. Negligible coincidences in the K-X-ray region indicate that 344 keV γ -ray in bulk must be present in the β branch. No appreciable coincidences were observed in the energy ranges higher than 770 keV. |
| 770 | K-X-rays, 121, 240, 344 | The X-rays, 121 and 244 keV coincidences are presumably due to 870 keV γ -rays present in the composite peak at 770 keV in the gate channel. No appreciable higher energy coincidences were observed after the intense 344 keV peak. |
| 970 | K-X-rays, 121, ≈ 240 | This γ -ray presumably leads to the 121 keV state in ^{152}Sm . |
| 1090 | K-X-rays, 121, 240, ≈ 330 | Coincidences with 121 keV γ -rays indicate that it is indeed the 1127 keV γ -ray which is in coincidence with the 121 keV γ -rays. |
| 1410 | No coincidences | The 1410 keV γ -rays did not show any appreciable coincidences either with K-X-rays or with the 121 keV photopeak. |

scanning the anthracene crystal spectrometer. Fig. 8 (a) represents the spectrum and one clearly sees two β -groups of end-point energies at 1500 and 750 keV in coincidence with the 344 keV γ -ray. In Fig. 8 (b) is shown

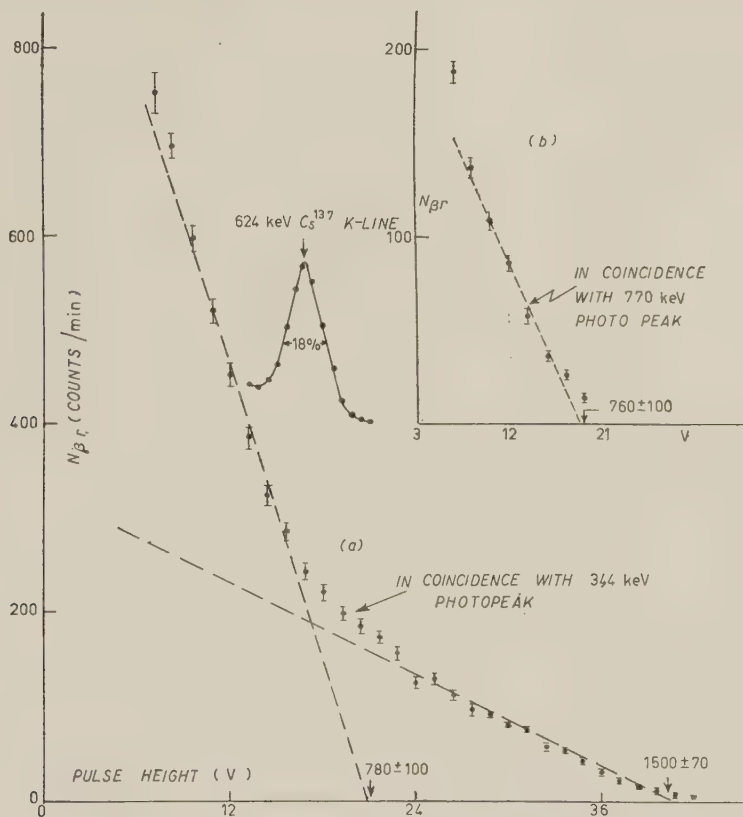


Fig. 8. — (a) β -spectrum of ^{152}Eu in coincidence with 344 keV γ -rays, the two β -components at 750 and 1500 keV end points are clearly discernible. (b) β -spectrum of ^{152}Eu in coincidence with 770 keV γ -rays. The only coincident β -group has the end point energy of ≈ 750 keV. The resolution of the anthracene crystal spectrometer for the 624 keV K -conversion line of ^{137}Cs is $\approx 18\%$.

the coincident β -spectrum when the full 770 keV photopeak was in the gate channel; the only β -group coincident with the 770 keV γ -rays had the end-point energy at ≈ 750 keV. In all these β - γ coincidences, the γ - γ background was separately determined and only the genuine β - γ coincidences are plotted in Fig. 8.

In order to ascertain the γ -rays that are present in the β -branch of ^{152}Eu , a band of β -particles of energy between 400 and 440 keV was selected as the

gate radiation and the coincident γ -spectrum is reproduced in Fig. 9. The two γ -rays at 344 and 770 keV are the ones that are strongly in coincidence, no γ -ray of energy higher than 770 keV shows any appreciable coincidence. The weak peak at about 410 keV is not well-resolved. The coincident peak at

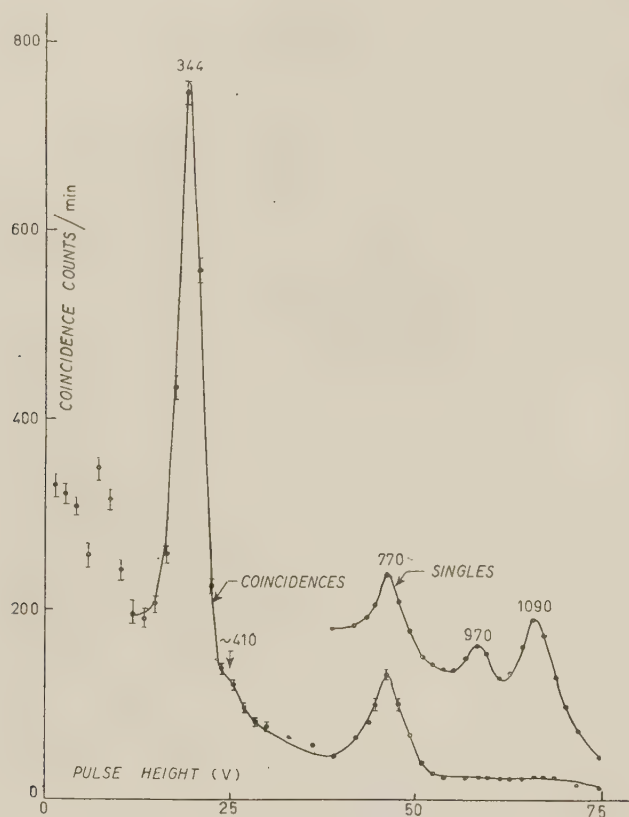


Fig. 9. — The γ -spectrum of ^{152}Eu in coincidence with a band of β -particles of energies between 400 and 440 keV. This band was particularly chosen as not to include the conversion electrons due to intense low energy γ -rays. No appreciable β - γ coincidences were observed with the γ -rays of energies higher than 770 keV. In all β - γ coincidences the γ - γ background was observed by absorbing all β -particles by means of a 3/16 in. perspex absorber. The spectra shown are the genuine β - γ coincidences.

≈ 150 keV is presumably due to the back scattering of the 344 keV γ -rays, since this experiment was done at 180° -geometry. The result of the β - γ coincidences are summarized in Table V.

TABLE V. — *Summary of β - γ coincidence measurements.*

| Gating radiation (keV) | Information about the coincident radiations | Remarks |
|---|---|--|
| 344 keV photopeak | β^- -groups of ≈ 1500 and ≈ 750 keV end-points. | The 344 keV γ -ray is in coincidence with two β^- -groups as is clearly shown in Fig. 8 (a). |
| 770 keV | β^- -group of ≈ 750 keV end-point. | The only β^- -group which is in coincidence with the 770 keV γ -ray is the one of 710 keV end-point energy (Fig. 8 (b)). |
| β^- -particles in the energy band $400 \div 440$ keV accepted in anthracene crystal | 344 and 770 keV photopeaks | This experiment clearly demonstrates (Fig. 9) that the strong γ -rays that are present in the β^- -branch of ^{152}Eu are 344 and 770 keV. No appreciable π - γ coincidences were observed for any γ -rays higher in energy than 770 keV. The slight coincidences near ≈ 150 keV might be due to back scattering of 344 keV γ -rays since this experiment was performed with counter axes oriented at 180° . |

3. — Multipole order assignment to the γ -rays.

From a knowledge of the relative intensities of the K -conversion lines and the γ -rays, it is possible to estimate the relative magnitude of the K -conversion coefficients of the different γ -rays. The relative values then can be converted to absolute conversion coefficients if the multipole order of one of the transitions is known in an independent way. The β -spectrum analysis and the β - γ coincidence experiments establish the fact that the 344 keV γ -ray arises due to the de-excitation of the first excited state in ^{152}Gd and the maximum β^- -group of 1450 keV terminates at this level; so it is concluded that no ground state β^- -transition takes place in ^{152}Gd , hence the 344 keV γ -ray intensity represents the total number of β -disintegrations from ^{152}Eu . The K -conversion coefficient α_K of the 344 keV γ -ray can then be determined from the following relation,

$$\alpha_K = 1 / \left(\frac{I_\beta}{I_K + I_L} - 1 \right) \left(1 + \frac{1}{K/L} \right).$$

The conversion contribution due to shells higher than L is neglected in this expression. $I_\beta = I_{\beta_1} + I_{\beta_2} + I_{\beta_3}$, I_K and I_L represent the intensities of the

K and L conversion lines and K/L is the measured ratio. From the lens spectrometer measurements (Fig. 2) it is found that the total γ -continuum intensity is 3390 as compared to 100 for the K -conversion line of 344 keV. Hence from the other measured data (Table I) i.e. $I_L = 29$ and $K/L = 100/29$ we get the value of the K -conversion coefficient for the 344 keV γ -ray as $\alpha_K = 0.032 \pm 0.005$. The theoretical K -conversion coefficient for a pure $E2$ transition is 0.033 and is in excellent agreement with the measured value. The K -conversion coefficient of 344 keV can now be used as a reference for calculating the absolute K -conversion coefficients of the other γ -rays. Table VI summarizes the experimental conversion coefficients calculated in this way; the theoretical K -conversion coefficients for the different multipole orders are obtained from ROSE's ⁽¹⁵⁾ tables.

TABLE VI. — K conversion coefficients and multipole order assignments.

| γ -ray energy (keV) | Iso- tope assign- ment | Relative intensity of K -con- version lines | Uncon- verted inten- sity (d) | α_K Experi- mental | Theoretical K -conversion coefficient | | | Proposed Multipole Order. |
|----------------------------|---------------------------------|---|---|---------------------------------|--|---------------------|---------------------|---------------------------------|
| | | | | | $E1$ | $E2$ | $M1$ | |
| 101 ^a | Sm | 220 | 5 | 1.32 | 0.25 | 1.1 | 1.6 | $E2$ |
| 121 ^b | Sm | 2355 | 88 | $8.0 \cdot 10^{-1}$ | — | $6.2 \cdot 10^{-1}$ | — | $E2$ |
| 244 | Sm | 83 | 30 | $8.3 \cdot 10^{-2}$ | $2.1 \cdot 10^{-2}$ | $8.0 \cdot 10^{-2}$ | $1.2 \cdot 10^{-1}$ | $E2$ |
| 315 ^c | Sm | 4 | 4 | $3.2 \cdot 10^{-2}$ | $1.2 \cdot 10^{-2}$ | $4.1 \cdot 10^{-2}$ | $8.0 \cdot 10^{-2}$ | ($E1$ or $E2$) ^e |
| 344 | Gd | 100 | 100 | $3.2 \cdot 10^{-2}$ | $1.0 \cdot 10^{-2}$ | $3.3 \cdot 10^{-2}$ | $6.6 \cdot 10^{-2}$ | $E2$ |
| 410 ^c | Gd | 4.5 | 9 | $1.5 \cdot 10^{-2}$ | $6.5 \cdot 10^{-3}$ | $2.0 \cdot 10^{-2}$ | $4.1 \cdot 10^{-2}$ | $E2$ |
| 442 ^c | Sm | 6 | 4 | $4.5 \cdot 10^{-2}$ | $4.9 \cdot 10^{-3}$ | $1.5 \cdot 10^{-2}$ | $2.7 \cdot 10^{-2}$ | ($E2 + M1$) |
| 710 | Sm | 4.5 | 13 | $1.0 \cdot 10^{-2}$ | $1.8 \cdot 10^{-3}$ | $4.6 \cdot 10^{-3}$ | $9.0 \cdot 10^{-3}$ | ($E2 + M1$) |
| 770 | Gd | 2.5 | 77 | $1.1 \cdot 10^{-3}$ | $1.6 \cdot 10^{-3}$ | $4.2 \cdot 10^{-3}$ | $8.4 \cdot 10^{-3}$ | $E1$ |
| 870 | Sm | — | 14 | — | — | — | — | — |
| 970 | Sm | 5 | 89 | $1.7 \cdot 10^{-3}$ | $9.0 \cdot 10^{-4}$ | $2.2 \cdot 10^{-3}$ | $3.9 \cdot 10^{-3}$ | $E2$ |
| 1090 ^c | Sm | 6 | 96 | $1.9 \cdot 10^{-3}$ | $7.4 \cdot 10^{-4}$ | $1.7 \cdot 10^{-3}$ | $3.0 \cdot 10^{-3}$ | $E2$ |
| 1127 ^c | Sm | 4 | 96 | $1.3 \cdot 10^{-3}$ | $7.0 \cdot 10^{-4}$ | $1.6 \cdot 10^{-3}$ | $2.7 \cdot 10^{-3}$ | $E2$ |
| 1417 | Sm | 2 | 135 | $4.4 \cdot 10^{-4}$ | $4.7 \cdot 10^{-4}$ | $1.0 \cdot 10^{-3}$ | $1.6 \cdot 10^{-3}$ | $E1$ |

(a) The conversion coefficient values quoted for this line are taken from F. K. MCGOWAN: *Phys. Rev.*, **93**, 163 (1954) for $Z = 61$.

(b) Quoted from ref. (3).

(c) The relative intensities of these lines were estimated from the coincidence data.

(d) The unconverted intensities are normalized with respect to the intensity of the 344 keV γ -ray.

(e) The assignments shown inside parentheses are to be considered as doubtful.

(¹⁵) M. E. ROSE, G. H. GOERTZEL and C. L. PERRY: ORNL-report 1023 (1951).

4. - Level scheme.

On the basis of the results of the present investigation a decay scheme is proposed for the 13 year ^{152}Eu (Fig. 10). The intensities of the various radiations together with the calculated transition probabilities are listed in Table VII. The proposed decay scheme explains satisfactorily the origin of most of the observed γ -rays as well as the various coincidence data.

TABLE VII. - Intensities (*) and calculated $\log ft$ (†) values of the radiations emitted by ^{152}Eu .

| Radiation | Abundance | $\log f_0 t$ | $\log f_1 t$ |
|-------------------------------|-----------|--------------|--------------|
| $\beta_1^- = 710 \pm 20$ keV | 13 | 10.7 | |
| $\beta_2^- = 1040 \pm 25$ keV | 1 | | 12.1 |
| $\beta_3^- = 1450 \pm 25$ keV | 3 | | 12.3 |
| EC to the level at 1417 keV | 29 | 7.2 (°) | |
| » 1248 keV | 20 | 8.7 | |
| » 1191 keV | 3 | 9.8 | |
| » 1090 keV | 29 | 9.1 | |
| » 807 keV | 1 | 11.0 | |

(*) Calculated per 100 disintegrations of ^{152}Eu .

(†) Calculated from the nomograph of MOSZKOWSKI: *Phys. Rev.*, **82**, 35 (1951).

(°) Calculated on the basis of maximum decay energy corresponding to K -binding energy of Sm i.e. 46.8 keV.

^{152}Sm -levels: From the earlier works (3,4) and also from Coulomb excitation experiments (8), it has been established that the 121 keV transition arises due to the de-excitation of the first excited state in ^{152}Sm , and it is of $E2$ character. The rotational character of this level is also evidenced from the half-life determination (16) of this state which shows an enhanced $E2$ transition probability as compared to the single particle estimate. The second state at 365 keV de-excites by 244 keV γ -ray, the measured K -conversion coefficient and the K/L ratio establish it as one of $E2$ type. The level at 870 keV de-excites by a weak γ -ray of energy 442 keV, observed both as a weak conversion line and also in the coincidence spectra with 121 and 244 keV γ -rays.

The levels at 1090, 1191 and 1248 keV are proposed on the basis of the γ - γ coincidence data, the energy fits the internal conversion lines and the observed intensities of the different γ -rays involved. The 1090 keV level de-excites by a γ -ray of 1090 keV going directly to the ground state and 970 keV γ -ray terminating at the 121 keV level; observed conversion coefficients

(16) A. W. SUNYAR: *Phys. Rev.*, **98**, 653 (1955).

characterize them as predominantly $E2$ types. The 1248 keV level also de-excites by two γ -rays; one of energy 1127 keV terminates at the 121 keV level and the other of 883 keV ends up at the 365 keV level. The 883 keV γ -intensity is low and no observable internal conversion line corresponding to this γ -ray has been observed; the 1127 keV γ -ray is mostly $E2$ in character. The observed intensities of the three radiations of 244, 970 and 1127 keV terminating at the 121 keV level account very well (Table VI) for the observed intensity of the 121 keV γ -ray after correcting for internal conversion of all the γ -rays. This leads us to conclude that the direct electron capture to this level is negligible. Similar arguments hold for the 365 keV level which de-excites only by the 244 keV γ -ray whose total intensity accounts rather well for the observed intensities of the 725 keV γ -ray (to be identified with the unresolved 710 keV γ -peak as observed in the singles spectrum, Fig. 4, and the broad conversion line of weak intensity corresponding to a γ -energy of ≈ 703 keV) and the 883 keV γ -ray, both terminating at this level. It is also seen that no appreciable electron capture transition takes place directly to this level.

The 1191 keV level is postulated in order to explain the existence of some weaker low-energy γ -rays that were observed both in the electron spectrum and in the coincidence experiments. It has been pointed out earlier that no appreciable KX -ray or 121 keV coincidences were observed with the 1417 keV γ -ray. The observed intensity of the 1417 keV γ -ray is about the same as due to that of 121 keV correcting for conversion and hence, according to the arguments put forward before, the 1417 keV γ -ray cannot terminate at the 121 keV level. The intensity consideration and the coincidence results force us to conclude that the 1417 keV γ -ray arises due to the de-excitation of the uppermost level at 1417 keV and it is predominantly fed by L capture. This shows that the total electron capture decay energy of ^{152}Eu is more than 1417 keV and less than 1464 keV.

^{152}Gd -levels: The Kurie analysis of the β -spectrum shows three groups at maximum energies 1450, 1040 and 710 keV. The β - γ coincidence experiments establish the level scheme in ^{152}Gd . No appreciable β -transition takes place to the ground state. No β - γ coincidences were observed for any γ -ray of energy higher than 770 keV (Fig. 9).

The highest energy β -group of 1450 keV has an α -shape corresponding to a unique first forbidden transition of the type $\Delta I = 2$, yes, the calculated $\log f_1 t = 12.3$. Since the 344 keV level is a $2+$ state, it is most likely that the ground state spin and parity of ^{152}Eu have the value $4-$. This assignment satisfactorily explains the existence of the 9.2 h isomer of ^{152}Eu , situated at ≈ 50 keV above, which emits a 1880 keV β -group to the ground state of ^{152}Gd with an allowed shape and $\log ft$ -value of 7.5.

The calculated $\log f_1 t = 12.1$ for the 1040 keV β -group also indicates that the level at 754 keV has spin $I = 2+$. Because of the $E1$ character of the 770 keV γ -ray as inferred from the measured K -conversion coefficient and in conformity with the angular correlation work ⁽¹⁷⁾, $I = 3-$ has been assigned to the 1114 keV level. The 710 keV β -group going to this level corresponds to a transition of the type $\Delta I = 1$, no; the calculated $\log ft$ -value is too high for an allowed transition. The total β -decay energy of ^{152}Eu is 1794 keV.

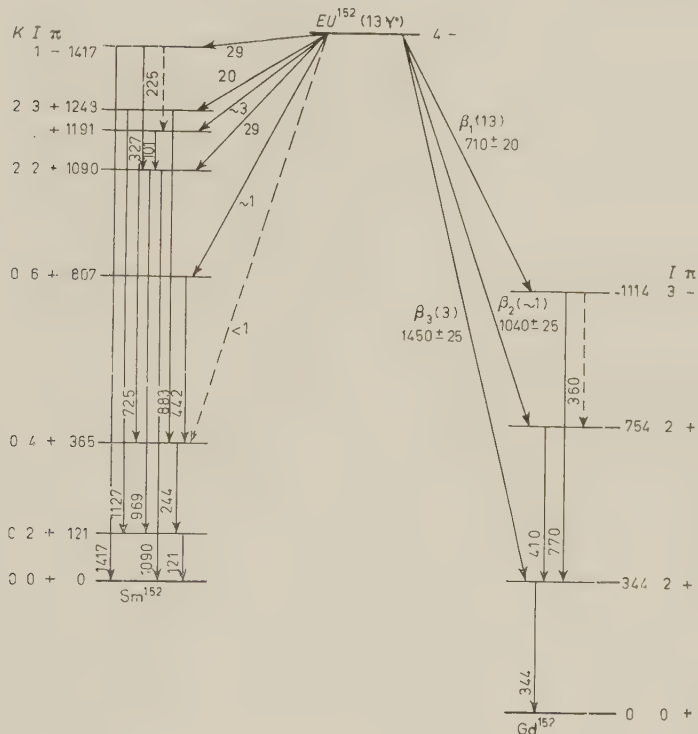


Fig. 10. — The proposed decay scheme for 13 yr ^{152}Eu . The transitions shown as dotted lines may be regarded as doubtful assignments. All energies are in keV.

From the proposed decay scheme, the ratio of total electron capture to β -emission is given by

$$\frac{EC}{\beta^-} = \frac{I_{121} + I_{1090} + I_{1417}}{I_{344}},$$

⁽¹⁷⁾ L. GRODZINS and H. KENDALL: *Bull. Am. Phys. Soc.*, **1**, No. 4, 164B11 (1956).

correcting for internal conversion, we get from Table VI

$$EC/\beta^- \approx 4.8.$$

The relative intensities and the transition probabilities of the different radiations from ^{152}Eu decay are summarized in Table VII.

5. - Discussion.

The decay of ^{152}Eu is unique in the sense that the level structure of ^{152}Sm , as reached by the electron capture decay, and that of ^{152}Gd , reached by β -decay, reveal quite different types of nuclear spectra in the region of $N=90$ and $N=88$. The large change in the nuclear structure is evident. This sharp change in the nuclear structure has been first observed in the study of the systematics⁽¹⁸⁾ of even-even nuclei. The nucleus ^{152}Sm with $N=90$ shows well-developed low-lying rotational states characteristic of the collective excitations of a nucleus of spheroidal shape. The energy interval rule for such rotational levels, corresponding to the ground state rotational band ($K=0$) is that the first, second and third excited states must have their energies in the ratio $E_1:E_2:E_3=3:10:21$ and of characters $2+$, $4+$ and $6+$; the ground state character of an even-nucleus is always $0+$. The levels in ^{152}Sm at 121, 365 and 807 keV conform very well to the interval rule and the measured K -conversion coefficient of the de-exciting γ -rays (pure $E2$ type) satisfy the required spin and parity assignments. On the other hand, in ^{152}Gd , the two low-lying levels at 344 and 754 keV are characteristic of the collective vibrations of the electric quadrupole type about a spherical equilibrium shape⁽⁵⁾. The shape oscillations of a spherical nucleus arise due to an oscillating electric multipole moment and are classified according to their multipole order, the lowest frequencies of collective vibration are in most cases expected to be of quadrupole type. Theory⁽⁵⁾ predicts that in the limit of harmonic oscillator approximation the energies of the first and second vibrational states must be in the ratio 1:2, the spin of the first vibrational state is always $I=2+$; there lies a degenerate triplet of character $0+$, $2+$, $4+$ at the second vibrational level. In ^{152}Gd we indeed observe that the energy ratio of these two states = 2.1; $I=2+$ character of the 344 keV level is established by the K -conversion coefficient of the corresponding γ -ray, and $2+$ assignment to the 754 keV level is also in agreement with the prediction of the theory. In the decay of vibrational states, $M1$ radiation is forbidden even when $\Delta I=0$; the 410 keV γ -ray corresponds to a $2+ \rightarrow 2+$ transition and the estimated K -conversion coefficient indicates an $E2$ character.

(18) G. SCHARFF-GOLDHABER and J. WENESER: *Phys. Rev.*, **98**, 212 (1955).

The level at 1114 keV in ^{152}Gd has been assigned a spin $I=3$. Recently, relatively low-lying odd-parity states of character $1-$, $3-$, $5-$ have been observed in a few even-even nuclei in the heavy elements ⁽¹⁹⁾. In the 9.2 h isomer decay of ^{152}Eu a state ^(3,20) in ^{152}Sm at 960 keV has been identified as $I=1-$ and $K=0$. Such odd-parity collective vibrational states are recently ⁽⁵⁾ interpreted as due to octupole vibrations of even-even nuclei, where the one phonon excitation has the character $I=3-$.

The Unified Nuclear Model ⁽⁵⁾ predicts for spheroidal nuclei two vibrational bands for even-even nuclei, each having one quantum of vibrational excitation. The so-called β -vibrational band ($K=0$) will have rotational band members $(0, 0+)$, $(0, 2+)$, $(0, 4+)$... The γ -vibrational band ($K=2$) will have members $(2, 2+)$, $(2, 3+)$, $(2, 4+)$... The rotational moment of inertia for these upper bands is about the same as that of the ground state band. The vibrational quantum energy may be of the order of 1 MeV for the heavy elements. The de-excitation of these levels to the members of the ground state rotational band will mainly proceed by $E2$ transitions even though $M1$ transitions are allowed. The intensity rules for the relative transition probabilities to the various members of a nuclear rotational band has been given by ALAGA ⁽²¹⁾ and others.

The respective ratios of the electric quadrupole transitions from the 1090 and 1248 keV levels in ^{152}Sm to the states of the ground state rotational band provide means of evaluating the K quantum numbers for these levels. After dividing out the fifth-power energy dependence we obtain the ratio of the reduced transition probabilities. The branching ratio of the 1090 keV level to the ground state ($I=0+$, $K=0$) and 121 keV ($I=2+$, $K=0$) yields $B(E2; 2, 2 \rightarrow 0, 0):B(E2; 2, 2 \rightarrow 0, 2)=0.6$, assuming pure $E2$ radiations for both transitions. The ratio calculated from the theory ⁽²¹⁾ is 0.7 thus establishing $K=2$ for the 1090 keV level. The branching ratio of the 1248 keV level to the $2+$ and $4+$ states of the ground state rotational band yields $B(E2; 2, 3 \rightarrow 0, 2):B(E2; 2, 3 \rightarrow 0, 4)=2.1$, the theoretically calculated ratio is 2.5; the agreement seems to indicate that the two γ -rays involved are probably predominantly of $E2$ character and the 1248 keV level has also $K=2$. Thus we may conclude that the 1090 keV $2+$ state and 1248 keV $3+$ state are quadrupole vibrational states corresponding to $K=2$ (γ -vibrations).

The 1191 keV level de-excites by the 101 keV transition to the 1090 keV level. The measured K -conversion coefficient of this γ -ray is ≈ 1.32 and

⁽¹⁹⁾ F. S. STEPHENS, F. ASARO and I. PERLMAN: *Phys. Rev.*, **96**, 1568 (1954).

⁽²⁰⁾ L. GRODZINS: *Bull. Am. Phys. Soc.*, **1**, No. 7, 329J7 (1956).

⁽²¹⁾ G. ALAGA, K. ALDER, A. BOHR and B. R. MOTTELSON: *Kgl. Danske Videnskab. Selskab. Mat. fys. Medd.*, **29**, No. 9 (1955).

$K/L \approx 2.3$; this γ -ray is predominantly of $E2$ type since for the $M1$ transition $K/L \approx 6$. This indicates that the level 1191 keV may have any spin-value from 0 to 4 and even parity. No spin assignments could, however, be made on the basis of our experimental results.

The assignment $I = 1 -$ as the spin and parity of the 1417 keV level in ^{152}Sm is consistent with the $E1$ nature of the 1417 keV γ -ray. This is the only odd-parity state discernible in ^{152}Sm . Theory ⁽⁵⁾ predicts that in an even-even nucleus the coupling between the quadrupole deformation and the octupole mode may give rise to a lowest odd-parity excitation $I = 1 -$. The only difficulty that one encounters in such an interpretation is that one expects a competing $E1$ transition of energy 1296 keV of relatively observable intensity to the 121 keV $2 +$ state. Because of this ambiguity no K quantum number has been assigned to this level. In order to ascertain the K -value of the ^{152}Eu ground state, the β -transition probabilities to the different levels in ^{152}Gd have to be known rather precisely; the experimental errors in the β -branching ratios are rather high (Table II) and this prevents us from assigning any K -value to ^{152}Eu . One fails to notice the K -forbiddenness of some electron capture and most of the β -transitions in this decay. The electron capture transition to $I = 4 +$ in ^{152}Sm is a first-forbidden transition ($\Delta I = 0$, yes), the higher order forbiddenness as revealed by the corresponding $\log ft$ -value is most likely due to K -forbiddenness. The same situation exists for all the three β -transitions.

Detailed studies of this isotope with a high resolution magnetic spectrometer and the experimental determination of the spin of ^{152}Eu would be of great interest.

* * *

The authors wish to thank Dr. R. RAMANNA for going through the manuscript and for many valuable comments. Our sincere thanks are due to Drs. S. JHA and J. VARMA for valuable comments. We are indebted to Dr. B. V. THOSAR for his kind co-operation in allowing us to use the magnetic spectrometers. Thanks are due to Mr. B. N. SUBBARAO for helping us in the measurements with the Intermediate Image Spectrometer. We gratefully acknowledge the ungrudging help we received from Mr. S. K. MITRA and Mr. S. V. GODBOLE at the various stages of this work.

Note added in the proof.

After this paper was sent for publication, the detailed work of CORK *et al.* (*Phys. Rev.*, **107**, 1621 (1957)) has been published; our results are, in essence, in agreement with theirs. Further, the ground state spin of ^{152}Eu has recently been measured to

be $I=3$. (M. ABRAHAM *et al.*: *Phys. Rev.*, **108**, 58 (1957)) by paramagnetic resonance method. This fact implies that the highest energy β -group of 1450 keV terminating at $2+$ state at 344 keV in ^{152}Gd is most probably a transition of the type $\Delta I=1$, yes, and it exhibits a forbidden spectral shape.

RIASSUNTO (*)

Le radiazioni del ^{152}Eu ($t_{1/2}=13$ anni) sono state studiate usando uno spettrometro a immagine intermedia, uno spettrometro a lente magnetica sottile e uno spettrometro a coincidenze a scintillazione. Si constatano tre gruppi β^- terminanti a 1450 ± 25 , 1040 ± 20 , 710 ± 20 keV; il gruppo di energia massima ha forma α . Opportune ricerche, mostrarono la presenza delle seguenti radiazioni γ : 101 (5), 121 (88), 244 (30), 315 (4), 344 (100), 410 (9), 442 (4), 710 (13), 770 (77), 888 (14), 970 (89), 1190 (96), 1027 (96) e 1410 (135) keV. I coefficienti di conversione K sono stati stimati per la maggior parte di queste transizioni e sono stati assegnati gli ordini dei multipoli. Esperienze di coincidenza raggi X- γ , γ - γ e β - γ ci permettono di costruire lo schema di decadimento del ^{152}Eu . La differenza nella struttura dei livelli del ^{152}Sm ($N=90$) e ^{152}Gd ($N=88$) risulta evidente dai risultati sperimentali. I primi tre stati eccitati del ^{152}Sm a 121, 365 e 807 keV si identificano come le tre parti della banda rotazionale dello stato fondamentale ($K=0$); i livelli a 1090 e 1248 keV con $I=2+$, e $3+$ rispettivamente, si dimostrano essere gli stati vibrazionali γ di quadrupolo corrispondenti a $K=2$. Lo stato eccitato più elevato del ^{152}Sm si trova a 1417 keV ed è probabilmente alimentato completamente per cattura L ; è questo l'unico stato con parità dispari del ^{152}Sm avente carattere $I=1-$. I livelli del ^{152}Gd a 344 e 754 keV, ambi con $I=2+$, raggiunti col decadimento β^- sono caratteristici delle vibrazioni collettive di tipo quadrupolo elettrico intorno a una configurazione d'equilibrio sferica. Il livello a 1114 keV del ^{152}Gd ha caratteristica $I=3-$ e si ritiene dovuto alle vibrazioni da ottupolo. Allo stato fondamentale del ^{152}Eu è stato assegnato lo spin $I=4-$; si sono calcolati i rapporti e le probabilità di transizione per i gruppi β^- e le transizioni per cattura elettronica. I risultati sperimentali si accordano con le previsioni del modello nucleare unificato.

(*) Traduzione a cura della Redazione.

The Influence of the Anomalous Magnetic Moment on the Spin Kinematics of Electrons in a Uniform Magnetic Field.

M. CARRASSI

Istituto di Fisica dell'Università - Genova
Istituto di Fisica Nucleare - Sezione Aggregata di Genova

(ricevuto il 20 Settembre 1957)

Summary. — The influence of a uniform magnetic field on the spin orientation of electrons, or other spin $\frac{1}{2}$ particles, in a beam is computed by assuming that the Dirac-Pauli equation correctly represents the electrons having anomalous magnetic moment. It is shown that, when the field is orthogonal to the electron beam, the anomalous magnetic moment causes the spin to turn about the field direction faster than in the normal condition. This effect depends on the energy of the electrons and becomes particularly large for energies which are high compared with the rest mass: for about 250 MeV energies a half circle path in the field would suffice to convert the longitudinal polarization state of the beam into the transverse one. The calculations are performed by making use of the exact solution of the Dirac-Pauli equation.

1. — It is interesting for many purposes to evaluate the effect of the anomalous magnetic moment on the spin kinematics of electrons, or of other Dirac particles, moving in a uniform magnetic field. This effect is at present of special interest due to the fact that polarized particles can now be injected directly into an accelerating machine.

MENDLOWITZ and CASE ⁽¹⁾ have recently derived the angular velocity of the spin precession of an electron having anomalous magnetic moment. Their starting point is the Dirac Hamiltonian with the additional term of Pauli type $a\mu_0\beta\sigma\cdot H$; subsequently, however, they have analyzed the problem in

⁽¹⁾ H. MENDLOWITZ and K. M. CASE: *Phys. Rev.*, **97**, 33 (1955).

the FOLDY-WOUTHUYSEN ⁽²⁾ representation obtaining the new Hamiltonian up to terms of the first order in $\mu_0 H$. By means of this method, the authors have found that, when the constant homogeneous magnetic field is perpendicular to the electron beam,

$$(*) \quad \omega_s = \omega_L \left(1 + \frac{a}{\sqrt{1 - \beta^2}} \right),$$

where ω_L is the relativistic cyclotron frequency, $a = \alpha/2\pi$ is the second order radiative correction to the spin magnetic moment, $\beta = v/c$. The result contained in the (*) deserves to be verified not only because of the importance it may have in the experiment of LOUISELL, CRANE and PIDD ⁽³⁾ for the direct measurement of the magnitude of the gyromagnetic ratio of the electron, but also for the large effect that it might produce when high energy particles are considered. In fact, for an electron energy of about 50 MeV, one should expect a 10 percent effect on the angular velocity; in other words, a few revolutions of the electron beam path should, in contrast to what is generally believed, suffice to obtain an observable anomalous spin rotation. Of course this statement is correct under the hypothesis that particles with anomalous magnetic moment are properly described by the Dirac equations in conjunction with the Pauli term $a\mu_0\beta\boldsymbol{\sigma}\cdot\mathbf{H}$. This assumption, of course, leaves open the question whether it is correct to interpret the anomalous magnetic moment as an intrinsic property of the particle or such moment should be attributed to radiative correction; in the latter case the Pauli term may not suffice to describe the behaviour of the particle, whatever its energy. Bearing this limitation in mind, the spin rotation has been directly calculated in the present work by using the exact solutions of the Dirac-Pauli ⁽⁴⁾ equation in a uniform magnetic field. In Sect. 2 it is shown that the generally used definition ⁽⁵⁾ of « spin direction » is again convenient using the Dirac-Pauli equation.

The solutions are derived in Sect. 3 according to the method used in a preceding work ⁽⁶⁾. In Sect. 4 the spin direction for the electron beam emerging from a magnetic field is explicitly obtained as a function of the spin direction of the incident beam. The result agrees with that obtained by MENDLOWITZ and CASE by using the Foldy-Wouthuysen representation.

⁽²⁾ L. L. FOLDY and S. A. WOUTHUYSEN: *Phys. Rev.*, **78**, 29 (1950) see also K. M. CASE: *Phys. Rev.*, **95**, 1323 (1954); furthermore H. MENDLOWITZ, in his thesis (unpublished), has treated, in the Foldy-Wouthuysen representation, an electron with an anomalous moment in a constant magnetic field, but we have not seen this work.

⁽³⁾ W. H. LUISELL, R. W. PIDD and H. R. CRANE: *Phys. Rev.* **94**, 7 (1954).

⁽⁴⁾ W. PAULI: *Hand. der Phys.*, **24**, 232; for a discussion of the Dirac-Pauli equation in a uniform magnetic field see also: P. CALDIROLA: *Rend. Ist. Lomb.*, **77**, 1 (1944).

⁽⁵⁾ See for example: N. F. MOTT and H. S. W. MASSEY: *The Theory of Atomic Collisions* (Oxford, 1949).

⁽⁶⁾ M. CARRASSI: *Nuovo Cimento*, **5**, 955 (1957). Referred to as (I) in the text.

2. - Let us consider the relativistic equation of Dirac-Pauli:

$$(1) \quad \left(\sum_{\mu} \beta^{\mu} \pi_{\mu} + i m_0 c + \frac{\lambda}{c} \frac{1}{2} \sum_{\mu\nu} \sigma^{\mu\nu} F_{\mu\nu} \right) \tilde{\psi} = 0,$$

were $\mu = 1, 2, 3, 4$; $\beta_{\mu} = (i\beta\alpha, \beta)$, α and β being the usual Dirac matrices; $\sigma_{\mu\nu} = \frac{1}{2}(\beta_{\mu}\beta_{\nu} - \beta_{\nu}\beta_{\mu})$; $F_{\mu\nu} = (\partial A_{\nu}/\partial x_{\mu} - \partial A_{\mu}/\partial x_{\nu})$ with $x_{\mu} = (\mathbf{r}, ict)$ and $A_{\mu} = (\mathbf{A}, i\Phi)$ $\pi_{\mu} = -i\hbar(\partial/\partial x_{\mu}) + (e/c)A_{\mu}$; λ is a constant of the dimensions of a magnetic moment so that the magnetic moment of the electron is $\mu = \mu_0 + \lambda$ (μ_0 is the Bohr magneton). If we express the electromagnetic tensor $F_{\mu\nu}$ in terms of the field intensities and write $\tilde{\psi} = \psi \exp[-(i/\hbar)\omega t]$, the equation (1) becomes:

$$(2) \quad \{w + e\Phi + c\boldsymbol{\alpha} \cdot \boldsymbol{\pi} + \beta m_0 c^2 + \lambda\beta[\boldsymbol{\sigma} \cdot \mathbf{H} + i(\boldsymbol{\alpha} \cdot \mathbf{E})]\} \psi = 0,$$

where ψ is now the spacial wave function with four components: ψ_j ($j=1, 2, 3, 4$) and $w = (p^2 c^2 + m_0^2 c^4)^{\frac{1}{2}}$.

Since our object is to study the spin kinematics in a magnetic field, the spin direction is taken to be defined, as we did in (I), in the usual way through the ratio:

$$(3) \quad \frac{\psi_3}{\psi_4} = \operatorname{tg} \frac{\chi}{2} \cdot \exp[i\omega],$$

where χ and ω are the polar angles of the « spin direction » in the co-ordinate system in which the electron is at rest.

This definition is the most convenient for all the problems concerning polarization states of the electrons, as TOLHOEK and DE GROOT (?) have clearly shown; furthermore, for a fast electron it is also the only method available at present by which the spin might be observed in practice since, as we already know (⁵), a decelerating electrostatic field does not change the ratio ψ_3/ψ_4 . This last property, indeed, might not be satisfied if we use equation (2) to describe the motion of the electron with anomalous magnetic moment. Actually, equation (2) contains a new term of interaction depending on the electric field; however, this term $i\lambda\beta\boldsymbol{\alpha} \cdot \mathbf{E}$, effects a mixture of the components in the same way as the term $c\boldsymbol{\alpha} \cdot \boldsymbol{\pi}$ and hence causes no difficulty. Indeed if we confine ourselves to the case of an electron moving parallel to the z axis, there being also an electrostatic field in this direction, we easily show that ψ_3 and ψ_4 both satisfy the same differential equation.

$$(4) \quad (w + e\Phi - m_0 c^2) \psi + \hbar^2 c^2 \left(\frac{\partial}{\partial z} - \frac{\lambda}{\hbar c} \frac{\partial \Phi}{\partial z} \right) \cdot \left[(w + e\Phi + m_0 c^2)^{-1} \left(\frac{\partial}{\partial z} + \frac{\lambda}{\hbar c} \frac{\partial \Phi}{\partial z} \right) \right] \psi = 0.$$

(?) H. A. TOLHOEK and S. R. DE GROOT: *Physica*, **17**, 17 (1951); H. A. TOLHOEK: *Rev. Mod. Phys.*, **28**, 277 (1956).

Thus, since the equation (4) is homogeneous and ψ_3 and ψ_4 both satisfy the analogous boundary conditions, it follows that the ratio ψ_3/ψ_4 does not change. The same result can be deduced calculating explicitly the solutions of equation (2) as TOLHOEK and DE GROOT have done for a Dirac particle ⁽⁸⁾.

This remark is also of interest since even when considering electrons with anomalous magnetic moment, any longitudinal electric field does not change the spin direction.

3. — If we consider the influence of the magnetic field alone, the equation (2) becomes:

$$(5) \quad \left[\frac{w}{c} + \boldsymbol{\alpha} \cdot \boldsymbol{\pi} + \beta m_0 c + \frac{\lambda}{c} \beta \boldsymbol{\sigma} \cdot \mathbf{H} \right] \psi = 0.$$

To solve the equation (5), we confine ourselves to the following case: $H=0$ for $x < 0$ and $H=H_z = \text{const.}$ for $x > 0$ (see the figure).

We proceed in a way analogous to that followed in I) in order to obtain the physically interesting solutions. Hence, putting $A_x = -\frac{1}{2}Hy$, $A_y = \frac{1}{2}Hx$, $A_z = 0$, the set of equations (5) can be reduced to the system of two second order differential equations

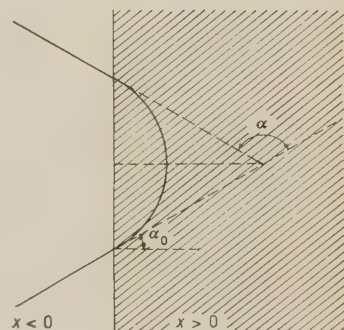


Fig. 1.

$$(6) \quad \left\{ \begin{aligned} & \left[\frac{(w - \lambda H)^2}{c^2} - m_0^2 c^2 - (\pi_x^2 + \pi_y^2) - \hbar \frac{e}{c} H - (1 - 2C_\lambda) \pi_z^2 \right] \cdot \psi_3 + \\ & \quad + 2C_\lambda (\pi_x - i\pi_y) \pi_z \psi_4 = 0, \\ & \left[\frac{(w + \lambda H)^2}{c^2} - m_0^2 c^2 - (\pi_x^2 + \pi_y^2) + \hbar \frac{e}{c} H - (1 + 2\bar{C}_\lambda) \pi_z^2 \right] \cdot \psi_4 + \\ & \quad + 2\bar{C}_\lambda (\pi_x + i\pi_y) \pi_z \psi_3 = 0, \end{aligned} \right.$$

where

$$C_\lambda = \frac{\lambda H}{w + m_0 c^2 + \lambda H}; \quad \bar{C}_\lambda = \frac{\lambda H}{w + m_0 c^2 - \lambda H}.$$

Among the four unknown functions there exist the relations:

$$(7) \quad \left\{ \begin{aligned} \psi_1 &= -\frac{C_\lambda}{\lambda H} [(\pi_x - i\pi_y) \psi_4 + \pi_z \psi_3], \\ \psi_2 &= -\frac{\bar{C}_\lambda}{\lambda H} [(\pi_x + i\pi_y) \psi_3 - \pi_z \psi_4]. \end{aligned} \right.$$

⁽⁸⁾ E. T. WHITTAKER and G. N. WATSON: *Modern Analysis* (Cambridge, 1952).

Since π_z commutes with π_x and π_y , it commutes also with the hamiltonian and therefore p_z is a constant of motion. Then we put $p_z = 0$ and so we treat the problem as independent of the z -coordinate. This assumption means that the propagation vector of the plane wave in the region $x < 0$ is perpendicular to the z -axis. The system (6) is reduced to two independent differential equations

$$(6') \quad \left[\frac{w^2 + \lambda^2 H^2}{c^2} - m_0^2 c^2 - (\pi_x^2 + \pi_y^2) - \left(\hbar \frac{e}{c} H + \frac{2w\lambda H}{c^2} \right) \sigma_z \right] \begin{pmatrix} \psi_3 \\ \psi_4 \end{pmatrix} = 0,$$

while equations (7) become

$$(7') \quad \begin{cases} \psi_1 = -\frac{C_\lambda}{\lambda H} (\pi_x - i\pi_y) \psi_4, \\ \psi_2 = -\frac{\bar{C}_\lambda}{\lambda H} (\pi_x + i\pi_y) \psi_3. \end{cases}$$

System (6'), putting $\omega = eH/2c$, can be written

$$(8) \quad \left[\frac{w^2 + \lambda^2 H^2}{c^2} - m_0^2 c^2 + \hbar^2 \nabla^2 - 2i\hbar\omega \left(y \frac{\partial}{\partial x} - x \frac{\partial}{\partial y} \right) - \omega^2 (x^2 + y^2) - 2 \left(\hbar\omega + \frac{w\lambda H}{c^2} \right) \sigma_z \right] \begin{pmatrix} \varphi_3 \\ \varphi_4 \end{pmatrix} = 0.$$

Using the same substitution as in (6,I) and also $\xi = 2(x + (\eta/2\omega))\sqrt{\omega/\hbar}$, we obtain

$$(8') \quad \left\{ \frac{d^2}{d\xi^2} + \frac{1}{4\omega\hbar} \left[p^2 + \frac{\lambda^2 H^2}{c^2} - \hbar\omega\xi^2 - 2 \left(\hbar\omega + \frac{w\lambda H}{c^2} \right) \sigma_z \right] \right\} \begin{pmatrix} \psi_3 \\ \psi_4 \end{pmatrix} = 0.$$

Putting finally

$$(9) \quad \begin{cases} \nu' = \nu \left(1 + \frac{\lambda^2 H^2}{p^2 c^2} - \frac{2w\lambda H}{p^2 c^2} \right), \\ \nu'' = \nu \left(1 + \frac{\lambda^2 H^2}{p^2 c^2} + \frac{2w\lambda H}{p^2 c^2} \right), \end{cases}$$

where $\nu = p^2/4\hbar\omega$ is the number of De Broglie wave lengths contained in a half circle of radius $r = cp/eH$, we can write the two equations

$$(10) \quad \begin{cases} \frac{d^2 \varphi_3}{d\xi^2} + \left(\nu' - \frac{1}{2} - \frac{1}{4} \xi^2 \right) \varphi_3 = 0, \\ \frac{d^2 \varphi_4}{d\xi^2} + \left(\nu'' + \frac{1}{2} - \frac{1}{4} \xi^2 \right) \varphi_4 = 0. \end{cases}$$

We observe that (10) differs from equations (7,I) obtained using the normal

Dirac equation, only for the values of the constants ν' and ν'' . Therefore, all terms of interaction with the anomalous magnetic moment are contained in these constants. The solutions are again the parabolic cylinder functions and we put $\varphi_3 = AD_{\nu'-1}(\xi)$ and $\varphi_4 = BD_{\nu''}(\xi)$. Using (7'), (6,I) and the known recurrence formulae of the D_ν functions, we find the solution of the equation (5) in the case $x > 0$

$$(11) \quad \psi = \begin{pmatrix} \frac{2i\sqrt{\hbar\omega}}{(w/c) + m_0c + (\lambda H/c)} B\nu'' D_{\nu''-1} \\ -\frac{2i\sqrt{\hbar\omega}}{(w/c) + m_0c - (\lambda H/c)} AD_{\nu'} \\ AD_{\nu'-1} \\ BD_{\nu''} \end{pmatrix} \exp \left[\frac{i}{\hbar} (\omega xy + \eta y) \right].$$

We now have to match, in $x = 0$, the solution (11) with that in the region $x < 0$ (see (9,I)). From this condition the following system is obtained

$$(12) \quad \begin{cases} (B_2 - B_1)p_x + i(B_1 + B_2)p_y = 2i\gamma_+ \sqrt{\hbar\omega} B\nu'' D_{\nu''-1}(\xi_0) \\ (A_2 - A_1)p_x - i(A_1 + A_2)p_y = -2i\gamma_- \sqrt{\hbar\omega} AD_{\nu'}(\xi_0) \\ A_1 + A_2 = AD_{\nu'-1}(\xi_0) \\ B_1 + B_2 = BD_{\nu''}(\xi_0), \end{cases}$$

where

$$\xi_0 = \frac{p_y}{\sqrt{\hbar\omega}}, \quad \gamma_+ = \left(1 + \frac{\lambda H}{w + m_0 c^2} \right)^{-1}, \quad \gamma_- = \left(1 - \frac{\lambda H}{w + m_0 c^2} \right)^{-1}.$$

From (12) we can easily derive the ratio B_2/A_2 , which specifies the polarization state of the reflected beam in terms of the initial data for the incident plane wave.

Let α be the angle between the momentum of the reflected beam and the momentum of the incident beam. Then, as shown in the figure, $\alpha = \pi - 2\alpha_0$, where $\alpha_0 = \text{tg}^{-1} p_y/p_x$.

Hence we have

$$(13) \quad \exp[i\alpha] = -\frac{p_x - ip_y}{p_x + ip_y}.$$

Using (13), from system (12) we deduce

$$(14) \quad \frac{B_2}{A_2} = \frac{B_1}{A_1} \exp[i\alpha] \frac{1 + i \left(\frac{p_y}{p_x} - \frac{p}{p_x} \frac{1}{\gamma_+} \sqrt{\frac{\nu}{\nu''}} R^+ \right) \frac{1 - i \left(\frac{p_y}{p_x} - \frac{p}{p_x} \gamma_- \sqrt{\frac{\nu'}{\nu}} R^- \right)}{1 - i \left(\frac{p_y}{p_x} - \frac{p}{p_x} \frac{1}{\gamma_+} \sqrt{\frac{\nu}{\nu''}} R^+ \right) \frac{1 + i \left(\frac{p_y}{p_x} - \frac{p}{p_x} \gamma_- \sqrt{\frac{\nu'}{\nu}} R^- \right)},$$

where we have used the definition $\nu = p^2/4\hbar\omega$ and we have put

$$R^+ = \frac{D_{\nu''}(\xi_0)}{\sqrt{\nu''} D_{\nu''-1}(\xi_0)}, \quad R^- = \frac{D_{\nu'}(\xi_0)}{\sqrt{\nu'} D_{\nu'-1}(\xi_0)}.$$

Now, putting

$$M = \frac{p_y}{p_x} - \frac{p}{p_x} \frac{1}{\gamma_+} \sqrt{\frac{\nu}{\nu''}} R^+ \quad \text{and} \quad N = \frac{p_y}{p_x} - \frac{p}{p_x} \gamma_- \sqrt{\frac{\nu'}{\nu}} R^-,$$

we have

$$\frac{1 + iM}{1 - iM} \frac{1 - iN}{1 + iN} = \frac{1 + i \frac{M - N}{1 + MN}}{1 - i \frac{M - N}{1 + MN}} = \frac{1 + i \operatorname{tg} \frac{\delta}{2}}{1 - i \operatorname{tg} \frac{\delta}{2}} = \exp[i\delta].$$

Therefore (14) can be written in the useful form

$$(15) \quad \frac{B_2}{A_2} = \frac{B_1}{A_1} \exp[i(\alpha + \delta)],$$

where δ is defined by the relation:

$$(16) \quad \operatorname{tg} \frac{\delta}{2} = \frac{M - N}{1 + MN} = \frac{p_x \left(\gamma_- \sqrt{\frac{\nu'}{\nu}} R^- - \frac{1}{\gamma_+} \sqrt{\frac{\nu}{\nu''}} R^+ \right)}{p - p_y \left(\gamma_- \sqrt{\frac{\nu'}{\nu}} R^- + \frac{1}{\gamma_+} \sqrt{\frac{\nu}{\nu''}} R^+ \right) + p \frac{\gamma_-}{\gamma_+} \sqrt{\frac{\nu'}{\nu''}} R^+ R^-}.$$

4. - It may be noted that (15) and (16) are exact formulae because till now no approximations have been made though we have considered particular conditions. However it will be convenient now to remember that $\nu \cong 10^8 \div 10^{15}$, in every case of interest; hence ν' and ν'' according to (9), are of the same order of magnitude. In addition we may observe that putting $\lambda = a\mu_0 = a(e\hbar/2m_0c)$, where a is the percentage correction to the magnetic moment, we can write

$$\lambda H = a\mu_0 H = a \frac{\hbar\omega}{m_0} = \frac{a}{4\nu} \frac{p^2}{m_0}$$

and therefore (9) gives

$$(17) \quad \begin{cases} \frac{\nu'}{\nu} = 1 - \frac{a}{2\nu} \frac{w}{m_0 c^2} + \left(\frac{a}{4\nu}\right)^2 \left(\frac{pc}{m_0 c^2}\right)^2 \\ \frac{\nu''}{\nu} = 1 + \frac{a}{2\nu} \frac{w}{m_0 c^2} + \left(\frac{a}{4\nu}\right)^2 \left(\frac{pc}{m_0 c^2}\right)^2. \end{cases}$$

Furthermore if a is of order 10^{-3} , it is clear that the last term in the two relations (17) is quite negligible both compared to unity and to the first order term. With this in mind and remembering the definitions of γ_+ and γ_- , we obtain

$$\gamma_- \sqrt{\frac{\nu'}{\nu}} = \frac{1}{\gamma_+} \sqrt{\frac{\nu}{\nu''}} = 1 - \frac{a}{4\nu} \cong 1.$$

With these simplifications, (16) becomes

$$(18) \quad \operatorname{tg} \frac{\delta}{2} = \frac{(p_x/p)(R^- - R^+)}{1 - (p_y/p)(R^- + R^+) + R^+ R^-}.$$

The functions R^+ and R^- can be evaluated asymptotically for large values of the parameters ν' and ν'' , as we have shown in the Appendix. Hence, we obtain:

$$(19) \quad \begin{cases} R^-(\xi_0) = \frac{D_{\nu'}(\xi_0)}{\sqrt{\nu'} D_{\nu'-1}(\xi_0)} = \frac{\cos(\gamma' - \beta_0)}{\sin \gamma'} = \operatorname{ctg} \gamma' \cos \beta_0 + \sin \beta_0, \\ R^+(\xi_0) = \frac{D_{\nu''}(\xi_0)}{\sqrt{\nu''} D_{\nu''-1}(\xi_0)} = \frac{\cos(\gamma'' - \beta_0)}{\sin \gamma''} = \operatorname{ctg} \gamma'' \cos \beta_0 + \sin \beta_0, \end{cases}$$

where

$$\gamma' = \frac{\pi \nu'}{2} - 2 \frac{p_y}{p} \left(\nu - \frac{a}{4} \frac{w}{m_0 c^2} \right) + \frac{1}{2} \frac{p_y}{p}, \quad \gamma'' = \frac{\pi \nu''}{2} - 2 \frac{p_y}{p} \left(\nu + \frac{a}{4} \frac{w}{m_0 c^2} \right) + \frac{1}{2} \frac{p_y}{p}.$$

By putting (19) into (18) and keeping terms up to the second order in $p_y/p = \beta_0$, we find:

$$\operatorname{tg} \frac{\delta}{2} = \frac{\operatorname{ctg} \gamma'' - \operatorname{ctg} \gamma'}{1 + \operatorname{ctg} \gamma' \operatorname{ctg} \gamma''} = \operatorname{tg}(\gamma'' - \gamma') = \operatorname{tg} \left[\frac{\pi}{2} (\nu'' - \nu') - \frac{p_y}{p} a \frac{w}{m_0 c^2} \right].$$

From the expressions of ν' and ν'' and assuming $p_y/p = \beta_0 \cong \alpha_0$ we obtain

$$(20) \quad \delta = a \frac{w}{m_0 c^2} (\pi - 2\alpha_0).$$

Hence from (15) finally we have

$$(21) \quad \frac{B_2}{A_2} = \frac{B_1}{A_1} \exp \left[i\alpha \left(1 + a \frac{w}{m_0 c^2} \right) \right] = \operatorname{tg} \frac{\chi}{2} \exp \left[i \left\{ \omega + \alpha \left(1 + a \frac{w}{m_0 c^2} \right) \right\} \right].$$

It appears from this result that the spin direction of the reflected beam is rotated around the direction of the magnetic field by an angle larger than the rotation angle of the momentum. If $\alpha = \pi$, one gets

$$\frac{B_2}{A_2} = -\frac{B_1}{A_1} \exp \left[i\pi a \frac{w}{m_0 c^2} \right].$$

The last result, corresponding to the particular condition $p_y = 0$, can be obtained directly, as we have shown in the Appendix, without using the asymptotic formula for the D_ν function. In this particular case the effect of the anomalous magnetic moment on the spin precession about the field direction might become particularly large for sufficiently large energies. Indeed, the rotation of the spin exceeds the «normal precession», by an angle $\Delta\alpha_\pi = \pi a(w/m_0 c^2)$ and therefore for an energy $w = 250$ MeV, one gets $\Delta\alpha_\pi \simeq \pi/2$. Thus, at this energy, an incident longitudinal polarized beam is «reflected» by the field with a transversal polarization.

The angular velocity of the spin precession can be easily obtained from (21); in fact, if $r = cp/eH$ is the radius of the classical half circle described by the electrons in the magnetic field, the time spent in traveling the path αr is:

$$t = \frac{1}{\sqrt{1-\beta^2}} \frac{m_0}{p} \alpha r = \frac{\alpha}{\sqrt{1-\beta^2}} \frac{m_0 c}{eH}.$$

Hence the angular velocity is

$$\omega_s = \frac{\alpha(1 + a(w/m_0 c^2))}{t} = \sqrt{1-\beta^2} \frac{eH}{m_0 c} \left(1 + a \frac{w}{m_0 c^2} \right) = \omega_L \left(1 + \frac{a}{\sqrt{1-\beta^2}} \right),$$

where ω_L is the angular velocity of the normal spin precession and therefore our result agrees with that obtained by MEDLOWITZ and CASE.

* * *

The author wishes to thank Professor A. BORSELLINO for encouragement and helpful advice received in working out this paper.

APPENDIX

For the calculation of the R^+ and R^- functions, it is necessary to find explicit expressions for the $D_{\nu}(\xi_0)$ and $D_{\nu'}(\xi_0)$ functions for large values of the parameters ν' and ν'' . In the mathematical literature ⁽⁹⁾ there are, under suitable hypotheses, several asymptotic expressions for the confluent hypergeometric functions for large value of the parameters on which these depend. In our case, the question is more complicated, because the variable $\xi_0 = p_{\nu}/\sqrt{\hbar\omega} = (p_{\nu}/p)2\sqrt{\nu}$ contains also the magnitude of the parameter itself. We refer to a detailed work of N. SCHWID ⁽¹⁰⁾, where two independent solutions of the Weber's equation are obtained assuming n to be very large. These solutions $w_1(z)$ and $w_2(z)$ are related to the usual parabolic cylinder functions as follows:

$$(1A) \quad \begin{cases} \Gamma\left(\frac{n+1}{2}\right) 2^{(n+1)/2} w_1(z) = \Gamma(n+1)[D_{-n-1}(iz) + D_{-n-1}(-iz)], \\ \Gamma\left(\frac{n}{2} + 1\right) 2^{(n+5)/2} w_2(z) = i\Gamma(n+1)[D_{-n-1}(iz) - D_{-n-1}(-iz)] \end{cases}$$

(n is real). Further, by using the relation:

$$(2A) \quad D_n(z) = \frac{\Gamma(n+1)}{\sqrt{2\pi}} \left\{ \cos \frac{n\pi}{2} [D_{-n-1}(iz) + D_{-n-1}(-iz)] + i \sin \frac{n\pi}{2} [D_{-n-1}(iz) - D_{-n-1}(-iz)] \right\},$$

the expressions of $w_1(z)$ and $w_2(z)$ and the asymptotic expressions of the $\Gamma(n)$ functions, from (1A) and (2A) one obtains:

$$(3A) \quad D_n(z) = \frac{e^{-n/2} n^{n/2} 2^{\frac{1}{2}}}{[1 - z^2/2(2n+1)]^{\frac{1}{2}}} \left\{ \cos \left[\frac{n\pi}{2} - z \left(n + \frac{1}{2} \right)^{\frac{1}{2}} \right] + O[n^{-\frac{1}{2}}] \right\}.$$

The relation (3A) holds good within the semicircle of radius $|z| = [2(2n+1)]^{\frac{1}{2}}$ contained in the half plane $R(z) \geq 0$ excluding the neighbourhood of the circumference. For the purpose of our calculation, we must consider that $z = \xi_0$ and that n will be either equal to ν' or $\nu'' - 1$ for the functions involved in R^+ , or, alternatively, to ν'' or $\nu' - 1$ for the functions involved in R^- . In order to ensure the validity of (3A) and noting that $\xi_0 = (p_{\nu}/p)2\sqrt{\nu}$, we shall assume, although this hypothesis is not strictly necessary, that $p_{\nu}/p \ll 1$ (i.e. we shall keep terms up to the second order in $p_{\nu}/p = \sin \alpha_0$). This hypothesis only means that we limit ourselves to consider those particular cases

⁽⁹⁾ A. ERDELYI, W. MAGNUS, F. OBERHETTINGER and F. TRICOMI: *Higher Transcendental Functions*, vol. I and II (New York, 1953); W. MAGNUS and F. OBERHETTINGER: *Special Functions of Mathematical Physics* (New York, 1949).

⁽¹⁰⁾ N. SCHWID: *Trans. American Math. Soc.*, **37**, 339 (1935).

in which the angle α_0 is not wider than a few degrees; furthermore, it allows considerable simplifications in the final formulae. Particular care shall be given to the simplifications of the arguments of the trigonometric functions contained in (3A). In fact it is permitted to neglect the terms of the order of $1/\nu'$ (or $1/\nu''$), but unity is not negligible compared to ν' (or ν''). Making use of (17), one obtains:

$$(4A) \quad \left\{ \begin{array}{l} \xi_0 \left(\nu' + \frac{1}{2} \right)^{\frac{1}{2}} = \frac{p_y}{p} 2 \left(\nu - \frac{a}{4} \frac{w}{m_0 c^2} + \frac{1}{4} \right), \\ \xi_0 \left(\nu' - \frac{1}{2} \right)^{\frac{1}{2}} = \frac{p_y}{p} 2 \left(\nu - \frac{a}{4} \frac{w}{m_0 c^2} - \frac{1}{4} \right), \\ \xi_0 \left(\nu'' + \frac{1}{2} \right)^{\frac{1}{2}} = \frac{p_y}{p} 2 \left(\nu + \frac{a}{4} \frac{w}{m_0 c^2} + \frac{1}{4} \right), \\ \xi_0 \left(\nu'' - \frac{1}{2} \right)^{\frac{1}{2}} = \frac{p_y}{p} 2 \left(\nu + \frac{a}{4} \frac{w}{m_0 c^2} - \frac{1}{4} \right). \end{array} \right.$$

From (4A) and (3A) one thus finds:

$$(5A) \quad \left\{ \begin{array}{l} D_{\nu'}(\xi_0) = \frac{\sqrt{2} e^{-\nu'/2} \nu'^{1/2}}{(1 - (\xi_0^2/4\nu'))^{\frac{1}{4}}} \cos \left[\frac{\pi \nu'}{2} - 2 \frac{p_y}{p} \left(\nu - \frac{a}{4} \frac{w}{m_0 c^2} \right) - \frac{1}{2} \frac{p_y}{p} \right], \\ D_{\nu'-1}(\xi_0) = \frac{\sqrt{2} e^{-(\nu'-1)/2} (\nu'-1)^{(\nu'-1)/2}}{(1 - (\xi_0^2/4\nu'))^{\frac{1}{4}}} \sin \left[\frac{\pi \nu'}{2} - 2 \frac{p_y}{p} \left(\nu - \frac{a}{4} \frac{w}{m_0 c^2} \right) + \frac{1}{2} \frac{p_y}{p} \right], \\ D_{\nu''}(\xi_0) = \frac{\sqrt{2} e^{-\nu''/2} \nu''^{1/2}}{(1 - (\xi_0^2/4\nu''))^{\frac{1}{4}}} \cos \left[\frac{\pi \nu''}{2} - 2 \frac{p_y}{p} \left(\nu + \frac{a}{4} \frac{w}{m_0 c^2} \right) - \frac{1}{2} \frac{p_y}{p} \right], \\ D_{\nu''-1}(\xi_0) = \frac{\sqrt{2} e^{-(\nu''-1)/2} (\nu''-1)^{(\nu''-1)/2}}{(1 - (\xi_0^2/4\nu''))^{\frac{1}{4}}} \sin \left[\frac{\pi \nu''}{2} - 2 \frac{p_y}{p} \left(\nu + \frac{a}{4} \frac{w}{m_0 c^2} \right) + \frac{1}{2} \frac{p_y}{p} \right]. \end{array} \right.$$

Since for large values of n , $(1 + (A/n))^n \cong e^A$, we may put in (5A)

$$(\nu' - 1)^{(\nu'-1)/2} = \nu'^{1/2} \left(\frac{e}{\nu'} \right)^{\frac{1}{2}} \quad \text{and} \quad (\nu'' - 1)^{(\nu''-1)/2} = \nu''^{1/2} \left(\frac{e}{\nu''} \right)^{\frac{1}{2}}.$$

Using these together with the (5A) and the definitions of R^+ and R , we at once get (19).

When $p_y = 0$, $p = p_x$, (18) becomes

$$(18') \quad \operatorname{tg} \frac{\delta}{2} = \frac{R^-(0) - R^+(0)}{1 + R^+(0) R^-(0)}.$$

Considering that

$$D_n(0) = \frac{\Gamma(\frac{1}{2}) 2^{n/2}}{\Gamma((1-n)/2)},$$

and using the well known relations satisfied by the Euler functions as well as the asymptotic expression

$$\Gamma(n) \cong e^{-n} n^{-\frac{1}{2}} \sqrt{2\pi},$$

while bearing in mind the definitions of R^+ , R^- , one immediately finds

$$R^+(0) = \cotg \frac{\pi \nu''}{2}, \quad R^-(0) = \cotg \frac{\pi \nu'}{2}.$$

From (18') then follows

$$\tg \frac{\delta}{2} = \tg \frac{\pi}{2} (\nu'' - \nu'),$$

from which (20) is directly obtained in the particular case in which $\alpha = \pi$ ($\alpha_0 = 0$).

RIASSUNTO

Viene calcolato l'effetto di un campo magnetico uniforme sulla orientazione dello spin di un fascio di elettroni, o di altre particelle di spin $\frac{1}{2}$, supponendo che il moto degli elettroni, dotati di momento magnetico anomalo, sia correttamente descritto dall'equazione di Dirac-Pauli. Si dimostra così che, quando il fascio di elettroni è normale alla direzione del campo, l'effetto dovuto al momento magnetico anomalo è di far precedere lo spin intorno alla direzione del campo più velocemente che nel caso normale. Tale effetto dipende dall'energia degli elettroni e diviene particolarmente vistoso per energie elevate rispetto a quella di riposo: per energie di circa 250 MeV, basta il percorso di una semicirconferenza nel campo per mutare lo stato di polarizzazione del fascio da longitudinale in trasversale. I calcoli sono stati eseguiti facendo uso delle soluzioni esatte dell'equazione di Dirac-Pauli.

An Experimental Test of the Fermi-Teller « Z-Law » ^(*)⁽⁺⁾.

J. C. SENS, R. A. SWANSON ^(×), V. L. TELEGDI
and D. D. YOVANOVITCH

*Enrico Fermi Institute for Nuclear Studies, University of Chicago
Chicago, Ill.*

(ricevuto il 2 Ottobre 1957)

Summary. — FERMI and TELLER predicted, in their classic paper on the slowing-down process of negative mesons, the relative probabilities with which the latter should be captured by the different atoms of a chemical compound. They concluded that these *atomic* capture probabilities should be proportional to the nuclear charges, Z_i , of the atoms considered. The experiments here described were carried out to check this prediction. They are based on the fact that negative muons reach rapidly the *K*-orbits around the nuclei of the atoms of the material in which they are slowed down, and disappear from these orbits (either by decay or absorption) at rates which are characteristic for the nuclei in question. Thus the time distribution of decay electrons emerging from a chemical compound in which muons are brought to rest presents in general as many exponential components as there are constituents; their intercepts at time zero (entry of the muons into the material) are directly proportional to $n_i p_i$, where n_i = fraction of component of atomic number Z_i , p_i = capture probability into the mesic *K*-shell of atom of same constituent. Neglecting the possibility of transfer of muons between neighbouring atoms, these p_i are equivalent to the capture probabilities predicted by Fermi and Teller. The present experiments show that at least in insulators (Al_2O_3 , P_2O_5 , SiO_2 , CCl_4 , KOH , KHF_2 , p-dichlorobenzene) the predictions of Fermi and Teller do not hold. No weighting of n_i with Z_i seems to arise, the lighter element being even preferred in some cases. As an explanation, it is pointed out that the energy loss to lattice vibrations, not considered by Fermi and Teller, may be an important mechanism in insulators for negative particles of nearly zero kinetic energy, i.e. at the point of being captured.

(*) A preliminary account of this work has been presented at the 1957 Denver Meeting of the APS (*Bull. Am. Phys. Soc.*, II, 2, No. 6, 320 (1957)).

(+) This research was supported in part by the U.S. Atomic Energy Commission and the Office of Naval Research.

(×) National Science Foundation Fellow, 1956-57.

1. - Introduction.

In the final section of their classic paper ⁽¹⁾ on the capture of negative mesons in matter, FERMI and TELLER proposed to predict the relative probabilities with which mesons are captured by the different kinds of atoms when the slowing-down takes place in a chemical compound. On the basis of some estimates which they themselves considered crude, these authors concluded that the atomic capture probabilities should be proportional to the respective nuclear charges, Z_i , of the atoms in question.

In many experiments, negative mesons are necessarily brought to rest in chemical compounds and mixtures thereof (e.g. in nuclear emulsions, bubble chamber liquids, radiochemical targets, etc.). The interpretation of such experiments depends often critically on the relative capture probabilities referred to above. Lacking direct experimental evidence on this point, many investigators have in the past relied on the theoretical conjecture of FERMI and TELLER, which has then become known as the « Z-law ».

No experiments specifically designed to test the validity of this « law » in a variety of substances appear to have been carried out so far, while sundry contradictory evidence has been obtained as a by-product of various experiments involving negative mesons ⁽²⁻⁴⁾. Among these, the work of STEARNS and STEARNS ⁽⁴⁾ is most significant and shall be discussed in detail later.

The present investigation, made possible by the availability of high intensity, high purity μ^- -beams at the Chicago synchrocyclotron ⁽⁵⁾, aims to provide reliable empirical data on the relative capture probabilities in a number of chemical compounds. It leads to the conclusion that the « Z-law » does not hold in practice, the distribution of captures among the various constituents being approximated more closely by the simple unweighted atomic ratios of the latter in the compound. While this conclusion is based exclusively on experiments performed with muons, it is reasonable to anticipate on the basis of our general understanding of the slowing-down processes that it will apply unchanged to the capture of negative pions.

2. - Experimental method.

Negative muons captured by an atom reach the mesic K -orbit in a time very short compared to their lifetimes in condensed matter, and disappear

⁽¹⁾ E. FERMI and E. TELLER: *Phys. Rev.*, **72**, 399 (1947).

⁽²⁾ W. K. H. PANOFSKY, R. L. AAMODT and J. HADLEY: *Phys. Rev.*, **81**, 565 (1951).

⁽³⁾ A. FAFARMAN and M. H. SHAMOS: *Phys. Rev.*, **100**, 874 (1955).

⁽⁴⁾ M. B. STEARNS and M. STEARNS: *Phys. Rev.*, **105**, 1573 (1957).

⁽⁵⁾ N. P. CAMPBELL and R. A. SWANSON: unpublished report.

from this orbit at a rate, Λ_d , that is characteristics of the nuclear charge Z . Indeed, $\Lambda_d = \Lambda_0 + \Lambda_c$, where Λ_0 is (to an excellent approximation) the muon decay rate in vacuo, and Λ_c the rate at which the muon is captured by the nucleus Z from the K -orbit. Λ_c is proportional to Z^4 , or rather Z_{eff}^4 ⁽⁶⁾.

Decay electrons will appear at a rate proportional to Λ_0/Λ_d , with an exponential time dependence characterized by Λ_d , time zero being that of the arrival in the K -shell. When muons are captured by the different constituents Z_i of a chemical compound, the time dependence of the electron decay rate will be a superposition of various exponentials, each with a different $\Lambda_d(Z_i)$. Indicating the relative capture probability into the K -shell of constituent atom Z_i by p_i , it is clear that the magnitude of any component of the observed electron decay rate at $t = 0$ will be proportional to $(\Lambda_0/\Lambda_d)\Lambda_d p_i n_i$, i.e. simply to $p_i n_i$, where n_i is the fraction of atoms Z_i in the compound. Barring the possibility ⁽⁷⁾ that a muon be transferred from one atom to another while cascading from its first bound orbit around a specific atom to its ultimate K -orbit, these p_i will represent directly the *atomic* capture probabilities sought by FERMI and TELLER. They will in any case represent the quantities of most immediate practical interest, being the relative capture probabilities into the orbits from which nuclear capture occurs.

To implement this method in practice, one has to determine accurately the time dependence of electron decays from negative muons stopped in a chemical compound. In principle it is not necessary to know a priori the Λ_d 's of the various elements contained in the compound, as these parameters can also be obtained from the analysis of the electron decay curves. It is however statistically advantageous to work with compounds consisting of elements which: (a) have been, or can be, investigated in the form of elemental targets, (b) have reasonably different disappearance rates, i.e. differ sufficiently in atomic number. It is obvious that binary compounds yield data that can be analysed less laboriously and more reliably than those from others.

The equipment used to determine the electron decay curves was the one repeatedly referred to in reports ^(8,9) on muon work done in this laboratory, and need not be described here in detail. It consists of a scintillation counter telescope defining the entry of muons onto the target under investigation, a scintillation counter telescope defining the exit of decay electrons from said target, and of a time-to-pulse height converter circuit fed by the coincidences from these two telescopes. The output of the converter is connected to a 100-channel pulse height analyzer. In the present experiment, the total useful

() J. A. WHEELER: *Rev. Mod. Phys.*, **21**, 133 (1949).

(7) T. B. DAY and P. MORRISON: *Phys. Rev.* (in print).

(8) R. A. SWANSON *et al.*: *Bull. Am. Phys. Soc.*, II, **2**, No. 4, 205 (1957).

(9) J. C. SENS, R. A. SWANSON, D. D. YOVANOVITCH and V. L. TELEGI: *Phys. Rev.*, Sept. 1, 1957.

range of the converter was 70 channels, corresponding to $5.15 \mu\text{s}$. The converter was repeatedly calibrated and checked for linearity during the experiment by means of a precision variable delay line (*).

For each of the compounds for which data are reported here, at least $3 \cdot 10^4$ electron counts within the useful range indicated above were collected. The counts from each successive 5 channels of the analyzer were totalled, and the data so obtained were first analysed graphically (+). The results so obtained were found to be somewhat subject to the uncertainties connected with the method, and in particular sensitive to the assumptions made about the « background » counts (these arise experimentally mainly from random coincidences). The data were hereafter subjected to least-squares fits to forms of the type $C_1 \exp [-\Lambda_d(1)t] + C_2 \exp [-\Lambda_d(2)t] + B$, assuming the Λ_d 's as known and weighting the points with the inverses of their variances. This analysis was carried out by means of punched cards on an IBM-650 computer. The relevant quantities $n_i p_i$ were derived from the C_i 's by applying corrections (a) for the lumping of data into groups of five channels, (b) for the known displacement of the « earliest » group of channels with respect to the true zero of time. In all cases the backgrounds B yielded by the least-squares analysis had magnitudes that were reasonable for the counting rates involved, as judged from our experience with elemental targets (3).

3. - Results.

We indicate underneath information relevant to specific targets and runs. The results are summarized in Table I, while Fig. 1 through 5 represent standard semilogarithmic plots of the electron decay rates for a number of targets.

(a) SiO_2 . Target: 6 g/cm² of Vitreosil, a commercial form of high purity fused quartz. Total electron counts: $3.18 \cdot 10^4$, $B = 6 \cdot 10^3$ counts/ μs .

(b) Al_2O_3 . Target: 10 g/cm² of refractory brick. Total electron counts: $14 \cdot 10^4$, $B = 4.6 \cdot 10^3$ counts/ μs .


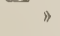
(c) P_2O_5 . Target: 6 g/cm² C.P. grade, anhydrous material, sealed in a thin polyethylene bag. Total electron counts: $4.9 \cdot 10^4$, $B = 1.4 \cdot 10^3$ counts/ μs .

(d) CCl_4 . Target: 6 g/cm² of liquid C.P. grade material, contained in a thin plastic bag. Total electron counts: $7.3 \cdot 10^4$, $B = 1.4 \cdot 10^3$ counts/ μs .

(*) Manufactured by Advance Electronics Co., Passaic, N.J.

(+) These results were quoted in our preliminary communication, *Bull. Am. Phys. Soc.*, II, 2, No. 6, 320 (1957).

TABLE I. — Summary of results on relative capture rates.

| Compound | Ratio | This expt. (*) | F.T. (+) | Atomic (x) |
|---|-------|----------------|----------|------------|
| P ₂ O ₅ | O/P | 2.7 ± .3 | 1.3 | 2.5 |
| CCl ₄ | Cl/C | 4.1 ± .8 | 11.3 | 4.0 |
| Al ₂ O ₃ | O/Al | 2.3 ± .2 | .92 | 1.5 |
| SiO ₂ | O/Si | 3.5 ± .3 | 1.1 | 2.0 |
| KHF ₂ | F/K | 1.7 ± .4 | .95 | 2.0 |
| KOH | O/K | 2.2 ± .4 | .42 | 1.0 |
| Cl  Cl (l) | C/Cl | 2.3 ± .2 | 1.06 | 3.0 |
| »  » (s) | C/Cl | 2.1 ± .2 | 1.06 | 3.0 |

(*) The errors assigned to these ratios are larger than those from statistics alone. Where the decay rates A_d are known from independent experiments (Al, O, P, Si, C) allowance has been made for the uncertainty in these rates; where the decay rates of one or more constituents were derived from the same data, the error has been additionally amplified by an estimated factor. For F, $A_d = 6.31 \cdot 10^8 \text{ s}^{-1}$ has been adopted, contrary to Ref. (9).

(+) The ratios indicated here are those conjectured by Fermi and Teller, i.e. correspond to the assumption that $p_i = Z_i$.

(x) The ratios indicated in this column are the stoichiometric ratios in the compounds, i.e. correspond to the assumption that all $p_i = 1$.

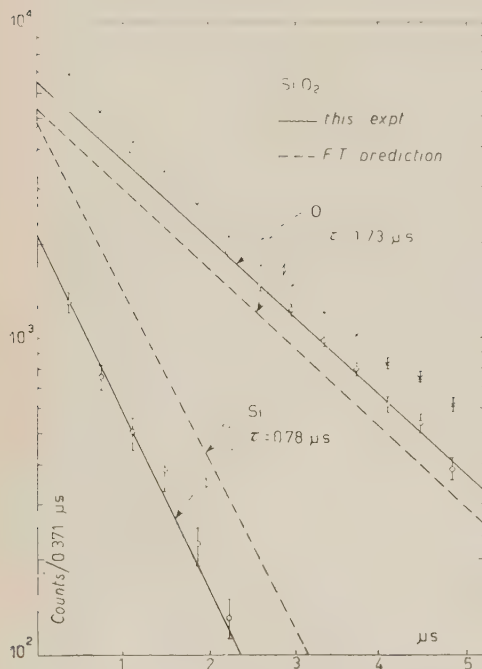


Fig. 1. — Time distribution of electron from μ^- decaying in SiO₂. xxxx: Experimental points. Errors are statistical standard deviations. Constant background is not indicated.

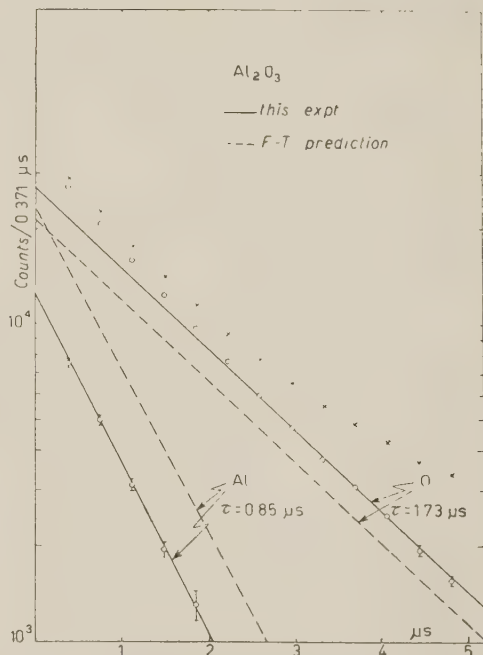


Fig. 2. — Time distribution of electrons from μ^- decaying in Al₂O₃. xxxx: Experimental points. Errors are statistical standard deviations. Constant background is not indicated.

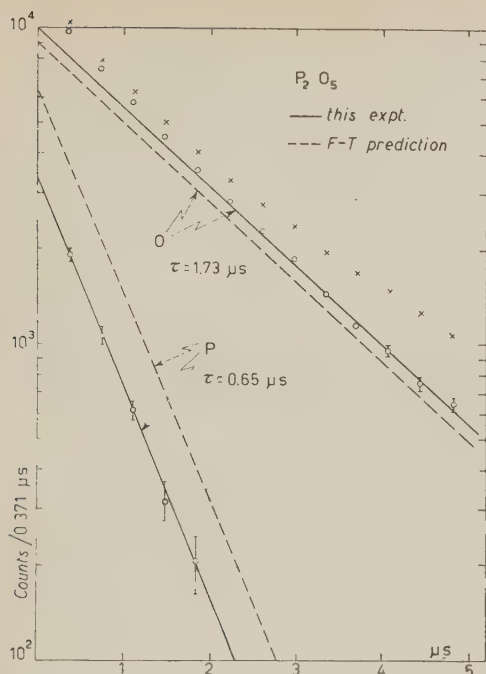


Fig. 3. — Time distribution of electrons from μ^- decaying in P_2O_5 . $\times\times\times\times$: Experimental points. Errors are statistical standard deviations. Constant background is not indicated.

(e) KOH. Target: 6 g/cm² of pellets of C.P. grade material, contained in thin polyethylene bag. Total electron counts: $3.1 \cdot 10^4$, $B = 7.7 \cdot 10^2$ counts/ μ s.

(f) KHF₂. Target: 6 g/cm² of C.P. grade material, contained in thin polyethylene bag. Total electron counts: $4.6 \cdot 10^4$, $B = 8.7 \cdot 10^2$ counts/ μ s.

(g) p-dichloro-benzene. Target: 6 g/cm² of solid, C.P. grade material

Fig. 5. — Time distribution of electrons from μ^- decaying in KOH. $\times\times\times\times$: Experimental points. Errors are statistical standard deviations. Constant background is not indicated.

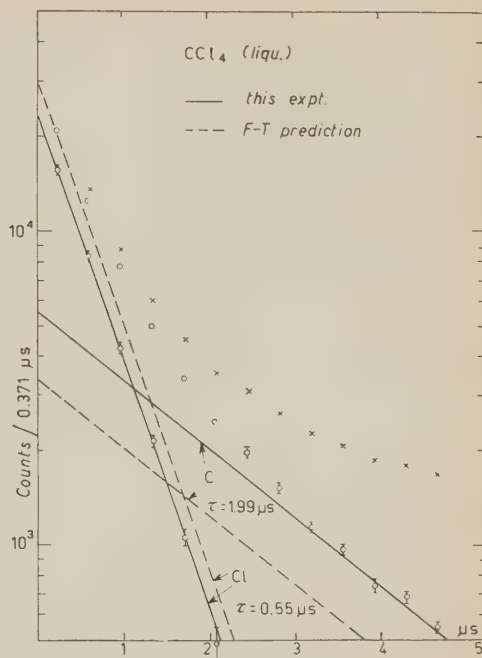
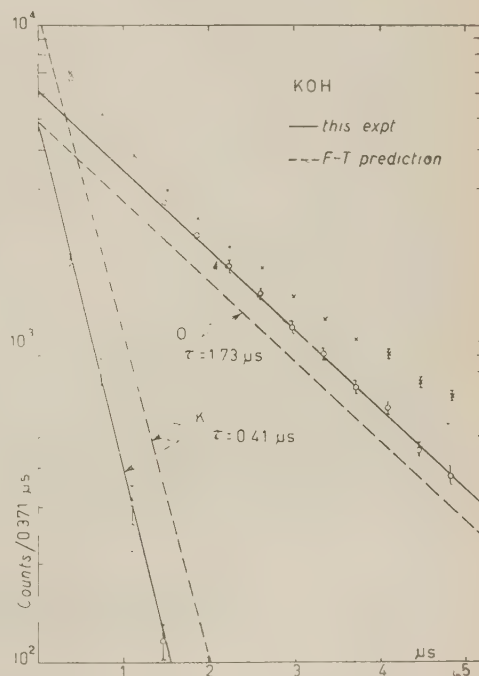


Fig. 4. — Time distribution of electrons from μ^- decaying in CCl_4 (liquid). $\times\times\times\times$: Experimental points. Errors are statistical standard deviations. Constant background is not indicated.



contained in a thin pyrex beaker. Total electron counts: $2.6 \cdot 10^4$, $B = 6 \cdot 10^2$ counts/ μ s.

(h) p-dichlorobenzene. Target: same as (g), but maintained in liquid state at about 70 °C. Total electron counts: $2.6 \cdot 10^4$, $B = 6 \cdot 10^2$ counts/ μ s.

4. - Interpretation of results and conclusion.

It is clear from Table I that the observed capture ratios depart in all cases from the Fermi-Teller prediction and follow more closely the simple atomic ratios, unweighted by the atomic numbers, indicated in the last column. In some cases the constituent of lesser Z appears even to be favored.

Before venturing into hypotheses about the reasons for this discrepancy, two rather obvious facts need consideration. First, not all the compounds investigated by us are equally reliable sources of information. Targets (a) through (d) consist of truly binary compounds, while the remainder contain hydrogen as a third element. The presence of hydrogen is not noticeable in the electron decay curves of these ternary compounds, where a component of A_d essentially equal to A_0 should appear, if protons were capable of capturing and retaining a muon in these substances. On the other hand, as anticipated by FERMI and TELLER ⁽¹⁾ and suggested by PANOFSKY's observations ⁽²⁾, the small neutral system formed by a hydrogen mesic atom would easily diffuse through matter and ultimately transfer the muon to a nucleus of higher charge. If we extrapolate the conclusion that the constituents of a compound capture mesons simply in their ratio to hydrogen, then in a compound like KOH the ratio of mesons found in the K -shells of K and O could be appreciably affected by this transfer mechanism. However, even under the unlikely assumption that in this compound (as contrasted with the true binary cases) the K atoms would have a 2 : 4 times larger relative capture probability than the O atoms, and that the mesic hydrogen atoms would transfer the mesons overwhelmingly to oxygen, the observed capture ratio could not be attained. It might be that practically no captures occur in hydrogen that is ionically bonded, as the protons have practically no electrons « of their own » to contribute effectively to the last stages of the stopping process ⁽¹⁰⁾.

Second, the case of Al_2O_3 needs clarification. This substance has been investigated by STEARNS and STEARNS ⁽⁴⁾ from the same point of view as in the present investigation, but by a different technique. These authors concluded that the « Z -law » is well borne out in this substance, in contrast with our results on this and other compounds. Their experiment consisted in com-

⁽¹⁰⁾ We are greatly indebted to Prof. A. TURKEVICH for pointing this out to us.

paring mesic X-ray spectra (and absolute yields) from two targets: (a) Al_2O_3 , (b) a macroscopic mixture of Al and O consisting of the same gram-amounts as the constituents of the oxide sample. The Al was in the form of 1 mm thick sheets, the oxygen in the form of water filling the interstices between these sheets. The spectra from these samples, involving K-X-rays from O and L-X-rays from Al, resulted essentially identical. From this we would conclude that the *macroscopic* law of stopping governing the distribution of captures among the adjacent sheets of water and aluminum is essentially the same as the *microscopic* law of stopping governing the distribution of captures among the Al and O atoms. The Stearnses assumed that the relevant macroscopic stopping powers are proportional to Z , and argued therefrom that the «Z-law» holds microscopically. While their assumption is reasonably justified at high velocities, the velocity range in which the stopping powers of Al and H_2O have to be compared is that of a muon that has barely enough energy to traverse one of the sheets. A rough estimate of this energy is 4 MeV. O is much more effective in stopping than Al at this energy, the ratio of stopping powers per gram being ⁽¹¹⁾ about 1.6 and increasing in favor of O as the particle velocity decreases. Thus the Stearns' data on Al_2O_3 are in reasonable, if not exact, agreement with ours.

The Stearnses also report that in CaS the «Z-law» is fulfilled to within $\pm 20\%$. The ratio of atomic numbers being 20/16, this conclusion is perfectly compatible with the captures occurring in this compound too in the simple atomic ratio.

The prediction of FERMI and TELLER was based on the behavior of the energy loss of negative mesons near zero kinetic energy, which these authors showed to be proportional to Z . In seeking the cause of the discrepancy between their prediction and experiment, it is perhaps worth pointing out that FERMI and TELLER gave a reliable estimate for the energy loss only for the case of metals. They indeed pointed out that in insulators certain difficulties arise at low meson velocities, these being due to the existence of a Brillouin gap in such materials. It might be that in insulators the energy loss near zero energy arises from mechanisms other than those considered by FERMI and TELLER, e.g. by inelastic collisions with the lattice. The dependence of such losses on Z , if any, is altogether unknown. Another theoretical possibility to explain our observations is that the mesons could be captured near zero kinetic energy not by any *individual* atom, but into a molecular orbital around a whole grouping of atoms. From such an orbital they would then transfer to individual atoms on a statistical basis. We hope to return to these points in more detail in a future publication.

Lastly, we wish to discuss the relevance of the «transfer mechanism»

⁽¹¹⁾ Stopping powers calculated from tables of proton ranges given in UCRL-2301.

suggested by DAY and MORRISON (7) to explain the anomalously high Auger rates observed in the K - and L -series of mesic X-rays from light elements (4). One could think that the mesons are *initially* captured according to the « Z -law » and get later transferred to the lighter constituents of the compounds. This possibility appears, however, rather improbable as the heavier constituents, both theoretically and experimentally, exhibit a much smaller fractional « external » Auger rate than the light ones. Thus the Day-Morrison mechanism, important anyhow only for the lightest elements, would operate in the reverse direction.

RIASSUNTO (*)

FERMI e TELLER hanno previsto, nel loro lavoro classico sul processo di rallentamento dei mesoni negativi, le relative probabilità della cattura di quest'ultimi da parte dei differenti atomi di un composto chimico, concludendo che queste probabilità di cattura *atomica* debbano essere proporzionali alle cariche nucleari Z_i degli atomi considerati. Gli esperimenti qui descritti furono eseguiti allo scopo di verificare tali previsioni: sono basati sul fatto che i muoni negativi raggiungono rapidamente le orbite K attorno ai nuclei degli atomi della materia nella quale sono rallentati e scompaiono da queste orbite (per decadimento o per assorbimento) in misura caratteristica per i nuclei in questione. Pertanto, la distribuzione nel tempo degli elettroni di decadimento emergenti da un composto chimico nel quale si arrestano dei muoni presenta in generale tante componenti esponenziali quanti sono i suoi costituenti; le loro intercette al tempo zero (ingresso dei muoni nella materia) sono direttamente proporzionali a $n_i p_i$, dove n_i è la frazione rappresentata dalla componente di numero atomico Z_i , e p_i è la probabilità di cattura nello strato mesico K dell'atomo dello stesso costituente. Trascurando la possibilità del passaggio dei muoni tra atomi vicini, le p_i equivalgono alle probabilità di cattura previste da Fermi e Teller. I presenti esperimenti mostrano che, almeno negli isolanti (Al_2O_3 , P_2O_5 , SiO_2 , CCl_4 , KOH , KHF_2 , p-diclorobenzene), le previsioni di Fermi e Teller falliscono. Non sembra intervenire nessuna ponderazione di n_i da parte di Z_i ; in alcuni casi, anzi, l'elemento più leggero sembra preferito. Come possibile spiegazione si fa rilevare che la cessione di energia alle vibrazioni del reticolo, non considerata da Fermi e Teller, può essere negli isolanti un importante meccanismo per la cattura di particelle negative dotate di energia cinetica quasi nulla.

(*) Traduzione a cura della Redazione.

On the Atomic Motions in Quasi-Crystalline Argon.

V. NARDI

*Istituto di Fisica dell'Università di Padova
Istituto Nazionale di Fisica Nucleare - Sezione di Padova*

(ricevuto il 17 Ottobre 1957)

Summary. — The direct exchange-energy E of two atoms in the quasi-crystalline picture of liquid argon is calculated. The result is $E_{\text{evap}}/E \simeq 1.4$. It is shown that the atomic motions in the liquid, enhanced with respect to the solid by the mutual correlations, can explain the differences experimentally determined in the structure of the two states.

1. — In order to investigate the physical consistency of the assumption that the elementary diffusion process in a non-associated liquid, near the melting point, consists in an exchange of position between two molecules, we have evaluated the energy associated with this exchange ⁽¹⁾. We have attributed to the liquid the f.c.c. structure which, in the case of argon that we consider, is also the structure of the solid. Obviously, the numerical result obtained depends essentially on this hypothesis, even if mitigated by the use of a liquid region with an extension of only few interatomic distances.

The idea of attributing to the liquid state a close-packed structure might be suggested by the fact that, at temperature not much higher than the melting point, X-ray analysis shows a nearest neighbours' number of about 10 for every liquid examined, which does not present molecular association, independently of the structure of the corresponding solid ⁽²⁾. This is consistent with a f.c.c. structure in which large and correlated molecular motions decrease the order-degree and the number of nearest neighbours. This point will be discussed again in Sect. 4.

⁽¹⁾ A similar calculation has been made for copper in the solid state, by F. SEITZ and H. B. HUNTINGTON: *Phys. Rev.*, **61**, 315 (1942). The activation energy found was too large with respect to the experimental value.

⁽²⁾ N. S. GINGRICH: *Rev. Mod. Phys.*, **15**, 90 (1943).

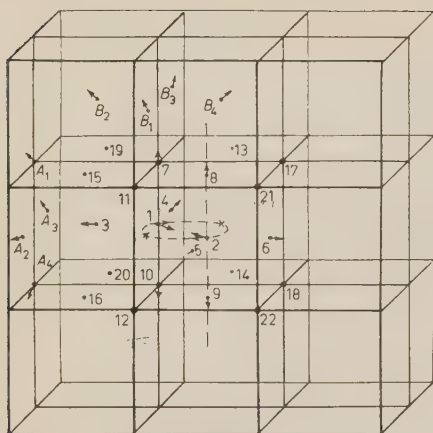


Fig. 1.

(0, 0, 1) plane through the cell-center, and about the $[0, 0, 1]$ axis which bisects perpendicularly the line 1, 2, because the corresponding saddle-point configuration has the least energy.

The nearest neighbours' distance in the f. c. c. lattice is $(\sqrt{2}/2)a = 4.04 \text{ \AA}$.

In the saddle-point configuration, which is reached after a rotation of the pair of 90° , we shall let the displacements, in the $[1, 1, 0]$ direction, of atoms 1 and 2 from their interstitial positions, situated respectively in the middle point of the edge 7, 10 and in the centre of the cubic cell, be $\lambda a(\sqrt{2}/2)$: here λ is a parameter to be determined. Let similarly $\mu(a/2)$ be the displacements of atoms 3, 4, 5, 6 from the equilibrium positions in the rotation plane and $\nu(a/2)$ those of atoms 7, 8, 9, 10 in the $[0, 0, 1]$ direction.

We consider also the displacements of A_1, A_2, \dots, A_{16} and B_1, B_2, \dots, B_{12} in the directions along the lines joining their equilibrium positions with the positions of 3, 4, ... 10 in the saddle-point configuration. We write the displacements of the atoms A_i , which are all equal, as $\pi a(\sqrt{2}/2)$, and the displacements of the atoms B_i , which are only approximately equal, as $(\pi + d\pi)a(\sqrt{2}/2)$. $d\pi$ is small with respect to the other parameters and may be expressed through μ, ν and π .

We assume an interaction potential between two argon-atoms at distance r , of the Lennard-Jones type:

$$(1) \quad V(r) = 4\varepsilon \left[\left(\frac{\sigma}{r} \right)^{12} - \left(\frac{\sigma}{r} \right)^6 \right],$$

with:

$$\varepsilon = 165.3 \cdot 10^{-16} \text{ erg}, \quad \sigma = 3.405 \text{ \AA},$$

determined by A. MICHELS from the second virial coefficient⁽³⁾.

We describe by means of (1) the interactions of atoms 1, 2, ..., 10 (Fig. 1) with the others and in particular with the A_i 's and B_i 's: the interactions of each A_i and B_i with the set of its other 11 first neighbours is described instead by means of the averaged

⁽³⁾ A. MICHELS, HUB. WIJCKER and H. K. WIJCKER: *Physica*, **15**, 627 (1949).

potential $11\Phi(r)$ used in the Lennard-Jones and Devonshire cell-theory. If r is the displacement of any A_i or B_i from its equilibrium position, this averaged potential is

$$(2) \quad 11\Phi(r) = 11 \frac{\varepsilon}{2} \left[\left(\frac{\sigma}{a(\sqrt{2}/2)} \right)^{12} \frac{a(\sqrt{2}/2)}{10r} \left\{ \left(1 - \frac{r}{a} \right)^{-10} - \left(1 + \frac{r}{a} \right)^{-10} \right\} + \right. \\ \left. - \left(\frac{\sigma}{a(\sqrt{2}/2)} \right)^6 \frac{a(\sqrt{2}/2)}{4r} \left\{ \left(1 - \frac{r}{a} \right)^{-4} - \left(1 + \frac{r}{a} \right)^{-4} \right\} \right],$$

with

$$\lim_{r \rightarrow 0} \Phi(r) = V \left(a \frac{\sqrt{2}}{2} \right).$$

In the saddle-point configuration the mutual distance between atoms 1 and 2 is $r_1 = (1 - 2\lambda)a(\sqrt{2}/2)$. The distance between atoms 1 and 3, and those of the same type (all indicated by the symbol $\langle 1-3 \rangle$), are: $r_2 = [(1 + \mu + \lambda)^2 + \lambda^2]^{\frac{1}{2}}(a/2)$ and, with a similar meaning of the symbol

$$\begin{array}{ll} \langle 1-7 \rangle: r_3 = [(1 + \nu)^2 + 2\lambda^2]^{\frac{1}{2}} \frac{a}{2}, & \langle 3-15 \rangle: r_7 = (2 + \mu^2)^{\frac{1}{2}} \frac{a}{2}, \\ \langle 3-A_1 \rangle: r_4 = [(1 - \mu)^2 + 1]^{\frac{1}{2}} \frac{a}{2} + \pi a \frac{\sqrt{2}}{2}, & \langle 7-15 \rangle: r_8 = (2 + \nu^2)^{\frac{1}{2}} \frac{a}{2}, \\ \langle 3-4 \rangle: r_5 = (1 + \mu)a \frac{\sqrt{2}}{2}, & \langle 7-B_1 \rangle: r_9 = [(1 - \nu)^2 + 1]^{\frac{1}{2}} \frac{a}{2} + (\pi + d\pi)a \frac{\sqrt{2}}{2}, \\ 3-7 \rangle: r_6 = [(1 + \mu)^2 + (1 + \nu)^2]^{\frac{1}{2}} \frac{a}{2}, & r_{10} = \pi a \frac{\sqrt{2}}{2}, \quad r_{11} = (\pi + d\pi)a \frac{\sqrt{2}}{2}, \end{array}$$

In this configuration, we have also for each B_i

$$(3) \quad \left(\frac{dV}{dr} \right)_{r=r_9} = -11 \left(\frac{d\Phi}{dr} \right)_{r=(\pi+d\pi)a(\sqrt{2}/2)}.$$

For the analogous relation available in the case of A_i , eq. (3) becomes

$$(4) \quad \left(\frac{d^2V}{dr^2} \right)_{r=r_4} dr = -11 \left(\frac{d^2\Phi}{dr^2} \right)_{r=\pi a(\sqrt{2}/2)} \cdot \frac{\sqrt{2}}{2} a d\pi.$$

From eq. (4) we have

$$d\pi = \frac{1}{2} (\nu - \mu) \frac{V''}{V'' + 11\Phi''} \simeq \frac{1}{2} (\nu - \mu) \left[0.15 + 4 \left(\frac{\mu}{2} - \pi \right) \right],$$

to the first order in $\mu/2 - \pi$ and with a parabolic approximation to $\Phi(r)$.

The energy difference E between saddle-point and equilibrium con-

figuration if one considers only changes in interaction energies between immediate neighbours is obtained determining the minimal value of

$$\begin{aligned}
 (5) \quad E(\lambda, \mu, \nu, \pi) = & V(r_1) + 4V(r_2) + 4V(r_3) - 23V\left(a\frac{\sqrt{2}}{2}\right) + \\
 & + 16V(r_4) + 2V(r_5) + 8V(r_6) + 16V(r_7) - 42V\left(a\frac{\sqrt{2}}{2}\right) + \\
 & + 12V(r_8) + 16V(r_9) - 28V\left(a\frac{\sqrt{2}}{2}\right) + 160\Phi(r_{10}) - 160V\left(a\frac{\sqrt{2}}{2}\right) + \\
 & + 106\Phi(r_{11}) - 106V\left(a\frac{\sqrt{2}}{2}\right). \quad (*)
 \end{aligned}$$

The result is

$$\begin{aligned}
 E = 796 \cdot 10^{-16} \text{ erg} \quad & \text{for } \lambda = 0.07, \\
 & \mu = 0.19, \\
 & \nu = 0.25, \\
 & \pi = 0.02.
 \end{aligned}$$

(Of Course the value of E might be lowered if one considers fluctuations in the density.)

3. — A comparison of the E -value, calculated in this way with the experimental E -value determined through the Arrhenius form of the diffusion coefficient

$$D = A \cdot \exp[-E/kT]$$

is not possible because of the scarcity of experimental data ⁽⁴⁾.

Although the elementary processes for momentum transmission and for molecular diffusion might be completely different, we observe that $E_{\text{vis}}/E \cong 0.67$. with $E_{\text{vis}} = 529 \cdot 10^{-16}$ erg derived from the experimental values ⁽⁵⁾ of the viscosity coefficient in the form

$$\eta = B \cdot \exp(E_{\text{vis}}/kT).$$

(*) The coefficients of $\Phi(r)$ in this expression are equal to the number of links between the A_i and B_i and their first neighbours in the equilibrium configuration. In this way we consider also the fact that both B_1 and B_4 interact with 7 and 8, and analogously for the symmetricals.

⁽⁴⁾ In the work of J. CORBETT and J. H. WANG: *Journ. Chem. Phys.*, **25**, 422 (1956); only one point of the curve $D = D(T)$ is determined.

⁽⁵⁾ N. S. RUDENKO and H. H. SCHUBNIKOV: *Phys. Zeit. Sowiet.*, **6**, 470 (1934).

From experimental data concerning the liquids, one has the general empirical relation $E_{\text{evap}}/E \sim 3$. In the case of Argon $E_{\text{evap}}/\text{atom} = 1103 \cdot 10^{-16}$ erg at $T = 87.3^\circ\text{K}$ and if we use the calculated E -value, we have the ratio $E_{\text{evap}}/E \cong 1.4$.

We may say that this calculation indicates that the direct-exchange of 2 atoms might be the basic mechanism for the molecular diffusion in the liquid, even though, obviously, it is not possible to exclude a vacancy motion or more complex processes involving a number of molecules higher than two. Against these more complex processes one can only say that they have a higher activation energy. Let us now examine in more detail this statement. For the high density of the solid, the greater contribution to the saddle-point energy in the exchange of two-molecules is given by the repulsive terms. If one takes into account exchange, for example through 4 atoms rings, one obtains repulsive terms with much smaller values than in the previous case and hence a smaller saddle-point energy ⁽⁶⁾. On the contrary, owing to the low density of the liquid, the larger contribution to the activation energy is not given by the few repulsive terms but by the many attractive terms. It follows that when one considers exchange through rings with 3 or more atoms, one has negligible decrease in the values of each repulsive term, while the increased number of attractive terms rises definitively the activation energy. We have verified this with a rough evaluation for the case of a three-atom ring (1, 2, 9 in Fig. 1) wheeling in the (1, 1, 1) plane, with the possibility of a small shift from it. Perhaps more definite information about the presence of these molecular ring motions will be supplied by experimental techniques such as neutron spectrometry.

4. — It is possible to believe that the essential difference between the liquid and solid states consists in the correlation of molecular motions, which is very strong in liquids, but negligible in solids, as is confirmed by the good results of the Einstein-model.

The order-degree, described by the radial distribution function $g(r)$, is smaller in liquids than in solids. This molecular disorder in liquids might be attributed to the larger displacements of the molecules from their equilibrium position, caused by the mutual correlation in their motions: the direct exchange of the position of two molecules is the most evident example of this correlation. We recall that X-rays analysis in argon at $T = 84.4^\circ\text{K}$ ⁽⁷⁾, gives the $g(r)$ function. According to the upper limit ϱ of the integration interval $(0, \varrho)$, chosen in order to evaluate the area under the first peak (at $r = 3.79 \text{ \AA}$) of the $4\pi r^2 g(r)$ function, one finds a first neighbours' number lying between 10.2 and 10.9. If we assume $\varrho = 4.69 \text{ \AA}$, the position of the first minimum,

⁽⁶⁾ C. ZENER: *Ac. Cryst.*, **3**, 346 (1950); (Evaluation for copper in the solid state).

⁽⁷⁾ A. EISENSTEIN and N. S. GINGRICH: *Phys. Rev.*, **62** (1942) 627.

any molecule placed at a distance larger than this from another fixed molecule can no longer be considered as its first neighbour. Now, in the model chosen 50 atoms are involved, essentially, for each elementary process. In the saddle-point configuration one has (in ångström):

$$\begin{array}{lll} r_1 \cong 3.5 & r_4 \cong 3.8 & r_6 \cong 4.9 \\ r_2 \cong r_3 \cong 3.6 & r_5 \cong 4.8 & r_7 \cong r_8 \cong 4.1 \end{array}$$

If one assigns to each atom of this group the first neighbours' number found for this configuration, one has five f.n. for the atoms 1 and 2, nine for the atoms 3, 4, ..., 10, eleven for the atoms 11, 12, ..., 18 and twelve for the remainder. The averaged f.n. number for the 50 atoms of the process comes out equal to 11. Naturally, if the model has to be consistent, the elementary processes of diffusion must be a prevailing cause of the diminution of the first neighbours' number with respect to the solid. On the other hand, such a diminution is not sufficient to obtain the experimental co-ordination number z , if we wish to exclude a frequency of these processes which is so large that there is appreciable interference amongst them. Therefore it is necessary to consider also the contribution to the decrease of z given by the large



Fig. 2.

oscillations, without exchange, about the respective equilibrium positions.

In order to discuss this point we use the characteristic methods of the Lennard-Jones and Devonshire cell-theory (Fig. 2). We consider an atom that during an oscillation shifts by r from the center of the spheric cell with a radius $a(\sqrt{2}/2)$ (Fig. 2). On the cell surface are uniformly distributed the 12 first neighbours.

If $r + a(\sqrt{2}/2) > \rho$, all the points of a spheric «calotte» with surface

$$\sigma = \pi a^2 \left[1 + \frac{\frac{1}{2}a^2 + r^2 - \rho^2}{\sqrt{2}ar} \right],$$

have a distance greater than ρ from the oscillating atom. The first neighbours' number for the atom so shifted from the sphere center is lowered to $z(r) = 12(1 - (\sigma/2\pi a^2))$. The averaged first neighbours number $\bar{z}(r)$ for the atom in oscillation, placed in the field of force described by eq. (2), results

$$\bar{z}(r) = \frac{12 \cdot \int_{r=0}^{r=\rho-a(\sqrt{2}/2)} \exp[-12\Phi(r)/kT] dr + \int_{r=\rho-a(\sqrt{2}/2)}^{r=a(\sqrt{2}/2)} z(r) \exp[-12\Phi(r)/kT] dr}{\int_{r=0}^{r=a(\sqrt{2}/2)} \exp[-12\Phi(r)/kT] dr} = 11.4.$$

From this result it follows that the first neighbours' number of the atoms 11, 12, ..., B_i and A_i might be lowered by 0.6. In this way the averaged f.n. numbers for the 50 atoms of the process results to be 10.6.

With a more refined cell-model, for example with no hard walls, it is certainly possible that this number can be reduced. In this way the number of elementary processes per unit volume necessary for obtaining the mean experimental number of first neighbours can be sufficiently low to give no appreciable interference between these processes.

In any case, from this estimate, it is clear that in order to explain the number of first neighbours in the liquid state, in particular for Argon, it is sufficient to consider the effect of the molecular motions.

* * *

The author would like to thank Prof. J. DE BOER for his kind hospitality at the Instituut voor theoretische Physica of Amsterdam and Prof. G. CARERI for helpful discussions.

He also wishes to thank Prof. J. F. KOKSMA and Prof. VAN WIJNGAARTEN of the Mathematisch Centrum of Amsterdam, who have carried out the minimum value calculation for the function $E(\lambda, \mu, r, \pi)$, contained in this note.

RIASSUNTO

Si è calcolata l'energia E per lo scambio diretto di due atomi, nel modello quasi-cristallino dell'argon liquido. Il risultato è $E_{\text{evap}}/E \cong 1.4$. Si mostra come i moti degli atomi nel liquido, esaltati rispetto al solido dalle correlazioni mutue, possono spiegare le differenze determinate sperimentalmente nella struttura dei due stati.

Heavy Primary Interactions in Water Loaded Emulsions.

V. D. HOPPER, J. E. LABY and Y. K. LIM

Physics Department, University of Melbourne

(ricevuto il 22 Ottobre 1957)

Summary. — Water loaded emulsions have been used to study cut-off energy, spectrum and flux of primary particles at geomagnetic latitude and longitude 47°S , 135°W . Results agree with Störmer cut-off energy for the latitude. Most interactions in the water loaded emulsions were shown to occur in light nuclei.

1. - Introduction.

A number of balloon flights ⁽¹⁾ were made during 1954-1956 in Victoria, Australia, at approximate geomagnetic latitude 47°S , dip 68° , and longitude 135°W (geographic longitude 145°E). A study of the fragmentation events of the heavy primaries recorded during these flights is of considerable interest in view of the recent work of WADDINGTON ⁽²⁾ and SIMPSON *et al.* ⁽³⁾ on the effective geomagnetic co-ordinates for cosmic rays. 600 μm Ilford G5 glass-backed emulsions were used and a large proportion of these were swollen to approximately three times the normal thickness ($k=3$) with water and exposed while wet. Details of the method will be described elsewhere but the main advantages for this particular investigation are that the paths of particles passing through the water-loaded emulsions are three times as long as in a single normal emulsion and that the chance of a collision with light nuclei including hydrogen is considerably increased. Expansions were limited to about three times since with greater expansions minimum ionization tracks could not be efficiently observed.

Sixty collisions of heavy primaries with nuclei in the emulsions have been analysed, 55 in the swollen emulsions, 4 in dry emulsions and 1 in the cello-

⁽¹⁾ J. E. LABY, Y. K. LIM and V. D. HOPPER: *Nuovo Cimento*, **5**, 249 (1957).

⁽²⁾ C. J. WADDINGTON: *Nuovo Cimento*, **3**, 930 (1956).

⁽³⁾ J. A. SIMPSON, K. B. FENTON, J. KATZMAN and D. C. ROSE: *Phys. Rev.*, **102**, 1648 (1956).

phane packing between two emulsions. The charge and energy of a primary particle were inferred from its δ -ray density combined with the grain count, angular distributions and nature of the disintegration fragments. In some cases scattering measurements could also be reliably made. From the zenith angle of the primary particle a correction was made to deduce the energy at the top of the atmosphere. Seven heavy primary particles were arrested in these emulsions and on the assumption that these particles had not changed charge an estimate was also made of their energy at the top of the atmosphere. From these results it is inferred that the cut-off energy at this latitude and longitude is 0.6 to 0.8 GeV/nucleon.

2. - Energy determination.

The interaction of an energetic nucleus with a hydrogen nucleus in the emulsion is the same as that due to an energetic proton bombarding the heavy nucleus at rest, but viewed from a different frame of reference. There are important advantages from a study of the former interaction, namely, the products of the disintegration can be more readily identified and the energy of the primary particle can be estimated from the angular spread of the fragments. If the energy of the primary particle is above 1 GeV/nucleon there is a possibility of mesons being created but these have a wider angular distribution than the fragments of the primary and can usually be separated from them.

In the case of a collision between a heavy primary particle with an atom other than hydrogen in the emulsion, the study is more complicated in that fragments are also emitted in the disintegration of the target nucleus; furthermore, the mesons created may be confused with the knock-on protons from the target nucleus. It is however in general possible in these events to separate most of the fragments of the incident nucleus from the mesons and the fast protons from the target nucleus.

The charged fragments consist mainly of protons and α -particles and one common method of estimating the momentum p per nucleon of the primary particle is to use the formulae ^(4,7),

$$(1) \qquad (\alpha\text{-particle}) \qquad \theta_{\text{rms}} = 0.056/p,$$

$$(2) \qquad (\text{proton}) \qquad \theta_{\text{rms}} = 0.12/p,$$

where θ_{rms} , the root mean square angle, is measured in radians and pc in

(4) M. F. KAPLON, B. PETERS, G. T. REYNOLDS and D. RITSON: *Phys. Rev.*, **85**, 292 (1952).

(5) K. GOTTSTEIN: *Phil. Mag.*, **45**, 347 (1954).

(6) F. HÄNNI: *Helv. Phys. Acta*, **28**, 345 (1955).

(7) Y. EISENBERG: *Phys. Rev.*, **96**, 1378 (1954).

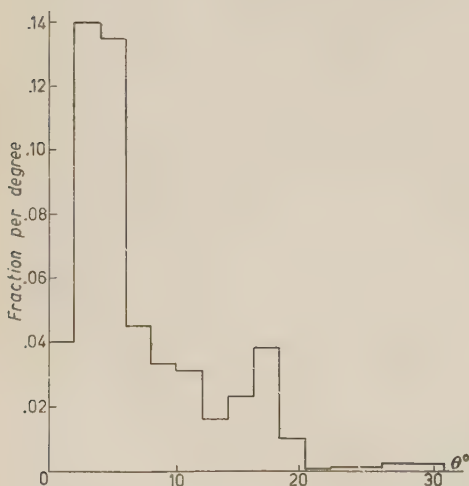
GeV/nucleon. The formulae are based on the assumption that the α -particles and protons observed as fragments of the primary particle are evaporation particles emitted isotropically in the centre of mass system of the primary particle with mean kinetic energies of 10 and 12 MeV respectively.

It became evident during the analysis that where both formulae are applicable they do not give identical results. This might be expected as a fraction of the protons are emitted in high energy disintegrations with much greater energy than can be attributed to a pure evaporation process. An analysis of high energy proton and neutron induced stars in normal emulsions by PARSONS *et al.* ⁽⁸⁾ shows that one-third of the protons with above minimum ionization have energies above 50 MeV and cannot be attributed to a pure evaporation process. The energy distribution of protons emitted in the disintegration of a light nucleus with production of mesons in normal emulsions obtained by these workers, after correcting for the presence of α -particles and heavier nuclei using fragmentation probabilities derived later, is given in Table I.

TABLE I. - *Energy distribution of protons from high energy stars induced by protons and neutrons.*

| Kinetic energy | 0 ÷ 8 | 8 ÷ 15 | 15 ÷ 30 | 30 ÷ 50 | 50 ÷ 85 | 85 ÷ 300 | 300 ÷ 800 |
|----------------|-------|--------|---------|---------|---------|----------|-----------|
| Protons/star | 0.7 | 1.3 | 0.4 | 0.3 | 0.4 | 0.8 | 0.1 |

It is possible to estimate from this distribution the angular distribution of protons emitted in the fragmentation of a light nucleus bombarding a stationary hydrogen nucleus on the as-



sumption of isotropic emission in the centre of mass system of the primary particle. The result for a primary energy of 1 GeV/nucleon is given in Fig. 1. It can be seen that a peak occurs at 2° to 6°. The root mean square angle occurs at 8.9° which is 2.1 times the value expected from Eq. (2). Agreement with Eq. (2) may

Fig. 1. - Angular distribution of protons from fragmentation of a light nucleus with energy 1 GeV incident on hydrogen.

⁽⁸⁾ R. W. PARSONS, F. A. BRISBOUT and V. D. HOPPER: *Phys. Rev.*, **95**, 193 (1954).

TABLE II. — *Summary of events recorded on flights.*

| Flight | k | Primary charge | Zenith angle | Energy GeV/n | | Fragments | | | | | n_s | N_p |
|--------------------------|-----------------|-------------------|-----------------|--------------|---------------|-----------|---|----|----------|-----|-------|-------|
| | | | | Ceil- ing | Above atm. | H | M | L | α | p | | |
| 26-3-1956 | 2.6 | 3 | 82 | — | > 0.75 | — | — | Li | — | — | — | 3 |
| At 20 g cm ⁻² | 2.6 | 3 | 29 | 2.8 | 2.9 | — | — | — | 1 | 1 | 1 | 3 |
| for 3.9 h | 2.6 | 3 | 24 | 4.0 | 4.1 | — | — | Li | — | — | — | 2 |
| | 2.6 | 3 | 24 | 4.0 | 4.1 | — | — | — | — | 3 | 18 | 30 |
| | 2.6 | 4 | 40 | 23 | 23 | — | — | — | 2 | — | 1 | 6 |
| | 2.6 | 5 | 15 | 18 | 18 | — | — | — | 2 | 1 | — | 4 |
| | 2.6 | 5 | 13 | 7 | 7 | — | — | Li | 1 | — | — | 5 |
| | 2.6 | 6 | 40 | 4.6 | 4.7 | — | — | — | 2 | 2 | 1 | 4 |
| | 2.6 | 6 | 58 | 0.4 | 0.67 | — | — | B | — | 1 | — | 5 |
| | 2.6 | 6 | 50 | 1.0 | 1.2 | — | — | — | — | 6 | 12 | 7 |
| | 2.6 | 6 | 38 | 2.5 | 2.7 | — | — | — | 1 | 4 | — | 1 |
| | 2.6 | 6 | 58 | 10 | 10 | — | — | Be | — | 2 | 1 | 0 |
| | 2.6 | 6 | 17 | 0.9 | 1.1 | — | — | Li | 1 | 1 | 2 | 1 |
| | 2.6 | 7 | 20 | 0.32 | 0.58 | — | — | — | — | 7 | — | 6 |
| | 2.6 | 7 | 80 | 0.3 | 1.12 | — | — | — | — | 7 | 1 | 6 |
| | 2.6 | 7 | 50 | 0.36 | 0.72 | — | C | — | — | 1 | — | 1 |
| | 2.6 | 7 | 30 | 1.2 | 1.4 | — | — | — | 2 | 3 | 3 | 0 |
| | 1.0 | 8 | 62 | 0.8 | 1.1 | — | — | — | 3 | 2 | 1 | 3 |
| | 2.6 | 9 | 7 | 3.8 | 4.0 | — | — | Be | — | 5 | 6 | 8 |
| | 2.6 | 9 | 37 | 0.93 | 1.2 | — | — | — | 3 | 3 | 2 | 7 |
| | 2.6 | 10 | 59 | 1.0 | 1.35 | — | F | — | — | 1 | — | 1 |
| | 2.6 | 10 | 67 | — | > 0.8 | Ne | — | — | — | — | — | 2 |
| | 2.6 | 12 | 65 | 0.41 | 1.0 | — | — | — | 4 | 4 | — | 4 |
| | 2.6 | 12 | 26 | 3.8 | 4.0 | — | — | Be | 3 | 1 | 4 | 0 |
| | 2.6 | 13 | 15 | 0.35 | 0.72 | — | — | B | — | 8 | — | 2 |
| | 1.0 | 13 | 20 | 3.0 | 3.2 | — | — | — | 3 | 7 | 6 | 0 |
| | 2.6 | 15 | 49 | 0.5 | 0.97 | — | C | — | 3 | 3 | — | 1 |
| | Cello- phane | 9 | 25 | 2.5 | 2.7 | — | — | B | 2 | — | — | — |
| 29-3-1956 | 2.6 | 4 | 44 | 3.0 | 3.1 | — | — | — | — | 4 | 28 | 12 |
| At 20 g cm ⁻² | 2.6 | 4 | 11 | 1.0 | 1.1 | — | — | — | — | 4 | — | 1 |
| for 6.3 h | 2.6 | 5 | 32 | 1.0 | 1.1 | — | — | Li | 1 | — | 1 | 5 |
| | 2.6 | 6 | 55 | 0.9 | 1.1 | — | — | — | 3 | — | 3 | 5 |
| | 2.6 | 10 | 53 | 0.63 | 1.0 | — | — | B | — | 5 | 3 | 3 |
| | 2.6 | 18 | 5 | 0.5 | 0.9 | Mg | — | — | 1 | 4 | — | 5 |
| | 2.6 | 21 | 57 | 0.14 | 1.0 | — | — | — | 3 | 14 | — | 5 |
| | 2.6 | 25 | 50 | 0.08 | 0.97 | — | — | — | 7 | 11 | — | 4 |
| 5-10-1955 | 1.8 | 4 | 55 | 0.54 | 0.65 | — | — | — | 2 | — | — | 6 |
| At 12 g cm ⁻² | 1.8 | 8 | 34 | 30 | 30 | — | — | Li | 1 | 3 | 2 | 1 |
| for 2 h | 1.8 | 9 | 57 | 0.75 | 0.95 | — | — | Li | 1 | 4 | 1 | 5 |
| | 1.8 | 15 | 40 | 0.8 | 1.05 | — | — | Be | — | 11 | — | 8 |
| | 1.8 | 17 | 56 | 0.36 | 0.85 | Si | — | — | 1 | 1 | — | 1 |

TABLE II (Continued).

| Flight | k | Primary charge | Zenith angle | Energy GeV/n | | Fragments | | | | | n_s | N_h |
|---|-----|----------------|--------------|--------------|---------------|-----------|---|-------|----------|-----|-------|-------|
| | | | | Ceil- ing | Above atm. | H | M | L | α | p | | |
| 5-10-1955 At 12 g cm ⁻² for > 4 h | 2.6 | 4 | 12 | 2.0 | 2.1 | — | — | — | — | 4 | 17 | 31 |
| | 2.6 | 4 | 29 | 0.3 | 0.45 | — | — | — | — | 4 | — | 10 |
| | 2.6 | 7 | 79 | — | — | — | N | — | — | — | — | 1 |
| | 2.6 | 8 | 57 | 1.9 | 2.1 | — | — | Be | 2 | — | — | 11 |
| | 3.2 | 8 | 32 | 0.5 | 0.7 | — | — | B | — | 1 | — | 5 |
| | 3.2 | 9 | 12 | 2.0 | 2.2 | — | — | Be | 1 | 3 | — | 1 |
| | 3.2 | 9 | 51 | 5.9 | 6.1 | — | — | Be | — | 5 | 3 | 0 |
| | 1.0 | 9 | 43 | 36 | 36 | — | — | — | 2 | 5 | 3 | 0 |
| | 2.6 | 10 | 18 | 4.0 | 4.2 | — | C | — | 1 | 2 | 3 | 0 |
| | 2.6 | 10 | 55 | 1.2 | 1.35 | — | — | — | 3 | 4 | 2 | 1 |
| | 3.2 | 20 | 40 | 0.75 | 1.10 | — | N | — | 4 | 5 | — | 1 |
| 21-12-1956 At 12 g cm ⁻² for > 5 h | 2.6 | 5 | 42 | 7 | 7.1 | — | — | — | 1 | 3 | 3 | 4 |
| | 2.6 | 6 | 55 | 1.5 | 1.7 | — | — | — | — | 6 | 4 | 4 |
| | 2.6 | 7 | 60 | 0.3 | 0.65 | — | — | — | 1 | 5 | 4 | 1 |
| | 2.6 | 8 | 38 | 2.2 | 2.4 | — | — | B | 2 | — | 3 | 5 |
| | 2.6 | 9 | 30 | 2.7 | 2.9 | — | — | — | 1 | 7 | 27 | 14 |
| | 2.6 | 15 | 46 | 3.0 | 3.4 | — | — | Li Li | 2 | 5 | 11 | 6 |
| 7-9-1955 At 20 g cm ⁻² | 3.1 | 5 | 55 | 0.4 | 0.65 | — | — | — | — | 5 | — | 16 |
| | 1.6 | 11 | 60 | 0.22 | 0.82 | — | — | — | 4 | 3 | — | 1 |
| 4-1-1954 At 20 g cm ⁻² | 1.0 | 19 | 36 | 1.5 | 1.9 | — | C | — | 3 | 7 | 2 | 6 |
| <i>Ending tracks</i> | | | | | | | | | | | | |
| 21-12-1956 | 2.6 | 6 | 43 | 0.03 | 0.38 | — | — | — | — | — | — | — |
| 5-10-1955 | 3.2 | 10 | 55 | 0.20 | 0.50 | — | — | — | — | — | — | — |
| 29- 3-1956 | 2.6 | 10 | 35 | 0.13 | 0.53 | — | — | — | — | — | — | — |
| 5-10-1955 | 2.6 | 12 | 28 | 0.4 | 0.6 | — | — | — | — | — | — | — |
| 26- 3-1956 | 2.6 | 12 | 53 | 0.35 | 0.82 | — | — | — | — | — | — | — |
| 21-12-1956 | 2.6 | 18 | 40 | 0.05 | 0.78 | — | — | — | — | — | — | — |
| 21-12-1956 | 2.6 | 20 | 30 | 0.30 | 0.82 | — | — | — | — | — | — | — |

be obtained by neglecting the outer third of the protons in computing θ_{rms} , as these are probably due to the non-evaporation protons. For collisions of primary particles with atoms heavier than hydrogen there is the possibility of still greater deviation from the formulae due to additional collisions. A similar method was applied to these events and the angle obtained by this method was combined with the θ_{rms} for α -particles to obtain the energy of the primary particle. The justification of this method is commented on later.

The grain densities and in some cases relative scattering of the secondary particles were taken into account in the energy estimation when the primary energy is low.

To correct for the ionization loss in the matter traversed before collision, use has been made of the stopping power given by BRADNER and BISHOP ⁽⁹⁾ for glass, the extrapolation of the stopping powers given by WILKINS ⁽¹⁰⁾ for dry emulsion and water and of the energy-range relation given by ROSSI ⁽¹¹⁾ for air. The stopping powers for glass, normal emulsion and $3 \times$ expanded emulsion, defined as ratio of range increment in g/cm² relative to air are respectively 0.96, 0.75 and 0.87. The corrections have been made individually for each primary particle and are listed in Table II.

3. - Charge determination.

It will be shown that in the loaded emulsions used, most of the interactions took place with the light nuclei of the target. This has the effect of limiting the target prongs to a small number and so reducing the possibility of target prongs being confused with the fragments of the primary particle. Thus it was possible to identify the primary nucleus from its fragments with reasonable certainty particularly in the several events where collisions occurred with hydrogen. These events served as the basis of γ -ray calibration from which other particles could be identified.

Results for the 60 primary particles undergoing fragmentation and 7 primary particles that ended in the emulsions are shown in Table II. The stack flown on 26 March 1956 was area-scanned and every star in 116 cm² of $2.6 \times$ loaded emulsion and 39 cm² of normal emulsion was examined carefully to determine whether it had been produced by a particle of charge greater than, or equal to 2. The remaining stacks were scanned for heavy primary disintegrations, mainly by the method of line scanning.

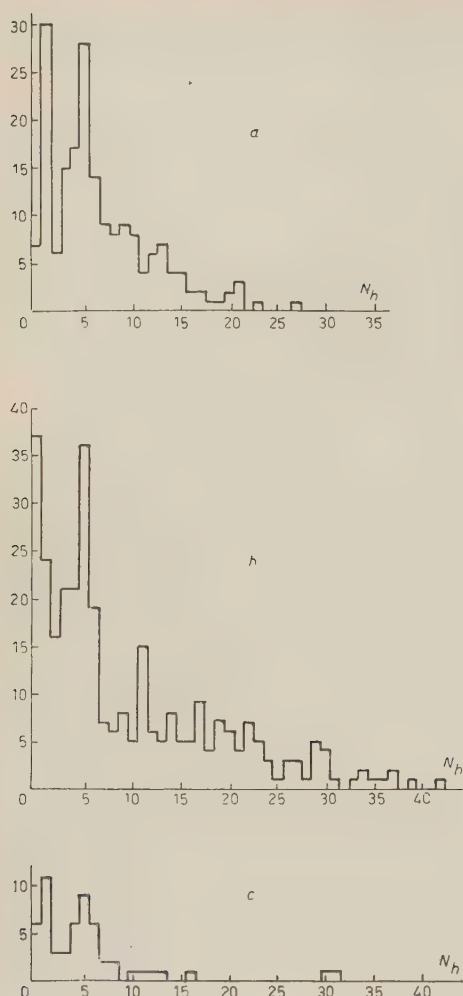
4. - Distribution of target prong number.

The distribution of target prong number N_h for events in the loaded emulsions (mean $k = 2.6$) are compared in Fig. 2 with the distribution obtained for normal emulsions. While the loaded emulsion data give a much smaller percentage of events with large prong numbers, the distributions at lower

⁽⁹⁾ H. BRADNER and A. S. BISHOP: *Phys. Rev.*, **76**, 587 (1949).

⁽¹⁰⁾ J. J. WILKINS: *A.E.R.E. Report G/R 664* (1951).

⁽¹¹⁾ B. ROSSI: *High Energy Particles* (New York, 1952), p. 40.



prong numbers are strikingly similar. This would be expected if in the normal emulsions the events in heavy target nuclei tended to occur with large prong numbers and in the loaded emulsions most of the events took place in light target nuclei. In particular the sudden decrease of frequency at $N_h = 7$ for both the normal and loaded emulsion distributions suggests that few light target nucleus events occur with $N_h \geq 7$. The distributions are also compared in Table III.

If it is assumed that events with $N_h > 6$ arise entirely from interactions in the heavy nuclei of the emulsion, one would expect the number of such events in a given area to remain unaffected by loading. The numbers in the table are therefore normalized so that the number of these events is equal

Fig. 2. — Distribution of target number: (a) normal emulsion, NOON and KAPLON⁽¹²⁾; (b) normal emulsion, FOWLER *et al.*⁽¹³⁾; (c) loaded emulsion, present work.

TABLE III. — Distribution of target prong number.

| Emulsion | Geomagnetic latitude λ^0 | Primary charge z | Observed frequency of stars with N_h | | | Normalized frequency of stars with N_h | | |
|------------------------|-------------------------------------|-----------------------|--|-------|-----|--|-------|-----|
| | | | 0 ÷ 1 | 0 ÷ 6 | > 6 | 0 ÷ 1 | 0 ÷ 6 | > 6 |
| Normal ⁽¹²⁾ | 41° and 55° N | ≥ 6 | 37 | 117 | 72 | 46 | 136 | 100 |
| Normal ⁽¹³⁾ | 46° N | ≥ 3 | 61 | 173 | 142 | | | |
| Loaded | 47° S | ≥ 3 | 19 | 44 | 11 | | | |

⁽¹²⁾ J. H. NOON and M. F. KAPLON: *Phys. Rev.*, **97**, 769 (1955).

⁽¹³⁾ P. H. FOWLER, R. R. HILLIER and C. J. WADDINGTON: *Phil. Mag.*, **2**, 293 (1957).

to 100 in each case. These results indicate that about 50% of the events in these loaded emulsions are due to the oxygen and hydrogen nuclei introduced by loading. It is of interest to note that for the flight on 26 March 1956 the loaded emulsion area of 116 cm² gave 24 events whereas one third of this area also carefully area scanned in the normal emulsion gave only two events. If one assumes that the gelatine and water nuclei have the same cross-section for the fragmentation of heavy primaries, the data of Table III combined with emulsion compositions show that of the events observed in the loaded emulsions 75% occurred in light nuclei; the corresponding value for the normal emulsion being 45%. The percentages calculated from the emulsion compositions are 70% and 40% for the loaded and normal emulsions using the cross-section formula given by BRADT and PETERS (¹⁴):

$$(3) \quad \sigma = \pi(R_i + R_t - 2\Delta R)^2,$$

R_i and R_t being the nuclear radii of the incident and the target nuclei given by $r_0 A^{\frac{1}{3}}$, $r_0 = 1.45 \cdot 10^{-13}$ cm, $\Delta R = 0.85 \cdot 10^{-13}$ cm. The same process may be applied to events with $N_h = 0$ and 1. It is found that 33% of the events in the loaded and 16% in the normal emulsions are due to interactions with hydrogen nuclei as target whereas the theoretical formula of Bradt and Peters gives 25% and 14% respectively. In the loaded emulsion 90% and in the normal emulsion 75% of the events with $N_h \leq 6$ are interactions with light nuclei. The hydrogen events account for about 85% of the normal emulsion events and 95% of the loaded emulsion events with $N_h = 0$ and 1. Thus it is reasonable to attribute the peaks at $N_h = 0$ and 1 and $N_h \approx 5$ in the distributions to interactions in hydrogen and C, N, O nucleus targets respectively.

5. - Fragmentation probabilities.

Since 90% of the fragmentation events with $N_h \leq 6$ observed in the loaded emulsions took place in light nuclei, the fragmentation probabilities derived from these must be characteristics of the collision of a heavy primary particle with a light nucleus of the emulsion or water. Detailed knowledge of fragmentation probabilities with light nuclei is required to estimate the nature of the primary flux from measurements of flux at balloon altitudes. The fragmentation probabilities P_{IJ} , i.e. the number of J -type nuclei emitted in the fragmentation of an I -type primary particle, are given in Table IV. The nomenclature of BRADT and PETERS (¹⁴) has been followed: H-nuclei, $10 \leq z$; M-nuclei $6 \leq z \leq 9$; L-nuclei $3 \leq z \leq 5$.

(¹⁴) H. L. BRADT and B. PETERS: *Phys. Rev.*, **77**, 54 (1950).

TABLE IV. — Fragmentation probabilities P_{IJ} from events with $N_h \leq 6$ in loaded emulsions.

| $I \backslash J$ | H | M | L | α | p |
|------------------|-----------------|-----------------|-----------------|-----------------|-----------------|
| H | 0.19 ± 0.11 | 0.25 ± 0.13 | 0.31 ± 0.14 | 2.25 ± 0.38 | 4.44 ± 0.53 |
| M | — | 0.11 ± 0.07 | 0.47 ± 0.16 | 0.79 ± 0.20 | 2.90 ± 0.39 |
| L | — | — | 0.40 ± 0.20 | 1.00 ± 0.32 | 0.90 ± 0.30 |

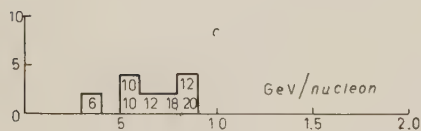
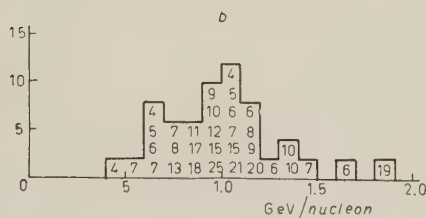
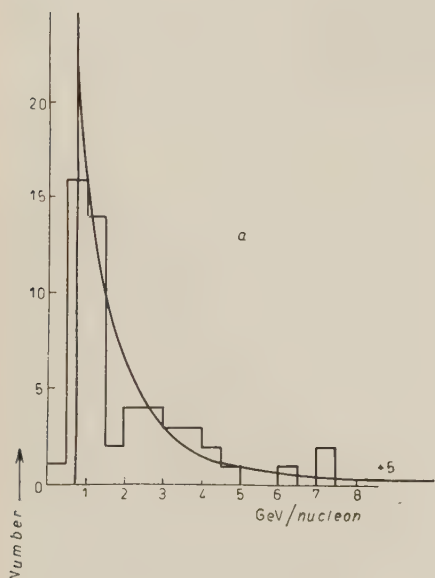


Fig. 3. — (a) Differential energy spectrum of primary particles which produced fragmentation; (b) lower end of spectrum of Fig. 3a; (c) energy spectrum at top of atmosphere of particles which ended in the emulsion.

The probability for L-nucleus emission in the fragmentation of H- and M-nuclei $P_{H+M,L}$ is 0.40 ± 0.11 and the α/p ratio is 0.45.

The values may be compared with those obtained by NOON and KAPLON⁽¹²⁾ and by FOWLER *et al.*⁽¹³⁾ for events in normal emulsions with $N_h \leq 7$. The probabilities of H- and M-nucleus emission are not significantly different from those listed by these workers, whereas for the L-nucleus and α -particle emission our results agree with those of NOON and KAPLON and correspond to a higher probability for L-nucleus emission and a lower probability for α -particle emission than the Bristol results.

6. — Energy spectrum and geomagnetic cut-off.

The differential energy spectrum, where for each particle the ionization loss has been corrected to correspond to energy at the top of the atmosphere, is shown in Fig. 3a. The lower end of the spectrum is given in 0.1 GeV/nucleon intervals in Fig. 3b, the number inside each square giving the charge of the particle. Seven tracks of energetic heavy nuclei have been observed to end in the emulsions. Their charges were determined from the thin-down lengths

and energies estimated by the range-energy relation. The energy distribution after correction for ionization loss in the overlying air on the assumption that they occurred at the ceiling height and suffered no loss of charge before reaching the detector is given in Fig. 3c.

The plates were attached to hang vertically and zenith angles were measured on the assumption that they did not swing during the level part of the flight. Visual observations support this contention. In addition, the measured zenith angular distribution of the primary particles which produce fragmentation in loaded emulsions is shown in Fig. 4, and it is seen that very few particles had calculated zenith angles greater than 60° . The smooth curve is the calculated angular distribution of the integrated track length based on the assumption of isotropy at the top of the atmosphere and normalized to the total number of interactions. This result supports our argument that the path of the primary particles may be assumed straight in passing through the bulk of the atmosphere above the plates.

The spread in the lower end of the energy spectrum shown in Fig. 3 may be due to the following: (a) the geomagnetic cut-off energy varies with direction; (b) the correction for ionization loss is made on the assumption that the primary particles reached the plates without loss of charge, but some were the secondary particles of some heavier nuclei. The corrections for these would be inadequate, since the ionization loss in energy per nucleon depends on zR , the product of charge and range. That this is an important factor giving rise to the observation of particles with energies apparently lower than the cut-off may be seen from Fig. 3b, where most of the lowest energy particles appear to have low charges. On the assumption that most of these were products of the fragmentation of the H-nuclei incident with near cut-off energies, this effect would account for about 5 of the low energy particles.

Thus from our results we conclude that the geomagnetic cut-off at geomagnetic latitude 47° S and geographic longitude 145° E occurs at $0.6 \div 0.8$ GeV/nucleon. This cut-off is in agreement with the energy distribution of heavy nuclei arrested in the stack shown in Fig. 3c.

The smooth curve in Fig. 3a is given by

$$dN/dE \sim (E + 0.94)^{-\gamma}; \quad \gamma \sim 2.4$$

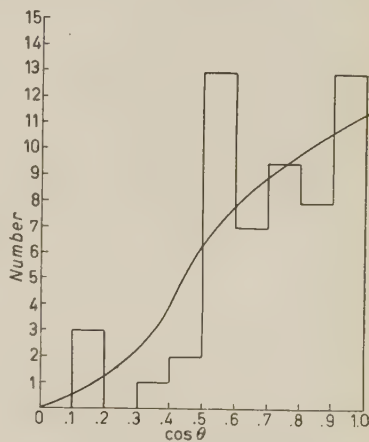


Fig. 4. — Zenith angular distribution of the primary particles which produced fragmentation. The smooth curve corresponds to the calculated angular distribution, assuming isotropy at the top of the atmosphere.

the area defined by the curve and $E = 0.7$ GeV/nucleon having been normalized to equal the total number of particles. The exponent is in agreement with the values given by other experimenters (⁷).

In view of the recent results of FOWLER *et al.* (¹³) which suggest that the mean kinetic energy of evaporation α -particles in the C -system of the incident nucleus increases with the charge of the incident particle, we have divided the events studied into two groups according to the primary charge $3 \leq z \leq 7$ and $z \geq 8$ and considered their distributions in energy after ionization correction. The two distributions were not significantly different and gave the same cut-off energy. We have also considered separately events with $N_h = 0$ and 1 which are mainly due to collisions with hydrogen nuclei and found this gave the same cut-off energy within the statistical error and this justifies the extension of the method of estimating energies to events $N_h > 1$.

7. — Flux of primary particles with $z \geq 6$.

It is possible to make a rough estimation of the flux of primary particles with $z \geq 6$ above Victoria from the number of fragmentation events produced by these particles using the interaction cross-sections calculated with the formula of Bradt et Peters (Eq. (3)). The calculated mean free paths of the M- and H-nuclei ($\bar{z} = 7$ and $\bar{z} = 15$) are respectively 26.5 and 18.0 g cm⁻² in air (¹²) and 33.2 and 22.0 g cm⁻² in the loaded emulsions exposed on 26 March 1956. 12 M-nucleus and 6 H-nucleus events were observed in an area of 97 cm² of emulsions of this stack swollen to 2.62 times the original thickness. With the fragmentation probabilities tabulated in Table III, which serve as an approximation to the case of interaction with air, the fluxes of primary M- and H-nuclei at the top of the atmosphere are evaluated as (5.7 ± 1.6) and (3.7 ± 1.5) particles m⁻² sr⁻¹ s⁻¹ respectively and these would be sufficient to create all seven L-nuclei events observed on the plates. The number of events occurring during ascent and descent has been estimated to be only 2% for these particles, which justifies the assumption made in the ionization loss correction that the events took place at the ceiling height.

8. — Discussion.

In a recent experiment of WADDINGTON (²) in which two stacks of plates exposed at the same geomagnetic latitude 55° N, one over England and the other over North America were studied, it was shown that the flux of primary α -particles over England was significantly lower than the flux over America. The cut-off energy over America from scattering measurements was estimated

as less than 0.15 GeV per nucleon and in England the method gave a value between 0.6 and 0.7 GeV per nucleon. The difference in flux could be attributed to the difference in cut-off energy. The cut-off energy calculated from the known geomagnetic latitude was 0.3 GeV per nucleon. If a shift in the geomagnetic latitude was entirely responsible for the change in the cut-off energy, it was pointed out that the observations would be consistent with a lowering of 5° and an increase of 3° or more in the accepted geomagnetic latitude of Europe and North America respectively. Later measurements (FOWLER and WADDINGTON⁽¹⁶⁾) carried out in North Italy gave a cut-off energy of 1.6 GeV per nucleon whereas from the known geomagnetic latitude (46° N) the expected value would be 1.0 GeV/nucleon.

SIMPSON *et al.*⁽³⁾ studied the position of the effective geomagnetic equator as defined by sea level cosmic ray intensity minima for different longitudes. These workers concluded that the effective geomagnetic equator did not coincide with the geomagnetic equator obtained by surface magnetic measurements. They suggested that a westward shift of the inclined magnetic dipole of the earth, whether centred or off-centred by about $40 \div 45^\circ$ without requiring an appreciable change in the angle of incidence would fit the sea level measurements made by them and other experimenters. This suggestion however did not fully explain the high altitude α -particle cut-off energy and flux measurements.

The cut-off energy at a given location depends strongly on the angle of incidence so that a sharp cut-off value is not obtained. It will be assumed that the measured cut-off is given approximately by the cut-off for vertical incidence. The Stoermer cut-off for vertical incidence of particles with $z \geq 2$ at 47° S is 0.9 GeV/nucleon. On the assumption that the centred dipole field of the earth is displaced 45° westward, the vertical cut-off at our location would be 1.8 GeV/nucleon. The extrapolation is more complicated if the dipole is displaced from the geographic centre. The effect of dipole eccentricity has been evaluated by JORY⁽¹⁷⁾. At the geomagnetic longitude of Victoria (135° W) the change of vertical rigidity due to this effect is about -14% . Thus the cut-off energy for Victoria based on the model of SIMPSON *et al.* and taking into account the dipole eccentricity is 1.5 GeV/nucleon. Alternatively, using the geomagnetic co-ordinates obtained by the surface surveys and allowing for dipole eccentricity a cut-off of 0.7 GeV/nucleon is expected. Our measurements thus give a cut-off value ranging from 0.6 to 0.8 GeV/nucleon,

(15) R. E. DANIELSON, P. S. FRIER, J. E. NAUGLE and E. P. NEY: *Phys. Rev.*, **103**, 1075 (1956).

(16) P. H. FOWLER and C. J. WADDINGTON: *Phil. Mag.*, **1**, 637 (1956).

(17) F. JORY: *Phys. Rev.*, **102**, 1167 (1956).

which is in agreement with values derived from the accepted geomagnetic co-ordinates but disagrees significantly with the Simpson *et al.* model.

No significant difference in cut-off value was detected over flights separated by several months, so it is possible that the best way of studying the effective magnetic field of the earth would be to measure cut-off energies at widely carefully selected points. To avoid any doubt of absolute energy determination it would be of value to determine the lines of constant cut-off energy and to compare these with the geomagnetic latitudes. The use of liquid loaded emulsions has considerable advantage over normal emulsions for such a study as they give a much greater density of fragmentation events for determining cut-off energies.

* * *

The authors wish to acknowledge the help received from the Commonwealth Meteorological Branch and for providing equipment for balloon tracking, and to thank Sir LESLIE MARTIN, F.R.S. for his interest and support. This work is supported by a grant from the Nuffield Foundation.

RIASSUNTO (*)

Per studiare il cut-off, lo spettro energetico e il flusso delle particelle primarie alla latitudine e longitudine geomagnetica 47° S e 135° W si sono usate emulsioni imbibite d'acqua. I risultati si accordano con l'energia di cut-off di Störmer per la latitudine. Si dimostra che la maggior parte delle interazioni nelle emulsioni imbibite d'acqua avvengono nei nuclei leggeri.

(*) Traduzione a cura della Redazione.

K^- Meson Exposures in Water-Soaked Emulsions.

G. ASCOLI, R. D. HILL and T. S. YOON

Physics Department, University of Illinois () - Urbana, Ill.*

(ricevuto il 12 Novembre 1957)

Summary. — A technique is described whereby pellicle strips of G5 emulsion are soaked in water and exposed as a stack of pellicles in intimate contact with one another. This technique allowed the normal process of tracing-through to be carried out and complete analysis of events was observed to be possible. The performance of the soaked emulsions, when they were exposed to a K^- -meson beam, is described and compared with that of unsoaked G5 emulsions exposed in the same beam.

In the following note we have been concerned with the problem of how to increase the frequency of K^- -free proton interactions in nuclear emulsions. Many experimenters ⁽¹⁻³⁾ have already used soaked or impregnated emulsions for this purpose, but as far as we are aware these experiments have been performed with single plates or pellicles. In order to retain as complete information as possible on the K^- -free proton interactions we set out to employ a stack of emulsion strips.

Two stacks of 30 pellicles of two different thicknesses, one of 600 μm and another of 1000 μm G5 emulsions, were prepared, exposed and processed. The dry pellicles, immediately after unpacking were weighed and measured for size. The pellicles were then placed in distilled water at 4 °C. The water was slowly circulated over the emulsions and nitrogen gas was bubbled through the water at the inlet. It is not known whether this was essential but it was

(*) Assisted by the joint program of the U.S.A.E.C. and the U.S.O.N.R.

(1) G. GOLDBABER: *Phys. Rev.*, **74**, 1725 (1948); S. GOLDBABER, J. C. BIELK, E. M. FRANKL and G. GOLDBABER: *A.E.C. Document N.Y.O.-6138*, 1953 (unpublished).

(2) DULKOVA, ROMANOVA, SOKOLOVA, SUKHOV, TOLSTOV and SHAFRONOVA: *Proc. Acad. Sci. USSR*, **107**, 43 (1956).

(3) C. J. BATTY: *Nuclear Inst.*, **1**, 138 (1957).

felt that the dissolved oxygen in the water should be expelled, especially as it might lead to fading of the image between the time of exposing and processing. Care was taken to turn the pellicles over several times especially at the start of the soaking. This tended to prevent sticking of the pellicles to the paper on which they rested and also might have allowed more uniform swelling of the emulsion.

After a soaking period of 12 hours, the pellicles were loaded into a lucite box which was specifically designed so as to contain the pellicles without allowing space either around the edges or above the pellicle stack. As each pellicle was transferred to the box, its area was measured and the average thickness of a pellicle was obtained by measuring the total thickness of the stack loaded into the box. It may be pointed out that the pellicles are readily handled as long as their temperature is kept low. Following soaking, the surfaces of the pellicles become very smooth and slippery and there is no tendency for the individual pellicles to stick to one another. In fact, a warning should be given that unless the pellicles are rather positively compressed within the box, they may slide over one another during transport and even between the time of exposing and processing. When all the pellicles had been transferred to the box and all the interstices had been filled with water, the box was tightly sealed with a rubber top plate and a lid of lucite which was screwed down.

During transport and exposure, the box of pellicle was maintained at a temperature of approximately 5 °C. During exposure the temperature was controlled by two copper plates which were clamped to the box and through which was circulated water from a reservoir of melting ice. After exposure the emulsions were X-rayed with a grid of lines spaced accurately 0.5 inches apart across the surfaces of the emulsion strips. We used X-rays of 150 kV filtered by 3 mm of copper and observed a penetration of approximately 4.5 cm into the wet stack of emulsions. For the X-ray slit system we found 50 μm lead slits of 1 inch thickness followed by 500 μm steel slits of 1 inch thickness to give satisfactory X-ray lines in the developed emulsion of the order 100 μm width.

Processing of the emulsions was started as soon as possible after exposure. No pre-soaking of the emulsions was, of course, necessary and a normal developing procedure was followed, except that necessarily the pellicles were unmounted on glass throughout. Although this has the advantage that the developing process, because of diffusion through both sides, is speeded up, and also any trouble of sticking-down is avoided, it introduces problems of uniform drying and of fixing down to glass backing in the later stages of the processing. Concerning the finished product of these actual two emulsion stacks it must be admitted that trouble was experienced with dichroic fog. However, in several previous tests using similar techniques no serious dichroic fog was

experienced. A considerable improvement in the transparency of the emulsions was brought about by refixing in ammonium thiosulphate.

On the average, the shrinkage factor of the dried emulsions measured from the wet state in which they were exposed was found to be 5.2 ± 0.2 . This figure undoubtedly depends to some extent on the manner of drying the pellicles; ours were soaked in increasing concentrations of alcohol and water and then finally dried on frames. The dried pellicles were mounted finally on glass.

TABLE I. — *Characteristics of soaked and normal emulsions.*

| Average values | 1000 μ m stack | 600 μ m stack |
|-------------------------------|--------------------------|--------------------------|
| Thickness, dry | 1.04 mm | 0.64 mm |
| Area, dry | 8.5 cm \times 11.6 cm | 8.3 cm \times 10.8 cm |
| Density, dry | 3.85 g/cm ³ | 3.91 g/cm ³ |
| Thickness, wet | 2.16 mm | 1.35 mm |
| Area, wet | 10.4 cm \times 14.1 cm | 10.0 cm \times 13.1 cm |
| Density, wet (*) | 1.92 g/cm ³ | 1.94 g/cm ³ |
| Volume swelling factor . . . | 3.1 | 3.1 |
| Thickness swelling factor . . | 2.1 | 2.1 |

(*) The density of the wet emulsion was estimated from volumetric measurements only and by assuming that the volume increase of the emulsion due to water uptake was 1 cm³ per g of water. The validity of this assumption is open to question as it has been shown experimentally by WALLER (3) and by BATTY (4) that the figure of water-uptake varies between 0.84 and 1.00 cm³ per g of water. Our preliminary experiments appeared to show for the batches we used that the value was, within 5 %, 1.0 cm³ per g. It may also be possible that emulsions in pellicle form take up water somewhat differently from those on glass backings, such as have been used in other experiments. It is abundantly clear from the information of Table I that the swelling of emulsion pellicles is anything but isotropic.

photographic plates on which had been printed grids of 0.5 mm spacings. The X-ray marks on the pellicles were located accurately for each individual pellicle on the sub-stratum of the 0.5 mm grid. The pellicles were cemented into position on the glass by a thermo-setting plastic used in a manner similar to that already described by YAGODA (4). It has been found that tracing through of the tracks from one emulsion to the next is straightforward; rarely are the beam tracks displaced from one emulsion grid to the next by more than a field under X22 power.

Data on the uptake of water and swelling of the emulsions are given in Table I, and approximate range-energy values, calculated from values for

(4) H. YAGODA: *Rev. Sci. Instr.*, **26**, 263 (1954).

dry G5 emulsions, are given for protons in our wet emulsions in Table II. The minimum grain density observed in the soaked emulsions was (16 ± 2) grains per $100 \mu\text{m}$, as compared with a normal grain density in dry G5 emulsion of the order of 30 grains per $100 \mu\text{m}$. In some earlier tests on different batches of G5 emulsions we observed minimum grain densities in wet emulsions as high as $(20 \div 22)$ grains per $100 \mu\text{m}$. The calculated scattering constant for $100 \mu\text{m}$ cells in the wet emulsion was approximately (read 14°-MeV/c), and this value has been found to agree with the observed multiple scattering of known particles of known momenta.

Some information on the frequencies of events produced by K^- mesons in wet emulsions is given in Table III. Also included in the table, for the purpose of comparing wet with dry emulsion performances, are some data

TABLE II. — *Comparison of proton ranges in wet and dry G5 emulsion.*

| E (MeV) | 1.0 | 5.0 | 10 | 20 | 100 |
|-------------------|--------------------|-------------------|-------------------|---------|-------|
| Range, dry G5 | 10.5 μm | 170 μm | 550 μm | 1.9 mm | 31 mm |
| Range, wet G5 (*) | 20 μm | 255 μm | 850 μm | 2.85 mm | 50 mm |

(*) These values are computed for the compositions of wet emulsions described by the characteristics of Table I and in accordance with the assumption discussed in the footnote of Table I. They have been checked satisfactorily against the μ -meson range from observed π - μ decays and also against the observed range of K-mesons of incident momentum of 300 MeV/c.

TABLE III. — *Comparison of events produced in soaked and normal G5 emulsions by K^- -mesons of initial momentum approximately 300 MeV/c.*

| Type of event | Stars at rest (*) | Zero-prong stars at rest | Stars in flight (*) | « Stoppings » in flight | Elastic hydrogen interactions |
|-----------------|-------------------|--------------------------|---------------------|-------------------------|-------------------------------|
| Water-soaked G5 | 500 (62.3%) | 143 (17.8%) | 128 (15.9%) | 32 (4%) | 5 (0.6%) |
| Normal G5 | 2557 (74 %) | 516 (14.7%) | 330 (9.5%) | 69 (2%) | 14 (0.4%) |
| -Ratio | 0.8 | 1.2 | 1.7 | 2.0 | 1.5 |

(*) Stars at rest and stars in flight have one or more visible heavy prongs. Stars in flight also include decays in flight.

by the Bristol workers (*) who used an identical K⁻-meson exposure with normal G5 emulsions to the Barkas beam at the Bevatron, University of California. The percentages in parentheses are those of the total numbers of K⁻-particle events observed. It is seen from the table that the ratios for those types of event which might be expected to show interactions between K-particles and hydrogen nuclei are consistently higher for wet emulsions than for dry emulsions. This increase is approximately what might have been expected from our emulsions which have $5.55 \cdot 10^{22}$ atoms of hydrogen per cm³ of emulsion as compared with $3.2 \cdot 10^{22}$ atoms per cm³ of normal G5 emulsion; a ratio of 1.74. This figure should also be multiplied by the ratio of the average path length of K⁻-mesons studied in our emulsions to that studied in the dry G5 emulsions. The range of a 300 MeV/c K-meson in normal G5 emulsion is 3.8 cm. The average path length of the K-mesons measured in our emulsion was only 3.92 cm. Although the range of a 300 MeV/c K-meson in the wet emulsions is 6.0 cm, we had a significant loss of range due, firstly, to penetration of the K-particles through the wall of the box, secondly, to the spoilage of the edges of the emulsions where they were clamped in the drying frames, and thirdly, due to the fact that the scanning for the particles was commenced in from the edge by about 0.5 cm. An estimated overall figure of improvement of 1.8 in favor of the wet emulsions over the dry emulsions in yielding K-free proton interactions is therefore reasonably consistent with the observations.

In conclusion it seems clear to us that on account of a number of adverse factors, such as the large shrinkage correction required, the presence of larger distortions to the tracks, the less well-known range-energy values involved, and the lower grain densities of tracks exhibited, the use of soaked emulsions for increasing the number of K⁻-hydrogen interactions does not justify the extra labor involved in the exposure and processing of the emulsions. It might be possible, however, that for special applications such as loading with deuterium or other elements the soaking techniques described here are advantageous.

(*) We are indebted to Dr. D. J. PROWSE and other workers at the University of Bristol for letting us have these figures from the K⁻-stack collaboration exposure which was reported on at the Conference in Venice and Padua, September 1957.

RIASSUNTO (*)

Si descrive una tecnica per la quale strisce di pellicole di emulsione G5 si fanno imbevare d'acqua e poi si spongono come un pacco di pellicole in intimo contatto reciproco. Tale tecnica consente di seguire le tracce e di fare l'analisi completa degli eventi osservati. Si descrive il comportamento delle emulsioni imbevute d'acqua e lo si confronta con quello di emulsioni G5 non bagnate esposte allo stesso fascio.

(*) Traduzione a cura della Redazione.

LETTERE ALLA REDAZIONE

(La responsabilità scientifica degli scritti inseriti in questa rubrica è completamente lasciata
dalla Direzione del periodico ai singoli autori)

The Electron-Electron Scattering with Longitudinal Polarized Electron Beam.

K. NAGY and I. FARKAS

Institute of theoretical Physics, Eötvös University - Budapest

(ricevuto il 2 Novembre 1957)

Recently several experiments have been carried out in order to verify the suggestion of LEE and YANG, namely the non-conservation of parity in weak interactions. The purpose of these experiments was to prove the asymmetry taking place as a consequence of the parity non-conservation as well as the polarization of particles produced in the interaction. From the available experimental data no unambiguous conclusions can be drawn on the nature of weak interactions, mainly of β -decay. Thus it is most desirable to carry out further experiments on several β -active nuclei. Recently a new experiment has been suggested to investigate the polarization of electrons released in β -decay of oriented nuclei. Namely the emerging electrons have to be scattered on polarized electrons (scattering by magnetized iron) and the scattering cross-section have to be measured. From the difference of this result and the result obtained from Møller-scattering the polarization of electrons emerging from β -decay can be determined (*) (+).

The idea of this experiment has suggested to investigate theoretically how the cross-section of electron-electron scattering will be modified if the electrons are longitudinally polarized. The calculations have been carried to the first non-vanishing approximation of the S -matrix. The graphs of the problem in the used approximation are



(*) This suggestion occurred simultaneously but independently to H. FRAUENFELDER (University of Illinois) and to I. BERKES (Central Research Institute of Physics, Budapest).

(+) After the completion of the present calculation we were informed about the experiment performed by H. FRAUENFELDER *et al.* [*Phys. Rev.*, **107**, 643 (1957)]. In this paper the authors mentioned, that this calculations were carried out by Dr. BINCER.

where p, q are the four-momenta of incident electrons, and p', q' the four-momenta of the emerging electrons.

The transition matrix element of the reduced S_2 -matrix is ⁽¹⁾

$$(1) \quad (p', q' | S_2 | p, q) = M \delta(p' + q' - p - q),$$

where

$$(2) \quad M = -\frac{ie^2}{c} \hbar^5 (2\pi)^4 \left[\frac{\bar{u}(\mathbf{p}') \gamma_\mu u(\mathbf{p}) \bar{v}(\mathbf{q}') \gamma_\mu v(\mathbf{q})}{(p' - p)^2} - \frac{\bar{u}(\mathbf{p}') \gamma_\mu v(\mathbf{q}) \bar{v}(\mathbf{q}') \gamma_\mu u(\mathbf{p})}{(q' - p)^2} \right].$$

The transition probability per unit time is

$$(3) \quad w = \frac{1}{T} \sum_{\text{final states}} |(p', q' | S_2 | p, q)|^2.$$

By summing over the spin and momenta of electrons in final states, we find

$$(4) \quad w = \frac{ie^4}{c(2\pi)^2} \int d\mathbf{p}' \delta(p'^2 + m^2 c^2) \delta(q'^2 + m^2 c^2) \cdot \\ \cdot \left\{ (p' - p)^{-4} \bar{u} \gamma_\nu (p'_\lambda \gamma_\lambda + imc) \gamma_\mu \bar{v} \gamma_\nu (q'_\rho \gamma_\rho + imc) \gamma_\mu v + \right. \\ + (q' - p)^{-4} \bar{u} \gamma_\nu (q'_\lambda \gamma_\lambda + imc) \gamma_\mu \bar{v} \gamma_\nu (p'_\rho \gamma_\rho + imc) \gamma_\mu v - \\ - (p' - p)^{-2} (q' - p)^{-2} \bar{u} \gamma_\nu (p'_\lambda \gamma_\lambda + imc) \gamma_\mu \bar{v} \gamma_\nu (q'_\rho \gamma_\rho + imc) \gamma_\mu u - \\ \left. - (p' - p)^{-2} (q' - p)^{-2} \bar{u} \gamma_\nu (q'_\lambda \gamma_\lambda + imc) \gamma_\mu \bar{v} \gamma_\nu (p'_\rho \gamma_\rho + imc) \gamma_\mu u \right\}.$$

It is assumed that the electrons in the initial state are polarized longitudinally, i.e. the spins are directed in the direction of the motion or in the opposite direction. Let us first consider the case when spin and momentum are parallel. The operator of the spin-projection $(1 + \sigma_p)/2$ be introduced as follows:

$$(5) \quad \frac{1 + \sigma_p}{2} u(\uparrow) = u(\uparrow); \quad \frac{1 + \sigma_p}{2} u(\downarrow) = 0.$$

Here $u(\uparrow)$ is the spinor belonging to the spin state parallel to the momentum and $u(\downarrow)$ belonging to the antiparallel state, σ_p is the scalar product of the spin-vector $\boldsymbol{\sigma}$ and the vector-unit $\mathbf{p}/|\mathbf{p}|$. By using the spin-projection operator $(1 + \sigma_p)/2$ and the energy-projection operator

$$(6) \quad A_+ = \frac{\mathcal{H} + |E|}{2|E|},$$

⁽¹⁾ J. M. JAUCH and F. ROHRlich. *The Theory of photons and electrons*, (Cambridge Mass., 1955), p. 253-257.

we get :

$$(7) \quad uOu = \sum_{s=1}^2 u^+ \frac{1+\sigma_p}{2} \gamma_4 O \frac{1+\sigma_p}{2} u = \sum_1^4 u^+ \frac{1+\sigma_p}{2} A_+ \gamma_4 O \frac{1+\sigma_p}{2} A_+ u = \\ = \text{Spur} \left(\frac{1+\sigma_p}{2} A_+ \gamma_4 O \right),$$

where O is an operator composed from γ_v matrices. Here the relations

$$(8) \quad \left(\frac{1+\sigma_p}{2} \right)^2 = \frac{1+\sigma_p}{2}; \quad A_+^2 = A_+ \quad \text{and} \quad \left[\frac{1+\sigma_p}{2}, A_+ \right] = 0$$

were used. Using equations (7) and (8) the transition probability (4) can be re-written in the form:

$$(9) \quad w = - \frac{ie^4}{c16(2\pi)^2} \int dp' \delta(p'^2 + m^2c^2) \delta(q'^2 + m^2c^2) \cdot \frac{1}{p_0 q_0} \cdot \\ \cdot \{ (p' - p)^{-4} \text{Spur} ((1 + \sigma_p)(p_\alpha \gamma_\alpha + imc) \gamma_v (p'_\lambda \gamma_\lambda + imc) \gamma_\mu) \cdot \\ \cdot \text{Spur} ((1 + \sigma_q)(q_\beta \gamma_\beta + imc) \gamma_v (q'_\epsilon \gamma_\epsilon + imc) \gamma_\mu) + \\ + (q' - p)^{-4} \text{Spur} ((1 + \sigma_p)(p_\alpha \gamma_\alpha + imc) \gamma_v (q'_\lambda \gamma_\lambda + imc) \gamma_\mu) \cdot \\ \cdot \text{Spur} ((1 + \sigma_q)(q_\beta \gamma_\beta + imc) \gamma_v (p'_\epsilon \gamma_\epsilon + imc) \gamma_\mu) - \\ - 2(p' - q)^{-2} (q' - p)^{-2} \text{Spur} ((1 + \sigma_p)(p_\alpha \gamma_\alpha + imc) \gamma_v (p'_\lambda \gamma_\lambda + imc) \gamma_\mu \cdot \\ \cdot (1 + \sigma_q)(q_\beta \gamma_\beta + imc) \gamma_v \cdot (q'_\epsilon \gamma_\epsilon + imc) \gamma_\mu) \} \cdot$$

From the transition probability we get for the cross-section:

$$(10) \quad \sigma = \frac{w}{v_1 + v_2}.$$

$v_1 + v_2$ is the relative velocity of the particles. In the following this formula will be specialized to the center-of-momentum system (CM-system), which is characterized by the relations:

$$(11) \quad \mathbf{p} = -\mathbf{q}, \quad \mathbf{p}' = -\mathbf{q}'; \quad |\mathbf{p}| = |\mathbf{p}'|; \quad p_0 = q_0 = p'_0 = q'_0.$$

Owing to the δ -functions the integral in (9) can be carried out easily. Using the relation

$$(12) \quad \gamma_\mu \gamma_\nu + \gamma_\nu \gamma_\mu = 2\delta_{\mu\nu}$$

the spures occured in (9) can be calculated in the well known manner. Finally we

get for the differential cross-section:

$$(13) \quad \frac{d\sigma}{d\Omega} = \left(\frac{d\sigma}{d\Omega} \right)_{\text{Møller}} + \frac{\alpha^2}{\kappa^2(\kappa^2 - 1)^2} \left\{ \frac{(2\kappa^2 - 1)(4\kappa^2 - 3)}{\sin^2 \vartheta} - (\kappa^4 - 1) \right\},$$

(in CM-system)

where

$$(14) \quad \left(\frac{d\sigma}{d\Omega} \right)_{\text{Møller}} = \frac{\alpha^2}{\kappa^2(\kappa^2 - 1)^2} \left\{ \frac{4(2\kappa^2 - 1)^2}{\sin^4 \vartheta} - \frac{4(2\kappa^4 - \kappa^2 - \frac{1}{4})}{\sin^2 \vartheta} + (\kappa^2 - 1)^2 \right\}$$

is the differential cross-section of Møller-scattering and we used the following abbreviations:

$$(15) \quad \alpha^2 = \frac{4}{1} \left(\frac{e^2}{4\pi mc^2} \right)^2; \quad \kappa = \frac{1}{\sqrt{1 - \beta^2}}, \quad \beta = v/c.$$

v is the velocity of electron, ϑ the angle between the vectors \mathbf{p} , \mathbf{p}' in CM-system.

If the spin of the two electrons is antiparallel to the direction of motion, operators $(1 - \sigma_p)/2$ and $(1 - \sigma_q)/2$ have to be used instead of $(1 + \sigma_p)/2$ and $(1 + \sigma_q)/2$, respectively. The result of the calculation will be the same as in the former case.

If the spin of one of the electrons is parallel to the direction of motion while that of the other is antiparallel, we get

$$(16) \quad \frac{d\sigma}{d\Omega} = \left(\frac{d\sigma}{d\Omega} \right)_{\text{Møller}} - \frac{\alpha^2}{\kappa^2(\kappa^2 - 1)^2} \left\{ \frac{(2\kappa^2 - 1)(4\kappa^2 - 3)}{\sin^2 \vartheta} - (\kappa^4 - 1) \right\}.$$

These two cases can be expressed in one form, namely:

$$(17) \quad \left(\frac{d\sigma}{d\Omega} \right)_{\pm} = \left(\frac{d\sigma}{d\Omega} \right)_{\text{Møller}} \pm \frac{\alpha^2}{\kappa^2(\kappa^2 - 1)^2} \left\{ \frac{(2\kappa^2 - 1)(4\kappa^2 - 3)}{\sin^2 \vartheta} - (\kappa^4 - 1) \right\}.$$

The notation (+) indicates the case when both spins are parallel to the momenta and notation (−) the case when only one of them is parallel.

From the experimental point of view the expression (17) has to be also transformed into laboratory system. The relations between the corresponding quantities of laboratory- and center of momentum-system are as follows (1):

$$\cos \vartheta = \frac{2 - (\gamma + 3) \sin^2 \theta}{2 + (\gamma - 1) \sin^2 \theta} = x,$$

$$(18) \quad \gamma = 2\kappa^2 - 1; \quad d\Omega = \frac{8 \cos \theta (\gamma + 1)}{[2 + (\gamma - 1) \sin^2 \theta]^2} d\omega.$$

Here θ and $d\omega$ refer to the laboratory-system. We used γ for the abbreviation of

the following expression

$$(19) \quad \gamma = \frac{1}{\sqrt{1 - v^2/c^2}}.$$

v is the velocity of electron in laboratory-system.

By using the relations (18), for the differential cross-section in laboratory-system, we get:

$$(20) \quad \frac{d\sigma}{d\omega} = \left(\frac{d\sigma}{d\omega} \right)_{\text{Møller}} \pm \frac{64x^2 \cos \theta}{(\gamma - 1)^2 [2 + (\gamma - 1) \sin^2 \theta]^2} \left\{ \frac{\gamma(2\gamma - 1)}{1 - x^2} - \frac{(\gamma + 1)^2}{4} + 1 \right\}.$$

(in L-system).

* * *

The authors wish to express their gratitude to Dr. G. MARX for suggesting this problem.

The first one hundred an fifty years; A history of John Wiley and Sons, Inc. 1807-1957. 1 Volume in-16° con 32 figure. J. Wiley & Sons, Inc. 1957, pp. xxv+242.

Questa rassegna che la nota casa editrice J. Wiley and Sons ha pubblicato sulla sua centocinquantenaria attività offre lo spunto a talune brevi riflessioni su la storia della scienza e della tecnica dall'inizio dell'ottocento ad oggi.

Sfogliando le pagine di questo volume dedicate alle pubblicazioni riguardanti le varie scienze si può notare innanzi tutto come le opere di fisica compaiano più tardi (1839) che non quelle di altre scienze quali ad esempi la matematica (1817). Questo probabilmente perchè allora scarsi erano ancora gli interessi culturali e pratici connessi a questa nuova scienza che riuscì durante l'ultimo cinquantennio a raggiungere e sorpassare le altre discipline.

A tale osservazione se ne aggiunge un'altra relativa al notevolissimo incremento della cultura, e quindi della editoria americana, sia sotto l'influsso dell'imponente processo di industrializzazione del paese sia per lo stimolo della numerosa emigrazione intellettuale europea dell'ultimo trentennio.

I volumi ricordati più interessanti per il fisico sono infatti per lo più di recente pubblicazione e ancora largamente usati, quali l'opera di LOEB su le scariche nei gas e i compendi di meccanica statistica del MAYER e di statistica per la fisica del LINDSAY. Per la fisica

nucleare basterà ricordare il volume di BLATT e WEISSKOPF e quello edito da EMILIO SEGRÈ.

Resta infine da notare quel classico della teoria dell'informazione che è la cibernetica del WIENER.

Spiace tuttavia che non compaiano in questa rassegna quadri statistici che documentino in modo più accurato il lettore sul numero di opere pubblicate nelle diverse discipline nei vari periodi.

A. ALBERIGI QUARANTA.

R. COURANT - *Vorlesungen über Differential- und Integralrechnung*; Zweiter Band (Funktionen Mehrerer Veränderlicher), Dritte Auflage, pp. 468; Springer-Verlag, Berlin-Göttingen-Heidelberg 1955.

Questa terza edizione ripresenta il noto e ottimo trattato del COURANT con leggere modifiche sulla seconda edizione tedesca. In esso l'A. tratta il calcolo differenziale ed integrale a varie variabili con notevole chiarezza di linguaggio ed esattezza dei concetti. Questi indubbi pregi sono dovuti anche alla mancanza di sottigliezze troppo formali: così il COURANT non trascina ovunque le n variabili ma tratta bensì con gran cura il caso di due variabili estendendo poi i concetti ed i risultati al caso più generale con assoluto rigore.

Nel primo capitolo l'A. dà alcuni ele-

menti di geometria analitica e calcolo vettoriale. Nel secondo capitolo introduce i concetti di funzione di varie variabili, continuità e limite, per poi definire le derivate parziali. Nel resto del 2° capitolo e nel 3° sviluppa il calcolo differenziale, applicando concetti geometrici con particolare riguardo. Nei capitoli 4° e 5° tratta il calcolo integrale, curando specialmente gli integrali curvilinei e superficiali e quindi i teoremi di Gauss, Stokes e Green; considera anche gli integrali impropri facendone poi applicazione agli integrali di Fresnel, a quelli di Fourier ed alla funzione gamma. Nel capitolo 7° introduce brevemente le equazioni differenziali (ordinarie ed alle derivate parziali) soffermandosi maggiormente su alcuni casi di particolare interesse.

Questo testo è da raccomandare caldamente, soprattutto agli studenti di Fisica ed Ingegneria che desiderino una solida preparazione matematica; infatti, oltre ai pregi già elencati esso ha quello di riportare numerose applicazioni di interesse fisico. Così, per esempio, lo

studio del calcolo degli errori, il confronto tra le rappresentazioni di Euler e Lagrange del moto dei fluidi, l'introduzione dei momenti ed applicazione a problemi fisici come quello del pentodo composto, le applicazioni delle equazioni del moto introducendo concetti di equilibrio e stabilità, lo studio del problema del potenziale, dell'equazione delle onde e delle equazioni di Maxwell nel vuoto ecc. Queste altre applicazioni inserite nel testo fanno sì che i concetti matematici vengano continuamente adoperati e quindi chiariti, rendendo inoltre più interessante e piacevole lo studio.

Bisogna però notare che è un peccato che non siano stati aggiunti i capitoli 7° e 8° dell'edizione inglese (calcolo delle variazioni e funzioni di variabile complessa) e gli interessanti problemi da risolvere che si trovano alla fine di ogni paragrafo di quella edizione.

Numerosi ed utili i diagrammi e le figure, ottima la presentazione tipografica.

D. AMATI

PROPRIETÀ LETTERARIA RISERVATA

Direttore responsabile: G. POLVANI

Tipografia Compositori - Bologna

Questo fascicolo è stato licenziato dai torchi il 25-II-1958